



# DEPARTAMENTO DE CIÊNCIAS DA VIDA

FACULDADE DE CIÊNCIAS E TECNOLOGIA  
UNIVERSIDADE DE COIMBRA

## The Role of Senescent Fibroblasts on Epithelial Cells Malignant Transformation

Luís André Lima da Gama Mendes

---

2011





**DEPARTAMENTO DE CIÊNCIAS DA VIDA**

FACULDADE DE CIÊNCIAS E TECNOLOGIA  
UNIVERSIDADE DE COIMBRA

## **The Role of Senescent Fibroblasts on Epithelial Cells Malignant Transformation**

Dissertação apresentada à Universidade de Coimbra para cumprimento dos requisitos necessários à obtenção do grau de Mestre em Bioquímica, realizada sob a orientação científica da Professora Doutora Maria Carmen Martins de Carvalho Alpoim (Universidade de Coimbra)

**Luís André Lima da Gama Mendes**

---

**2011**



*Canto noite fora, alma dentro  
Sinto que a Coimbra me entrego  
Tempos d'ouro, leva-os o vento  
Minhas mágoas, o Mondego*

*Eis que chega a hora de partir  
Hora derradeira do adeus  
Levo na memória  
Risos, prantos, histórias  
Coisas que não esqueço  
Peço só poder voltar*

*Choro este sonho que se acaba  
Sonho de que acordo, triste fado  
Dos meus ombros solta-se a capa  
Dos meus olhos, a saudade...*

Balada de Despedida 6º Ano Médico 2006/07



## ACKNOWLEDGMENTS

Ao dar início à apresentação deste trabalho, não posso deixar de dedicar algumas palavras de agradecimento, em particular:

À Professora Doutora **Maria Carmen Alpoim**, por me ter dado a oportunidade de realizar este projecto, dando-me a conhecer um mundo totalmente novo, além das horas de discussão de ideias e pontos de vista, a força e a motivação que me transmitiu com a sua infindável energia, mesmo quando as coisas não corriam tão bem.

Ao **Carlos Rodrigues**, pela paciência e disponibilidade com que sempre se apresentou, pelas suas chamadas de atenção, a sua exigência consigo próprio e ambição, sendo um exemplo a seguir em certos aspectos, ainda que nem sempre devidamente reconhecido.

À Professora Doutora **Isabel Carreira**, tal como a todo o grupo do **Laboratório de Citogenética e Genómica na Faculdade de Medicina da Universidade de Coimbra** por todo o apoio e ajuda com que se disponibilizaram durante este projecto, pelo ambiente de trabalho que proporcionaram, demonstrando que é possível trabalhar a sorrir.

A todos os **estagiários e alunos de mestrado**, que durante o último ano passaram pelo Laboratório, gostaria também de agradecer pela companhia durante dias e dias a fio na sala do café e pelo ambiente de camaradagem que tanto facilitou a tarefa quando não havia resultados.

À Professora Doutora **Ana Urbano**, graças a quem tomei o gosto pela área do cancro e cultura de células e cujo rigor me motivou a querer sempre mais de mim.

Ao Professor Doutor **Marc Chanson** e o seu grupo no **Laboratoire d'Investigation Clinique III, Hôpitaux Universitaires de Genève** por me ter aceite no seu grupo de trabalho e ter reconhecido que, ainda que Portugal seja um país pequeno, é capaz de criar pessoas com valor e capazes.

Pessoalmente gostava de agradecer:

À minha **família** mas principalmente ao meu **Pai**, à minha **Mãe** e à minha **Irmã**, simplesmente por serem eles próprios, terem feito o maior esforço em educar-me com todo o carinho e por me terem ensinado as virtudes do respeito e confiança, lembrando-me nas

acções do dia-a-dia que “Casa” não é o sítio onde se vive mas sim onde se encontra o Coração, a eles dedico todo o meu êxito.

A todos os meus **amigos** que desde sempre me fizeram sorrir, saltar, rir, algumas vezes chorar (de riso), com quem partilhei bons e maus momentos, aventuras e amores, não interessando a distância que nos separa, bastando um segundo para regressar a cumplicidade. Nesse sentido gostava de particularmente agradecer ao **Nöel Yeh Martin** por me demonstrar que a amizade não tem fronteiras e, principalmente ao **André Melo, Joana Francisco e José Brás da Luz**, por me conhecerem como mais ninguém, me terem aturado todas as minhas loucuras.

À **Tuna Académica da Universidade de Coimbra** por todos os ensaios, concertos, reuniões, copos e saídas, por me permitir continuar um sonho de criança com a música, por serem a minha fuga a uma vida rotineira e ser algo mais do que um estudante universitário comum, proporcionando-me o “espaço” onde me refugiava, sendo o meu escape do trabalho.

Por último e talvez ainda mais importante, gostava também de dar um muito obrigado sentido à **Catarina Ferrão**, por toda a paciência e carinho que teve por mim, tal como a motivação que não me deixou de dar, por me ter aturado nos dias bons e dias maus e ter tido compreensão para quase todas as minhas loucuras. Agradeço do fundo do meu coração todos os bons momentos que se proporcionaram e por me lembrar, todos os dias, que por muita expectativa que tenham de nós e exigência que nos seja colocada, acima de tudo somos humanos e precisamos de Amor.

## TABLE OF CONTENTS

	Symbols and Abbreviations	XI
	Summary	XV
	Resumo	XVII
<b>1.</b>	<b>Introduction</b>	<b>1</b>
1.1.	The Respiratory System	3
1.2.	The Bronchial Epithelium	4
1.3.	The Connective Tissue and The Extracellular Matrix	7
1.3.1.	Fibroblasts	8
1.4.	Lung Cancer	10
1.4.1.	Genomic Hallmarks of Lung Carcinomas	13
1.4.2.	The Invasive Properties of Lung Carcinomas	17
1.4.3.	Metabolic Reprogramming of Carcinoma Cells	19
1.5.	Microenvironment and Cancer	20
1.6.	Senescence	22
1.6.1.	Molecular Mechanisms of Senescence	26
1.7.	Chromium, Hexavalent Chromium and Cancer	28
1.8.	Cell Culture	31
1.8.1.	Primary Cell Cultures	32
1.8.2.	BEAS-2B Cell Line	33
1.8.3.	Co-Cultures	34
1.8.3.1.	Co-Culture of Lung Fibroblasts and Bronchial Epithelial Cells	34
1.9.	Objective	36

<b>2.</b>	<b>Material &amp; Methods</b>	<b>37</b>
2.1.	Reagents and Material	39
2.2.	Equipment and Software	43
2.3.	Solutions and Nutrient Medium Preparation	45
2.4.	Methods	47
2.4.1.	Cell Culture	48
2.4.1.1.	Human Bronchial Fibroblasts (HBF) Primary Cultures	49
2.4.1.2.	Human Bronchial Epithelial Cells (HBEC) Primary Cultures	50
2.4.1.3.	BEAS-2B Cell Line Cultures	51
2.4.1.4.	Cell Passage	51
2.4.1.5.	Cell Counting	52
2.4.1.6.	Cell Freezing/Unfreezing	53
2.4.1.6.1.	Cells' Freezing	53
2.4.1.6.2.	Cells' Unfreezing	54
2.5.	Establishment of Cr(VI) Exposure Conditions That Induced Senescence on HBF	54
2.6.	Co-Cultures	55
2.7.	Cells' Viability Evaluation - MTT Assay	55
2.8.	Cells' Morphology and Growth Pattern Evaluation	56
2.9.	Senescent Phenotype Evaluation	56
2.10.	Immunocytochemistry	57
<b>3.</b>	<b>Results &amp; Discussion</b>	<b>59</b>
3.1.	Human Bronchial Fibroblasts (HBF) Primary Cultures	61
3.2.	Primary Cultures of Human Bronchial Epithelial Cells (HBEC)	63
3.3.	Cr(VI) Exposure Conditions That Induce Senescence on Human Bronchial Fibroblasts (HBF)	64
3.3.1.	Determination of the Cr(VI) Exposure Conditions That Induce Growth Arrest	65

3.3.2.	Determination of the Cr(VI) Exposure Conditions That Induce Senescence	74
3.3.3.	Immunocytochemical Characterization of Senescent Fibroblasts	87
3.4.	Co-Cultures: The Effect of Senescent Fibroblasts on BEAS-2B Cells Proliferation	92
<b>4.</b>	<b>Conclusion &amp; Final Remarks</b>	<b>95</b>
<b>5.</b>	<b>References</b>	<b>99</b>



## SYMBOLS AND ABBREVIATIONS

<b><math>\alpha</math>-SMA</b>	- Alpha Smooth Muscle Actin
<b>Akt</b>	- Serine/threonine protein kinase
<b>ALK</b>	- Anaplastic Lymphoma Kinase
<b>AMPK</b>	- 5' Adenosine Monophosphate-activated Protein Kinase
<b>ATP</b>	- Adenosine Triphosphate
<b>BEAS-2B</b>	- Bronchial Epithelial Airway System – 2B
<b>BEBM</b>	- Bronchial Epithelial Basal Medium
<b>BEGM</b>	- Bronchial Epithelial Growth Medium
<b>BPE</b>	- Bovine Pituitary Extract
<b>BRAF</b>	- v-Raf Murine Sarcoma Viral Oncogene Homolog B1
<b>BRCA (1,2)</b>	- Breast Cancer (type 1, 2) Susceptibility Protein
<b>BSA</b>	- Bovine Serum Albumin
<b>CAF</b>	- Carcinoma-Associated-Fibroblasts
<b>CCL5 / RANTES</b>	- Chemokine (C-C motif) ligand 5
<b>CD34</b>	- Cluster of Differentiation Molecule - 34
<b>CDK4</b>	- Cyclin-Dependent-Kinase 4
<b>CDK6</b>	- Cyclin-Dependent-Kinase 6
<b>CHK2</b>	- Checkpoint kinase 2
<b>Cr(VI)</b>	- Hexavalent Chromium
<b>CP</b>	- Cancro do Pulmão (Portuguese for Lung Cancer)
<b>c-MET</b>	- MET or MNNG HOS Transforming gene
<b>DAB</b>	- 3,3-Diaminobenzidine Tetrahydrochloride
<b>DMEM</b>	- Dulbecco's Modified Eagle Medium
<b>DMSO</b>	- Dimethyl Sulfoxide
<b>DNA</b>	- Deoxyribonucleic Acid
<b>E2F</b>	- Group of genes that codifies a family of transcription factors (TF) in higher eukaryotes
<b>ECACC</b>	- European Collection of Cell Cultures
<b>ECM</b>	- Extracellular Matrix
<b>EGFR</b>	- Epidermal Growth Factor Receptor
<b>EMT</b>	- Epithelial-Mesenchymal Transition
<b>ERCC-1</b>	- DNA excision repair protein ERCC-1

<b>EU-27</b>	- European Union
<b>FBS</b>	- Foetal Bovine Serum
<b>FDA</b>	- Food and Drug Administration
<b>FDG</b>	- 18F-fluorodeoxyglucose
<b>FGF-7</b>	- Fibroblast Growth Factor 7
<b>FOX</b>	- Forkhead Orthologs Protein Family
<b>GLUT</b>	- Glucose Transporter
<b>HAEC</b>	- Human Airway Epithelial Cells
<b>HBEC</b>	- Human Bronchial Epithelial Cells
<b>HBF</b>	- Human Bronchial Fibroblasts
<b>HBSS</b>	- Hank's Balance Salt Solution
<b>HER-2</b>	- Human Epidermal Growth Factor Receptor 2
<b>HGF</b>	- Hepatocyte Growth Factor
<b>HIF</b>	- Hypoxia-Inducible Factor 1
<b>HIF 1<math>\alpha</math></b>	- Hypoxia-Inducible Factor 1 $\alpha$
<b>HIF 2<math>\alpha</math></b>	- Hypoxia-Inducible Factor 2 $\alpha$
<b>IDH</b>	- Isocitrate Dehydrogenase
<b>IGF (1, 2)</b>	- Insulin-like Growth Factor (1, 2)
<b>IL(6, 8)</b>	- Interleukin (6,8)
<b>KRAS</b>	- V-Ki-ras2 Kirsten rat sarcoma viral oncogene homolog
<b>LC</b>	- Lung Cancer
<b>LKB1</b>	- Serine/Threonine Kinase 11
<b>Mek</b>	- Mitogen-activated protein kinase kinase, also known as MAP2K
<b>MET</b>	- Mesenchymal-Epithelial Transition
<b>MMP (3,9)</b>	- Matrix Metalloproteinases (3 and 9)
<b>MSC</b>	- Mesenchymal Stem Cells
<b>mTOR</b>	- Mammalian Target Of Rapamycin
<b>MTT</b>	- 3-(4,5-Dimethylthiazol-2-yl)-2,5-diphenyltetrazolium bromide
<b>MYC</b>	- V-myc myelocytomatosis viral oncogene homolog, a oncogene express in tumor cells
<b>NHBE</b>	- Normal Human Bronchial Epithelium
<b>NKX2-8</b>	- NKX-homeodomain factors
<b>NSCLC</b>	- Non-Small Cell Lung Cancer
<b>p16</b>	- Protein 16, product of the p16 tumor suppressor gene

<b>p21</b>	- Protein 21, mediator of p53 activity on cell cycle
<b>p53</b>	- Protein 53, regulator of cell proliferation
<b>PAX-9</b>	- Paired box gene 9
<b>PBS</b>	- Phosphate Buffer Solution
<b>PDGF</b>	- Platelets-Derived Growth Factor
<b>PET</b>	- Positron Emission Tomography
<b>PI3K</b>	- Phosphatidylinositol 3-Kinase
<b>PIK3CA</b>	- Phosphatidylinositol 3-kinase 110 kDa Catalytic Subunit
<b>pRb</b>	- Retinoblastoma Protein
<b>Raf</b>	- RAF proto-oncogene serine/threonine-protein kinase
<b>RAS</b>	- Oncogene that encodes the Ras protein, named after RAt Sarcoma
<b>RER</b>	- Rough Endoplasmic Reticulum
<b>rhEGF</b>	- Human Recombinant Epidermal Growth Factor
<b>ROS</b>	- Reactive Oxygen Species
<b>RRM1</b>	- Ribonucleoside-diphosphate Reductase Large Subunit
<b>SASP</b>	- Senescence-Associated Secretory Phenotype
<b>SA-<math>\beta</math>gal</b>	- Senescence-Associated Beta Galactosidase
<b>SCLC</b>	- Small Cell Lung Cancer
<b>SF</b>	- Senescent Fibroblasts
<b>SM</b>	- Smooth Muscle
<b>SNP</b>	- Single Nucleotide Polymorphism
<b>SP-C</b>	- Surfactant Protein-C
<b>SV-40</b>	- Simian Virus 40
<b>T3</b>	- Thiiodoethionine
<b>TGF-<math>\beta</math></b>	- Transforming and Growth Factor Beta
<b>TITF-1</b>	- Thyroid Transcription Factor 1
<b>TNF<math>\alpha</math></b>	- Tumour Necrotic Factor alpha
<b>TNF<math>\beta</math></b>	- Tumour Necrotic Factor beta
<b>Tp53</b>	- tumor protein 53
<b>TSC2</b>	- Tuberous Sclerosis protein 2
<b>TSP-1</b>	- Thrombospondin 1
<b>USA</b>	- United States of America
<b>UV</b>	- Ultraviolet Radiation
<b>VEGF</b>	- Vascular Endothelial Growth Factor



## SUMMARY

As the vast majority of human cancers, hexavalent chromium [Cr(VI)] induced lung cancers (LC) are carcinomas that arise from epithelial cells. Though there is little doubt that multiple genetic alterations are necessary for epithelial cells malignant transformation to take place, several lines of evidence suggest that the progress towards full malignancy, of cells that bear potentially oncogenic mutations, requires a permissive tissue microenvironment. Therefore, to obtain reliable information on the mechanisms underlying the onset and progression of cancer a system resembling the *in vivo* epithelium is needed. In the case of LC such a system requires the use of normal human bronchial epithelial cells (NBEC). However, NBEC proliferate poorly and most epithelial cells quickly lose their differentiated features *in vitro*, probably because appropriate signals from extracellular matrix, growth factors and hormones have not been fully defined. The number of cultures that can be initiated is therefore limited by the yield of NBEC obtained from tissues or commercially available sources.

Recently, however, it was established a new cultivation method in which epithelial cells and fibroblasts co-evolve together, which can be used to study the role of fibroblasts, the major stroma component intimately involved in tissue homeostasis, on epithelial cells malignant transformation.

Fibroblasts portray a wide range of molecular, biochemical and morphological features which allow them to adapt to normal and pathological situations. Factors secreted by senescent fibroblasts (SF) can stimulate epithelial cells proliferation and disrupt epithelial differentiation, which may explain age-related cancers.

The main targets of Cr(VI)-toxicity are bronchial epithelial cells (BEC) and bronchial fibroblasts. Although, Cr(VI) is known to induce senescence in human foreskin fibroblasts, it's unknown whether Cr(VI) also induces senescence in human bronchial fibroblasts and the role of this senescent fibroblasts on bronchial epithelial cells malignant transformation.

This dissertation describes the impact of Cr(VI)-exposure regimens on normal bronchial fibroblasts phenotype and the effects of the Cr(VI)-induced senescent fibroblasts on SV-40 immortalised human bronchial epithelial cells phenotype using a co-culture method.

To fulfill the objective of this dissertation several cultures of normal bronchial fibroblasts and normal bronchial epithelial cells were established out of lung biopsies. Thereafter, it was possible to established which Cr(VI)-exposure regimen was inducing a stable senescent

phenotype on human bronchial fibroblasts. Finally, co-cultures of bronchial fibroblasts both normal and Cr(VI)-senescent were cultured together with bronchial epithelial cells. These co-cultures allowed the evaluation of how normal and senescent fibroblasts and epithelial cells co-evolved together in presence and absence of Cr(VI).

## RESUMO

O cancro de pulmão (CP) induzido por crómio hexavalente [Cr(VI)] emerge em células epiteliais sendo, por este motivo, designado carcinoma. Muito embora a ocorrência de múltiplas alterações genéticas seja um factor crucial na malignização de células recentemente, verificou-se que o processo requer a existência de um microambiente permissivo em torno das células com potenciais mutações oncogénicas. Por isso, a obtenção *in vitro* de dados precisos sobre os mecanismos subjacentes ao aparecimento e desenvolvimento da patologia maligna necessita, no caso do CP, de utilizar modelos que tenham características semelhantes ao epitélio bronquial humano. É um facto que células normais do epitélio bronquial humano (NBEC) terão de ser usadas, o que é muito limitativo dado que estas células, *in vitro*, se tornam indiferenciadas devido, possivelmente, à ausência de factores de crescimento e hormonas provenientes da matrix. Por isso, o uso de culturas primárias de NBEC, obtidas comercialmente ou de tecidos, é muito restrito.

Recentemente foi implementada uma nova metodologia que permite cultivar células epiteliais conjuntamente com fibroblastos e, conseqüentemente, estudar o papel dos fibroblastos, o maior componente do estroma envolvido na homeostasia dos tecidos, na transformação maligna de células epiteliais.

Os fibroblastos apresentam características moleculares, bioquímicas e morfológicas que favorecem a sua adaptação a situações normais e patológicas. É já do conhecimento que os factores segregados por fibroblastos senescentes (SF) têm capacidade para estimular a proliferação de células epiteliais, interferindo com a diferenciação celular e potenciando o eclodir de cancro em idosos.

Os principais alvos de toxicidade de Cr(VI) são células epiteliais bronquiais e fibroblastos bronquiais. Apesar de se saber que Cr(VI) é capaz de induzir senescência em fibroblastos do prepúcio, desconhece-se se o Cr(VI) também induz senescência em fibroblastos bronquiais humanos e o papel deste fibroblastos senescentes na transformação maligna de células epiteliais bronquiais.

Esta dissertação descreve o estudo realizado tendo em vista avaliar se o Cr(VI) induzia o desenvolvimento do fenótipo senescente em fibroblastos bronquiais normais, e o efeito da senescência em fibroblastos no fenótipo de células epiteliais bronquiais normais, imortalizadas por SV-40, usando um método de co-cultura.

Para cumprir os objectivos desta dissertação diversas culturas de fibroblastos bronquiais normais e células epiteliais bronquiais normais foram estabelecidas a partir de biopsias de pulmão. Posteriormente, foi possível determinar qual o regime de exposição a Cr(VI) induzia um fenótipo senescente estável em fibroblastos bronquiais humanos. Finalmente, co-culturas de fibroblastos bronquiais, tanto normais como senescentes devido a Cr(VI), e células epiteliais bronquiais foram realizadas. Estas co-culturas permitiram a avaliação de como fibroblastos, normais e senescentes, e células epiteliais co-evoluíram em conjunto, na presença e ausência de Cr(VI).

# Introduction



## 1.1. THE RESPIRATORY SYSTEM

In humans and other mammals the respiratory system is essentially composed by the airways, the lungs and the respiratory musculature. The bronchial airways, also called the bronchial tree, besides conducting the air to and from the lungs, also account for its conditioning, warming and humidification. In the alveolar regions of the lungs, the oxygen and the carbon dioxide passively diffuse between the conditioned air and the outside atmosphere a process called pulmonary haematosis [Junqueira and Carneiro, 2008].

The two primary bronchi are originated from a bifurcation of the terminal part of the trachea. These cartilaginous structures penetrate each lung at the hilum, where they subdivide into secondary, tertiary and smaller bronchi, forming a tree-like structure called bronchopulmonary segment. This structure has its own connective tissue capsule and blood supply and represents 10–12% of each lung. The existence of such lung segments facilitates the specific surgical resection of unhealthy lung tissue without affecting nearby healthy tissue, being of most interest for our work.

As the number of segments multiplies, becoming smaller, each bronchus reaches a diameter of approximately 5 mm. In this region of the respiratory system the lung tissue forms a pseudostratified epithelium with ciliated cells interspersed with goblet cells. This entire cellular complex is supported by a thin lamina propria of smooth muscle, elastic fibres and connective tissue that also functions as a feeder layer to the epithelium [Junqueira and Carneiro, 2008].

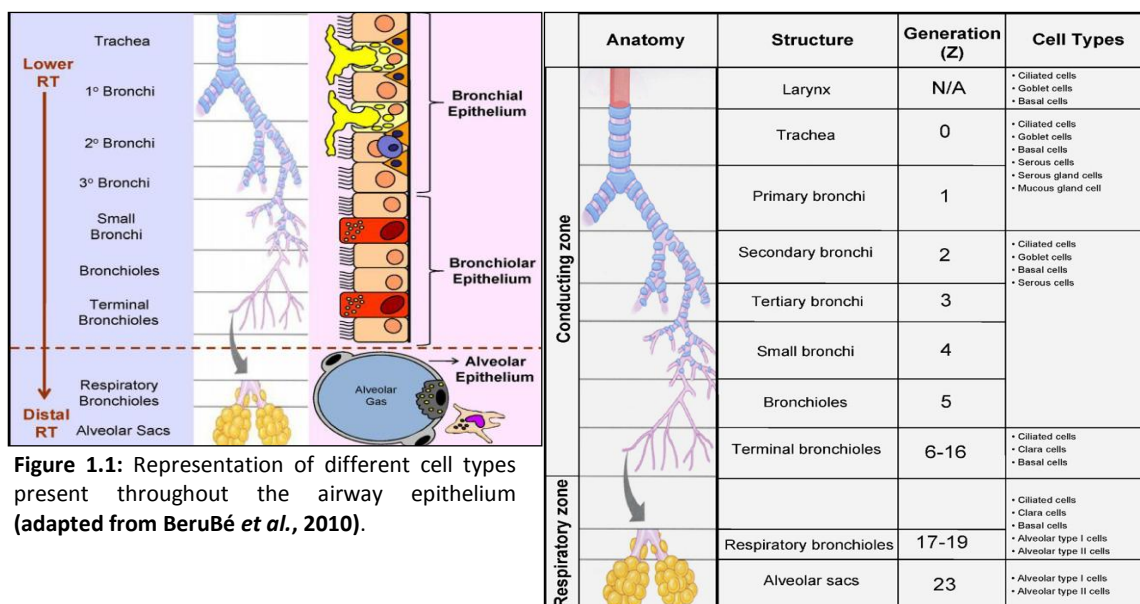


Figure 1.1: Representation of different cell types present throughout the airway epithelium (adapted from BeruBé et al., 2010).

## 1.2. THE BRONCHIAL EPITHELIUM

The bronchial epithelium is characterized by the aggregation of polyhedral epithelial cells that produce a small amount of extracellular matrix [Junqueira and Carneiro, 2008]. The characteristic shape of these cells results from their close juxtaposition in cellular layers, and is similar to what would be observed if a large number of inflated balloons were compressed into a limited space. The strong intercellular adhesion observed in these cells allows the formation of large cellular layers that cover all the body surfaces and cavities. Their protective and contractile features allow the simultaneous absorption and secretion of molecules inside and outside the organs. Additionally, in certain cases like in the olfactory epithelium, some specialized cells act as sensory cells.

The nuclei of bronchial epithelial cells are spherical, a characteristic of cuboidal cells, and their long axis are always parallel to the main axis of the cell [Junqueira and Carneiro, 2008]. The nuclei can be localized at different levels within the cell, giving the false appearance of cellular stratification [Junqueira and Carneiro, 2008]. As the lipid-rich membranes between cells are frequently indistinguishable under the light microscope, stained cells' nuclei are frequently used to infer the shape and number of cells.

Human bronchial epithelial cells (HBEC) generally show polarity, with organelles and membrane proteins distributed unevenly in different parts of the cell [Junqueira and Carneiro, 2008]. The region of the cell that faces the connective tissue is called the basal pole, whereas the opposite pole, usually facing a respiratory cavity, is the apical pole. The intervening sides apposed in neighbouring cells are called the lateral surfaces [Junqueira and Carneiro, 2008]. The membranes on the lateral surfaces of adjoining cells often have numerous infoldings to increase the contact area and these cells' functional capacity. The different regions of polarized cells may have different functions.



**Figure 1.2:** Image of bronchial epithelium, primarily columnar cells with cilia (arrows), with fewer goblet cells. The lamina propria has both smooth muscle (SM) and small serous glands (G) near cartilage (C) (adapted from Junqueira and Carneiro, 2008).

The lateral membranes of epithelial cells also exhibit several specialized intercellular junctions. These junctions can function as seals, preventing the flow of materials between the cells (occluding junctions), sites of adhesion (adhesive or anchoring junctions) or channels for communication between adjacent cells (gap junctions) (Figure 1.3).

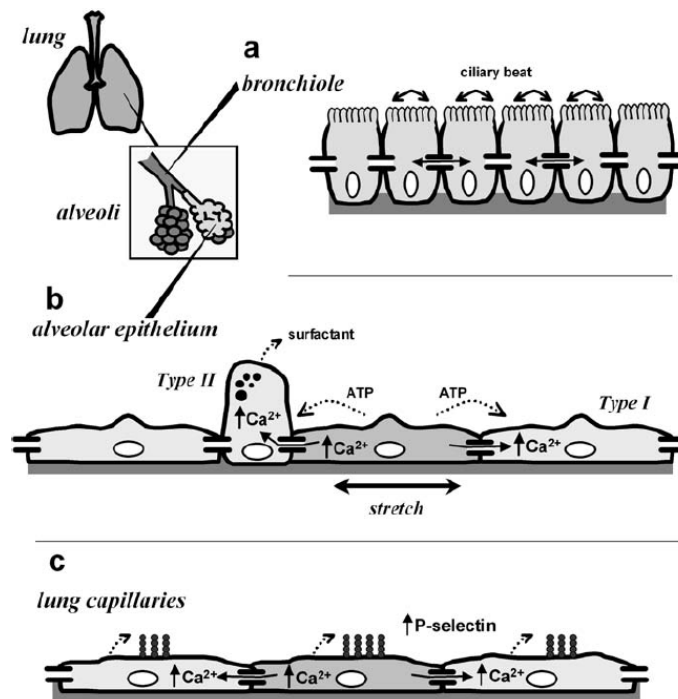


**Figure 1.3:** Intercellular communication in the lung through gap junctions (adapted from Johnson and Koval, 2009).

HBEC have elongated (5–10  $\mu\text{m}$  long and 0.2  $\mu\text{m}$  diameter), high motile cilia on their apical surface. Each cilium is bounded to the cell membrane by the basal bodies and contains at the base an axoneme with a central pair of microtubules surrounded by nine peripheral microtubule pairs [Junqueira and Carneiro, 2008]. Cilia are electron-dense structures localized at the apical pole, just below the cellular membrane, exhibiting coordinated rapid back-and-forth movements to propel a current of fluid and suspended matter in one direction over the ciliated epithelium [Junqueira and Carneiro, 2008]. This movement depends upon the hydrolysis of the adenosine triphosphate (ATP) bounded to the ciliary dynein present on the peripheral microtubule doublets of the axoneme. Each ciliated cell of the trachea is estimated to have about 250 cilia. [Junqueira and Carneiro, 2008].

The HBEC can cover up to  $2^{21}$  to  $2^{23}$  branches of the respiratory zone. However, they only cover 1% of the whole respiratory surface [BéruBé *et al.*, 2010]. These cells have an essential role in the maintenance of the respiratory capacity, being able to work as an alveolar defence against several pathogenic agents, for example, by keeping the mucosa secretion levels. Therefore, the HBEC have a critical role in respiratory disorders, such as asthma and lung cancer [Crystal, Randell, Engelhardt, *et al.*, 2008].

Because the bronchial epithelium is directly exposed to a wide range of injurious agents, HBEC are very susceptible to pro-inflammatory signals that easily modulate their function [Crystal, Randell, Engelhardt, *et al.*, 2008]. In addition, the multiplicity of microenvironments throughout the respiratory tract, by inducing different levels of cellular differentiation, renders HBEC to adopt rather diverse cellular phenotypes. For instance, HBEC able to produce secretoglobin, glycoprotein capable of cell adhesion (cluster of differentiation molecule CD34) and surfactant protein-C (SP-C) are able to proliferate easily in response to tissue wounds [Crystal, Randell, Engelhardt, *et al.*, 2008].

Bronchial epithelial cells can easily go into mitosis, although this renewal process varies accordingly to the tissue. Growth factors, such as hepatocyte growth factor (HGF), insulin growth factor-1 (IGF-1) and fibroblast growth factor-7 and 10 (FGF-7; FGF-10) [Skibinski *et al.*, 2007; Lebeche *et al.*, 1999], as well as collagen type IV [Freshney, 2002], induce HBECs' proliferation, while differentiation depend on thyroid transcription factor-1 (TTF-1), forkhead orthologs protein family (FOX) and  $\beta$ -Cadherin, following interaction with several transcript factors [Maeda, Davé, Whitsett, 2007].

Myoepithelial cells are found in the glandular epithelium as a thin layer above the basement membrane but, generally, beneath the luminal cells. In the mammary gland myoepithelial cells constitute the basal cell layer of an epithelium that harbours the epithelial progenitor/stem cells [Freshney, 2004; Ghajar and Bissell, 2008]. Easily distinguished from epithelial cells, that just express keratins, myoepithelial cells express simultaneously keratins and alpha smooth muscle actin ( $\alpha$ -SMA) [Berman, 2009]. In wound healing, myoepithelial cells reactively proliferate, and their presence in a hyperplastic tissue usually suggests absence of cancer. Only rare cancers, like adenoid cystic carcinomas, contain myoepithelial cells as one of their malignant components [Berman, 2009].

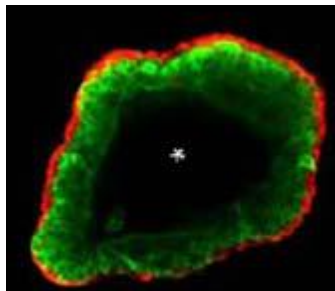


**Figure 1.4:** K8 (*green*), an epithelial marker, stains throughout mammary structures while K14 (*red*), indicative of myoepithelial cells *in vivo*, is confined to the basal surface (\* denotes lumen) (adapted from Ghajar and Bissell, 2008).

### 1.3. THE CONNECTIVE TISSUE AND THE EXTRACELLULAR MATRIX

The connective tissue has a central role in the human body because it is responsible, as its name suggests, for connecting and supporting all the other tissues of the body. Fibroblasts are a prominent component of this tissue that makes up the stromal compartment [Olumi *et al.*, 1999]. They are originated from undifferentiated mesenchymal cells and they orchestrate the crosstalk between the stroma and the epithelial cells, driving to tissue homeostasis [Junqueira and Carneiro, 2008; Olumi *et al.*, 1999].

In connective tissue are found: cells, fibers, and ground substance. Fibroblasts are prominent cells of the connective tissue that makes up the stromal compartment [Olumi *et al.*, 1999]. These cells are originated from undifferentiated mesenchymal cells and orchestrate the crosstalk between the stroma and the epithelial cells, driving to tissue homeostasis [Junqueira and Carneiro, 2008; Olumi *et al.*, 1999]. During the connective tissue' formation, fibroblasts synthesize collagen, elastin, glycosaminoglycans, proteoglycans and multiadhesive

glycoproteins, building up the ECM. Subsequently, a wide combination of protein fibers (collagen and elastic fibers) forms and creates the so called ground substance. This highly hydrophilic viscous complex of anionic substances stabilizes the ECM by binding it to receptor proteins, integrins, on the surface of cells and to the other matrix components [Junqueira and Carneiro, 2008].

In addition to its major structural role, ECM is a reservoir of factors controlling cell growth and differentiation [Junqueira and Carneiro, 2008], and the hydrophilic nature of the majority of the connective tissue provides the medium through which nutrients and metabolic wastes are exchanged between cells and their blood supply [Junqueira and Carneiro, 2008].

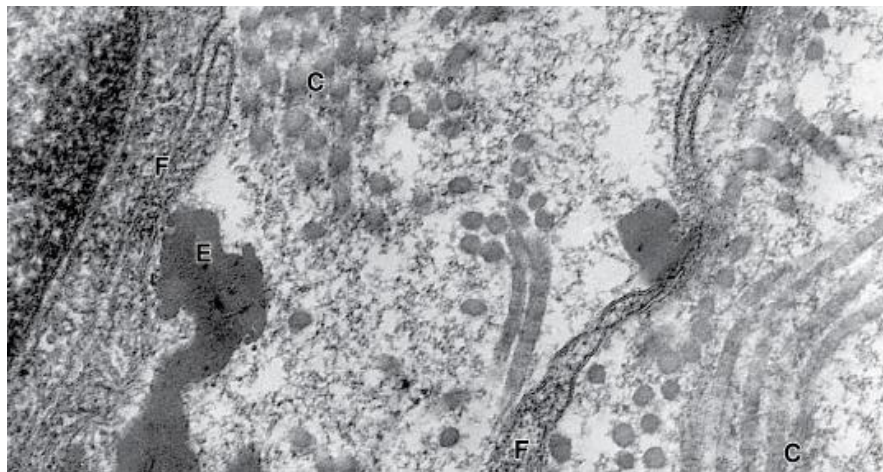


**Figure 1.5:** Electronic Microscopy image of ECM ultrastructure, showing ground substance, collagen (C); elastic fibers (E) and fibroblasts (F) (adapted from Junqueira and Carneiro, 2008).

### 1.3.1. FIBROBLASTS

Fibroblasts are important to epithelial function, particularly in the lung, more specifically in the bronchus, due to the predominance of a pseudostratified epithelial layer that is greatly dependent on a stable and rich connective tissue, being responsive to the presence of collagen,  $\beta$ -integrins and EGF for stability. Recent studies revealed that fibroblasts and epithelial cells cooperate in response to airway inflammation [Knight, 2001], and fibroblasts were also able to induce stress in lung epithelial cells *in vitro* [Bartling *et al.*, 2006].

In human adults, the connective tissue' fibroblasts rarely undergo division. Nevertheless, mitosis can resume whenever an organ requires additional fibroblasts as during the process of

wound healing [Junqueira and Carneiro, 2008]. In accordance, two stages of activity are often observed in fibroblasts: active and quiescent [Junqueira and Carneiro, 2008].

Active fibroblasts are morphologically distinct from quiescent fibroblasts that are scattered within the matrix they have already synthesized. As a consequence, some histologists reserve the term fibroblast to denote the active cell and fibrocyte to designate the quiescent fibroblast [Junqueira and Carneiro, 2008]. Active fibroblasts typically display large active nuclei and an eosinophilic cytoplasm tapering off in both directions along the axis of the nucleus, morphology usually called "spindle-shaped". In addition, these fibroblasts also have an abundant and irregularly branched cytoplasm [Junqueira and Carneiro, 2008]. Their nuclei are ovoid, large and pale-staining, with fine chromatin and a prominent nucleolus [Junqueira and Carneiro, 2008]. The cytoplasm is rich in rough endoplasmic reticulum (RER), and the Golgi apparatus is well developed [Junqueira and Carneiro, 2008]. Active fibroblasts are the targets of various growth factors that influence cell growth and differentiation, such as TGF- $\beta$ , and Vascular Endothelial Growth Factor (VEGF) [Sugiura *et al.*, 2007].

Quiescent fibroblasts are smaller than active fibroblasts. Usually spindle-shaped, they have a smaller and darker elongated nucleus and more acidophilic cytoplasm with much less RER [Junqueira and Carneiro, 2008].

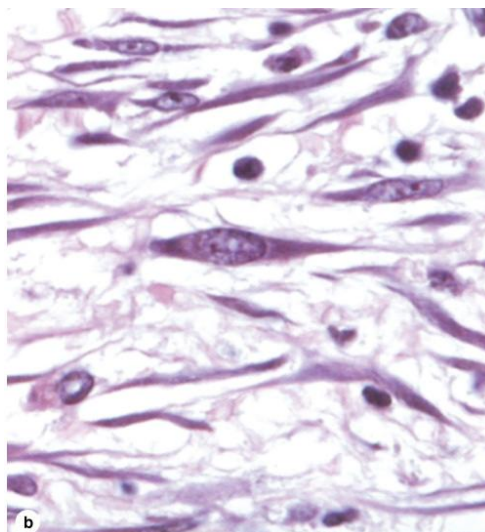


**Figure 1.6:** Image of both active and quiescent fibroblasts from the dermis (adapted from Junqueira and Carneiro, 2008).

Myofibroblasts, a specific sub-population of fibroblasts, are found sub-epithelially in many mucosal surfaces, acting as a regulator of the shape but also as stem cells niche. They can be distinguished from fibroblasts because they express, in addition to vimentin,  $\alpha$ -SMA.

Myofibroblasts have both support and paracrine functions. In wound healing they play a central role by depositing extracellular collagen fibers and wound contraction [Komuro, 1990]. They contain smooth muscle myosin isoforms in addition to  $\alpha$ -SMA, the requisite machinery for contraction and/or motility, and respond to proinflammatory cytokines by producing matrix proteins and additional growth factors [Mori *et al.*, 1992].

#### 1.4. LUNG CANCER

Although cancer has been known since the early Egypt, only in the latter 30 years it has been extensively studied [Knowles *et al.*, 2005; Weber, 2007]. According to the literature, cancer can be characterized as a complex disease occurring as a result of a progressive accumulation of genetic and epigenetic alterations that enable cells' escape from normal cellular and environmental controls [Mills, 2002]. Nowadays, cancer represents one of the trending causes of death [Knowles *et al.*, 2005; Weber, 2007].

Lung cancer (LC) is the most frequent cause of cancer deaths in both men and women in industrialized countries [Cancer Research UK, 2011]. The highest rates of lung cancer are found in Central and Eastern Europe and in northern America [Cancer Research UK, 2011]. Within the European Union (EU-27) the countries with the highest male rates are Hungary and Poland and the ones with the lowest rates are Sweden and Cyprus [Cancer Research UK, 2011]. In 2005, in the United States, the combined annual number of deaths from breast, colon and prostate cancer would not equal the death toll from lung cancer, and in 2004 more than 150,000 patients died of this disease [Spiro and Silvestri, 2005]. The lowest lung cancer rates are found in Middle African countries [Panno, 2005].

**Table 1.1:** Resume of new cases and deaths for different types of cancer in the United States of America in 2003 (adapted from Panno, 2005).

NEW CANCER CASES AND DEATHS FOR 2003			
Cancer	New Cases	Deaths	Mortality (%)
Bladder	57,400	12,500	22
Brain	18,300	13,100	72
Breast	212,600	40,200	19
Digestive tract	204,400	89,200	44
Leukemia	30,600	21,900	72
Lymphoma	61,000	24,700	41
Liver	17,300	14,400	83
Lung	185,800	163,700	88
Mouth and throat	27,700	7,200	26
Pancreas	30,700	30,000	98
Prostate	220,900	28,900	13
Skin (melanoma)	54,200	7,600	14

Data is for the United States and was compiled from information provided by the American Cancer Society. Mortality is the number of deaths divided by new cases times 100. The values are rounded off to the nearest percentage point.

Several environmental and industrial carcinogens like tobacco smoke, nickel, arsenic, chromium and polycyclic hydrocarbons have been accepted as major causes of LC [Coppé *et al.*, 2008a; Salnikow and Zhitkovich, 2008; Urbano *et al.*, 2008]. Non-ferrous metal production industry as well as painting and leather industries have been considered of high-risk to LC development. There is also evidence that heavy occupational exposure to diesel exhaust increases LC risk and the large American prospective Agricultural Health Study Exposure suggests that exposure to herbicides and insecticides also increases LC risk [Ruddon, 2007]. Occupational exposures to silica can result in silicosis, which represents an increased risk for LC [Cancer Research UK, 2011]. Finally, evidence supports an increased risk of LC development following exposures to asbestos in non-smokers as well as for recent smokers who also have previously worked with that material [Cancer Research UK, 2011].

LC susceptibility and risk are also increased in inherited cancer syndromes caused by rare germ-line mutations in *Tp53*, retinoblastoma (*RB*) and the epidermal growth factor receptor (*EGFR*) gene [Herbst, Heymach and Lippman, 2008]. More recently, three large genome wide association studies identified an association between single-nucleotide polymorphism (SNP) variation at 15q24–15q25.1 and a higher susceptibility to LC development [Herbst, Heymach and Lippman, 2008]. This newly identified LC-associated SNP variation region includes two genes encoding subunits of the nicotinic acetylcholine receptor alpha, which is regulated by nicotine exposure [Herbst, Heymach and Lippman, 2008].

DNA repair capacity is also very important in what regards LC development. In agreement, germ-line alterations in nucleotide excision repair system genes, like *ERCC1*, increase LC susceptibility and risk **[Herbst, Heymach and Lippman, 2008]**. This scenario is worsened when accompanied by exposure to tobacco smoke **[Herbst, Heymach and Lippman, 2008]**. Increased expression of DNA synthesis and repair genes, including *RRM1* (the regulatory subunit of ribonucleotide reductase) and *ERCC1*, in non-small-cell LC correlates with a better overall prognosis but no benefit from platinum-based chemotherapy **[Herbst, Heymach and Lippman, 2008]**.

Commonly documented LCs have an epithelial origin and, as a consequence, are classified as carcinomas **[Panno, 2005]**. Carcinomas are generally divided into two major types: small cell lung cancer (SCLC), which accounts for about 25% of all lung tumours, and non-small cell lung cancer (NSCLC), that accounts for about 75% of the total LCs **[Freshney, 2004]**. NSCLC can additionally be sub-divided in three major histological types: squamous carcinoma, adenocarcinoma, and large cell carcinoma **[Freshney, 2004]**.

SCLC typically disseminates widely and is seldom cured by surgical resection, whereas NSCLC may be cured by surgery if diagnosed at early stages **[Freshney, 2004]**. In addition, SCLC tumours have a better initial response to cytotoxic therapies than do NSCLC.

**Table 1.2:** Genetic abnormalities related to non-small-cell lung cancer and small-cell lung cancer (**adapted from Herbst, Heymach and Lippman, 2008**). Non-small-cell lung cancer includes squamous-cell carcinoma and adenocarcinoma. Neuroendocrine fields have been detected only in tissue surrounding tumors and have been characterized by extremely high rates of allelic loss and by c-MET overexpression (Salgia R: personal communication). Variations are based in part on smoking profiles. The percentages include increased gene copy numbers from amplification or polysomy and represent percentages from resected cancers. The percentages are higher in primary tumors from patients with metastatic disease. Increased copy numbers have been reported in squamous dysplastic lesions but not in adenocarcinoma precursors. Genomic *EGFR* variant III mutations have been detected only in lung squamous-cell carcinoma, and these tumors are sensitive preclinically to irreversible EGFR tyrosine kinase inhibitors. The incidence of 5% is substantially lower than that of 30 to 40% for the detection in squamous-cell carcinoma or adenocarcinoma by immunohistochemical analysis or other techniques. The anaplastic lymphoma kinase (*ALK*) fusion gene (involving chromosome 2p), consisting of parts of *EML4* and *ALK*, is transforming in fibroblasts and occurs in adenocarcinoma but not in other types of non-small-cell lung cancer or other non-lung cancers.

Abnormality	Non-Small-Cell Lung Cancer		Small-Cell Lung Cancer
	Squamous-Cell Carcinoma	Adenocarcinoma	
<b>Precursor</b>			
Lesion	Known (dysplasia)	Probable (atypical adenomatous hyperplasia)	Possible (neuroendocrine field) <sup>†</sup>
Genetic change	<i>p53</i> mutation	<i>KRAS</i> mutation (atypical adenomatous hyperplasia in smokers), <i>EGFR</i> kinase domain mutation (in nonsmokers)	Overexpression of c-MET
<b>Cancer</b>			
<i>KRAS</i> mutation	Very rare	10 to 30% <sup>‡</sup>	Very rare
<i>BRAF</i> mutation	3%	2%	Very rare
<b><i>EGFR</i></b>			
Kinase domain mutation	Very rare	10 to 40% <sup>‡</sup>	Very rare
Amplification <sup>§</sup>	30%	15%	Very rare
Variant III mutation	5% <sup>¶</sup>	Very rare	Very rare
<b><i>HER2</i></b>			
Kinase domain mutation	Very rare	4%	Very rare
Amplification	2%	6%	Not known
<i>ALK</i> fusion <sup>  </sup>	Very rare	7%	Not known
<b><i>MET</i></b>			
Mutation	12%	14%	13%
Amplification	21%	20%	Not known
<i>TTF-1</i> amplification	15%	15%	Very rare
<i>p53</i> mutation	60 to 70%	50 to 70% <sup>‡</sup>	75%
<i>LKB1</i> mutation	19%	34%	Very rare
<b><i>PIK3CA</i></b>			
Mutation	2%	2%	Very rare
Amplification	33%	6%	4%

### 1.4.1. GENOMIC HALLMARKS OF LUNG CARCINOMAS

The first phase of carcinomas' development, and as a consequence, of lung epithelium malignant transformation, is dysplasia. Dysplasia is characterized by a disordered growth of cells in a tissue or organ, accompanied by cell differentiation [Panno, 2005; Schulz, 2005]. *EGFR* amplification is commonly associated with this process, particularly in higher grades dysplasias, and is a renowned lung-cancer risk factor when detected in the sputum of smokers

[Herbst, Heymach and Lippman, 2008]. Gain of function of this receptor leads to the activation of several signalling pathways, such as the Ras–Raf–Mek, responsible for the growth of cancer cells and tumour progression (Figure 1.7).

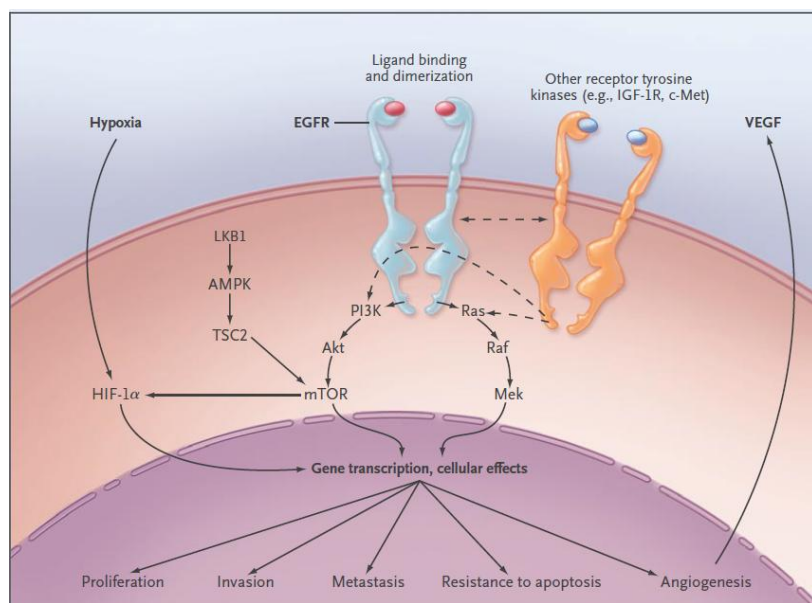


**Figure 1.7:** Some EGFR-dependent signaling Pathways. EGFR activates several major downstream signaling pathways, including Ras–Raf–Mek and the pathway consisting of phosphoinositide 3-kinase (PI3K), Akt, and mammalian target of rapamycin (mTOR), which in turn may have an effect on proliferation, survival, invasiveness, metastatic spread, and tumor angiogenesis through pathways that are either dependent on or independent of the hypoxia inducible factor (HIF). These pathways also may be modulated by other receptor tyrosine kinases, such as insulin-like growth factor 1 receptor (IGF-1R) and cMET, and by the LKB1–amp-activated protein kinase (AMPK) pathway, which is involved in energy sensing and cellular stress. Most of these functions depend on signaling through the kinase domain. However, kinase-independent functions, such as maintaining glucose transport, have been reported. TSC2 denotes tuberous sclerosis complex 2, and VEGF vascular endothelial growth factor (**adapted from Herbst, Heymach and Lippman, 2008**).

Activating *KRAS* mutations are limited to NSCLC (predominantly adenocarcinomas), and mutually exclusive to mutations in the *EGFR* and *HER2* kinase. They are associated with an increased resistance to EGFR inhibitors (tyrosine kinase inhibitors and cetuximab). *KRAS* mutations are chiefly smoking-related G→T transversions affecting the exon 12 (in 90% of patients) or exon 13 of the *KRAS* gene. A distinct *KRAS* mutational profile consisting of G→A transition mutations was recently detected in patients with adenocarcinoma who had never smoked [Herbst, Heymach and Lippman, 2008]. Nevertheless, its functional significance is unclear. *KRAS* mutations appear to be an early event (e.g., detectable in the pre-invasive lesions of atypical adenomatous hyperplasia and bronchoalveolar carcinoma) that precedes smoking-related lung adenocarcinoma. They are generally correlated with poor prognosis [Herbst, Heymach and Lippman, 2008]. Further evidence supporting this gene’s role in the pathogenesis of LC comes from transgenic mice that bear a mutated *KRAS*. These mice

developed multifocal atypical adenomatous hyperplasia and adenocarcinoma with early *MET* gene activation following KRAS-induced carcinogenesis [Herbst, Heymach and Lippman, 2008].

*BRAF* mutations have also been detected in NSCLC and may be an early event in lung tumourigenesis [Herbst, Heymach and Lippman, 2008]. Additionally, transversions (smokers) and transitions (non-smokers) also have been reported for the *Tp53* gene in lung adenocarcinoma [Herbst, Heymach and Lippman, 2008].

A recent SNP array screening in human lung adenocarcinoma samples identified a wide range of genomic amplifications, namely in regions containing the *KRAS*, *MYC*, *VEGF* genes and several cell-cycle-associated genes [Weir, 2007]. Nevertheless, the most common focal event in this high-resolution analysis was an amplification of the *TITF1* (also called *NKX2-1*) gene at the 14q13.3 chromosomal region 14q13.3. *TITF1* encodes a lineage-specific transcription factor that is essential for the formation of the cells lining the lung alveoli (type II pneumocytes). *In vitro*, transfection of immortalized normal human lung epithelial cells with at least two of the three genes (*TITF1*, *NKX2-8*, and *PAX-9*) in the 14q13.3 region caused increased growth potential of the cells, suggesting that these three genes may work cooperatively in the pathogenesis of LC [Herbst, Heymach and Lippman, 2008]. Recent data indicate that squamous-cell carcinoma also exhibits *TITF1* amplification, as detected by fluorescence *in situ* hybridization (FISH). Yet, in contrast with adenocarcinoma, *TITF1* protein levels are kept untouched [Herbst, Heymach and Lippman, 2008].

In its struggle to survive in the absence of nutrients and in the presence of accumulated metabolic by-products, tumours build up a new tumour-associated microvessel network following a process called angiogenic switch [Schulz, 2005]. VEGF is the main orchestrator of this process, as the increase in its levels, in pre-malignant bronchial epithelial cells, induces the progression from low grade to high grade bronchial dysplasia [Herbst, Heymach and Lippman, 2008].

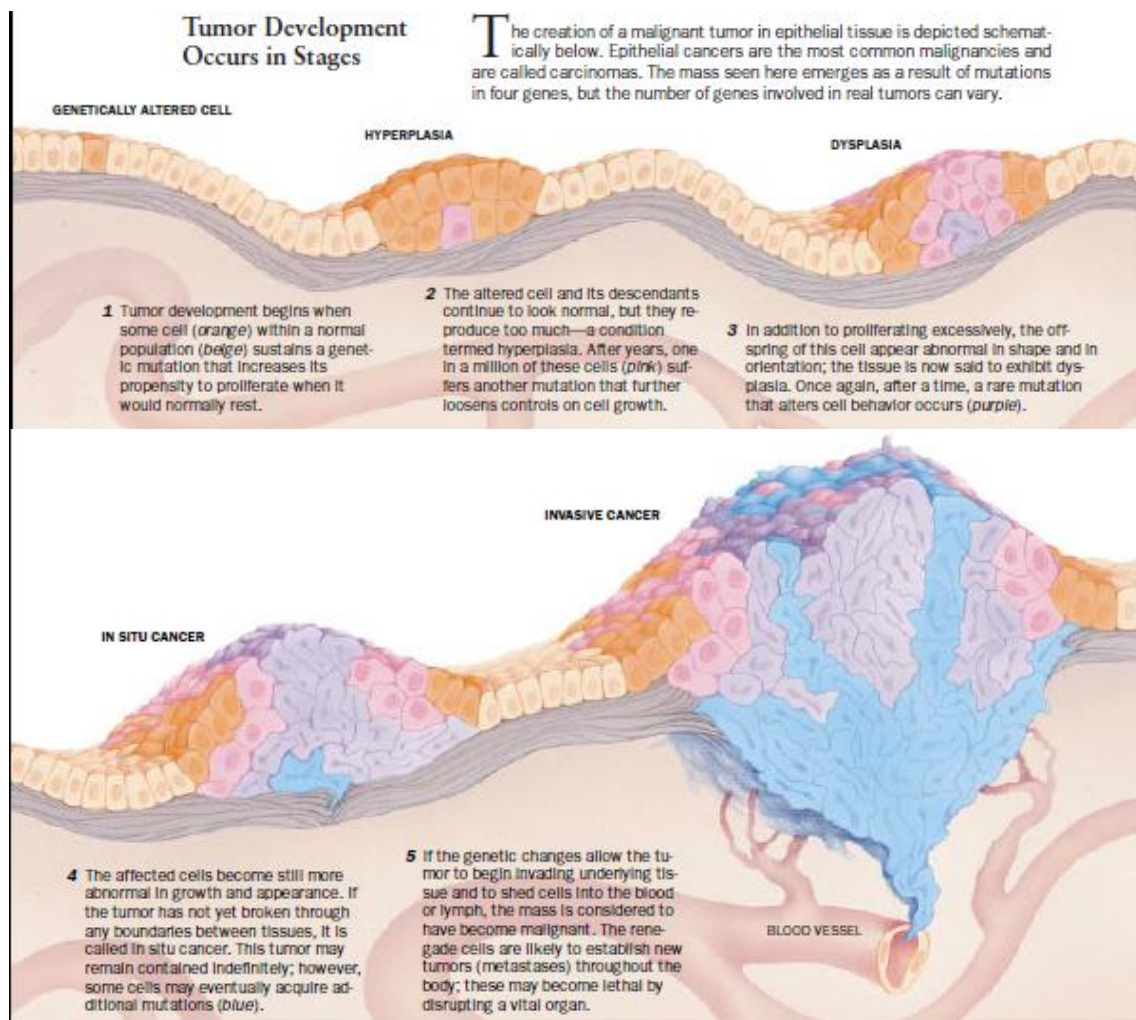


**Figure 1.8:** Representation of the tumor development from a genetically altered cell to hyperplasia, dysplasia, in situ cancer (this case carcinoma) and invasive cancer (adapted from Weinberg, 1996).

During the subsequent steps of malignant progression, namely hyperplasia, metaplasia, and carcinoma *in situ* (Figure 1.8), the intense angiogenic activity continues, allowing a correlation between the factors associated with increased tumour angiogenesis, namely VEGF, and the LC development to be established. As a consequence, circulating VEGF levels are used to predict the clinical benefit of using VEGF inhibitors in LC patients [Herbst, Heymach and Lippman, 2008]. Whenever positive results are expected, the VEGF monoclonal antibody bevacizumab is used in combination with standard chemotherapy to block angiogenesis and reduce the growing ability of NSCLC [Herbst, Heymach and Lippman, 2008].

The PI3K/Akt and the mTOR, pathways (Figure 1.7) are also activated during early in lung carcinogenesis, even though *Akt* overexpression starts during bronchial dysplasia [Herbst, Heymach and Lippman, 2008]. Mutations or amplifications of *PIK3CA*, which encodes the PI3K catalytic subunit, are frequently found in a subgroup of NSCLC, especially the squamous-cell

carcinoma, and associate with increased PI3K activity and *Akt* expression [Herbst, Heymach and Lippman, 2008]. Inhibition of Akt was reported to induce apoptosis of human pre-malignant and malignant lung cells and to prevent lung carcinogenesis in an animal model [Herbst, Heymach and Lippman, 2008]. mTOR inhibitors also blocked malignant progression of atypical adenomatous hyperplasia lesions in the *KRAS* mouse model [Herbst, Heymach and Lippman, 2008]. Since mTOR drives tumorigenesis in part through macrophages, the anti-tumour effect of mTOR inhibition is mainly directed to the tumour microenvironment [Herbst, Heymach and Lippman, 2008].

#### 1.4.2. THE INVASIVE PROPERTIES OF CARCINOMA CELLS

As to the mechanisms underlying LC invasion and metastasis, they are largely an enigma. It is clear that, as carcinomas arising from epithelial tissues progressed to higher pathological grades of malignancy with local invasion and distant metastasis establishment, the associated cancer cells typically develop morphological changes and alter their attachment to neighbour cells and to the ECM [Parrinello *et al.*, 2005; Hu and Polyak, 2008]. In the process of dissemination, the best characterized alteration is the loss, by the tumour epithelial cells, of E-Cadherin, a key cell-to-cell adhesion molecule [Hanahan and Weinberg, 2011]. By forming adherent junctions in adjacent epithelial cells, E-Cadherin helps to assemble epithelial cell sheets and to maintain the proliferation arrest of the cells within these sheets, avoiding unregulated epithelial proliferation and hyperplasia. Increased expression of E-Cadherin is a well-established antagonist of invasion and metastasis, whereas the reduction of its expression is known to potentiate invasive and metastatic phenotypes [Hanahan and Weinberg, 2011]. The frequently observed down-regulation and occasional mutational inactivation of E-Cadherin in human carcinomas provided strong support for its role as a tumor suppressor [Hanahan and Weinberg, 2011].

A developmental regulatory program, referred to as the “epithelial-mesenchymal transition” (EMT), has become prominently implicated as a means by which transformed epithelial cells can acquire the ability to invade, to resist apoptosis and to disseminate [Hanahan and Weinberg, 2011]. By co-opting a process involved in various steps of embryonic morphogenesis and wound healing, carcinoma cells can concomitantly acquire multiple attributes that enable invasion and metastasis. This multifaceted EMT program can be

activated transiently or stably, and to differing degrees, by carcinoma cells during the course of invasion and metastasis [Hanahan and Weinberg, 2011].

A set of pleiotropic transcriptional factors, including Snail, Slug, Twist, and Zeb1/2, mostly identified by developmental genetics, orchestrate the EMT and EMT-related migratory processes during embryogenesis [Hanahan and Weinberg, 2011]. These transcriptional regulators are expressed in various combinations in a number of malignant tumour types, and have been shown in experimental models of carcinoma to be determinant for programming invasion and to elicit metastasis when ectopically overexpressed [Hanahan and Weinberg, 2011]. Such transcription factors have been associated with the loss of adherent junctions [Hanahan and Weinberg, 2011], the conversion from a polygonal/epithelial to a spindly/fibroblastic morphology [Hanahan and Weinberg, 2011], the expression of matrix-degrading enzymes [Hanahan and Weinberg, 2011], an increased motility and a heightened resistance to apoptosis [Hanahan and Weinberg, 2011], all traits implicated in the processes of invasion and metastasis. Several of these transcription factors can directly repress E-Cadherin gene expression, thereby depriving neoplastic epithelial cells of this key suppressor of motility and invasiveness [Hanahan and Weinberg, 2011].

An important factor during invasion and metastasis is the VEGF. The *VEGF-A* gene encodes ligands involved in orchestrating new blood vessel growth during embryonic and postnatal development, in homeostatic survival of endothelial cells and in physiological and pathological situations in the adult. VEGF signaling via three receptor tyrosine kinases (VEGFR-1–3) is regulated at multiple levels, reflecting this complexity of purpose. Thus, *VEGF* gene expression can be upregulated both by hypoxia and by oncogene signaling [Hanahan and Weinberg, 2011], favouring tumour growth and dissemination. In addition, VEGF ligands can also be sequestered in the extracellular matrix in latent forms that are subject to release and activation by extracellular matrix-degrading proteases (e.g., MMP-9) [Hanahan and Weinberg, 2011]. Other pro-angiogenic signals, such as members of the fibroblast growth factor (FGF) family, have been implicated in sustaining tumour angiogenesis when their expression is chronically up-regulated [Hanahan and Weinberg, 2011]. Thrombospondin 1 (TSP-1), a key counterbalance in the angiogenic switch, also binds transmembrane receptors displayed by endothelial cells and thereby evokes suppressive signals that can counteract pro-angiogenic stimuli [Hanahan and Weinberg, 2011].

At the epithelium level, the formation of tumours requires loss of growth control, unlimited proliferation ability, resistance to apoptosis and finally, angiogenic ability to

potentiate the formation of metastasis [Krtolica and Campisi, 2002; Bissell *et al.*, 2003]. In addition, malignant cells have to undergo changes in the expression of organizational proteins such as  $\beta$ 1-integrins and/or  $\beta$ 3-integrins [Bissell *et al.*, 2003; Kenny and Bissell, 2003; Ghajar and Bissell, 2008], dystroglycan [Bissell *et al.*, 2003; Kenny and Bissell, 2003; Ghajar and Bissell, 2008], TGF- $\beta$  [Bissell *et al.*, 2003; Ghajar and Bissell, 2008] and the IL-6 or IL-8 cytokines [Skibinski *et al.*, 2007; Ghajar and Bissell, 2008]. The expression of the EGF receptors (EGFR) is also frequently found up-regulated which, by triggering an EGF-mediated intracellular signal pathways response, allows tumour development [Bissell *et al.*, 2003; Kenny and Bissell, 2003; Bissell *et al.*, 2005]. Finally, loss of function of tumour-suppressor genes such as *Rb*, the breast-cancer susceptibility proteins 1 and 2 (BRCA1 e BRCA2) and the cell-cycle checkpoint protein 2 homologous (CHK2), have been proved to contribute to the morphology changes associated with deregulated cell proliferation [Bissell *et al.*, 2005].

During the invasion process, the ECM also suffers a tremendous remodelling, mainly driven by its fibroblasts. Those fibroblasts are no longer normal; instead, during the malignization process of the epithelial cells, they underwent series of phenotypic and genomic alterations that transformed them and committed them to the tumour [Olumi *et al.*, 1999]. These newly designated carcinoma-associated-fibroblasts (CAFs) have an abnormal migratory behaviour *in vitro* and an altered expression of growth factors such as platelet-derived growth factor, IGF-I and -II, TGF- $\beta$ 1, HGF/epithelial scatter factor, and keratinocyte growth factor [Olumi *et al.*, 1999]. Nevertheless, although these phenotypic changes have been documented in CAFs, their impact on tumour growth and development has not yet been investigated [Olumi *et al.*, 1999].

### 1.4.3 METABOLIC REPROGRAMMING OF CARCINOMA CELLS

The existence of a metabolic switch in cancer cells has been proposed for decades [Hsu and Sabatini, 2008; Hanahan and Weinberg, 2011]]. Such reprogramming of energy metabolism is seemingly counterintuitive, as cancer cells must compensate for the 18-fold lower efficiency of ATP production afforded by glycolysis relative to mitochondrial oxidative phosphorylation. It is accomplished, in part, by up-regulating glucose transporters (GLUT), notably GLUT1, which substantially increases glucose cellular uptake [Hanahan and Weinberg, 2011]. Indeed, markedly increased uptake and utilization of glucose have been documented in

many human tumour types, using positron emission tomography (PET) with a radiolabelled analogue of glucose ( $^{18}\text{F}$ -fluorodeoxyglucose, FDG) as a reporter [Hanahan and Weinberg, 2011]. Glycolytic fuelling has been shown to be associated with activated oncogenes (e.g., *RAS*, *MYC*) and mutant tumour suppressors (e.g., *TP53*), whose changes in tumour cells have been selected, primarily, for their benefits in conferring the hallmark capabilities of cells' proliferation, avoidance of cytostatic controls, and attenuation of apoptosis. This reliance on glycolysis can be further accentuated under the hypoxic conditions that operate within many tumours. In fact, the hypoxia response system acts pleiotropically to up-regulate glucose transporters and multiple enzymes of the glycolytic pathway. Thus, both the Ras oncoprotein and hypoxia can independently increase the levels of the hypoxia-induced factor (HIF), HIF1 $\alpha$  and HIF2 $\alpha$ , which in turn up-regulate glycolysis [Hanahan and Weinberg, 2011].

Activating (gain-of-function) mutations in the isocitrate dehydrogenase 1/2 (*IDH*) enzymes genes have been reported in glioma and other human tumours [Hanahan and Weinberg, 2011]. Cells with these mutations were possibly clonally selected for their ability to alter energy metabolism, as data associates IDH activity with elevated stability of the HIF-1 transcription factors which in turn affects genome stability and angiogenesis/invasion, blurring the lines of phenotypic demarcation [Hanahan and Weinberg, 2011]. As a consequence, the designation of reprogrammed energy metabolism as an emerging hallmark seems most appropriate to highlight both its evident importance and the unresolved issues surrounding its functional independence from the core hallmarks [Hanahan and Weinberg, 2011].

## 1.5. MICROENVIRONMENT AND CANCER

Cellular microenvironment is, by definition, the cell-surrounding medium, constituted by a diversity of molecules secreted by the neighbouring cells and by cells, namely the fibroblasts that form the ECM [Bissell *et al.*, 2005; Hu and Polyak, 2008]. Though there is little doubt that multiple genetic alterations are necessary for epithelial cells malignant transformation to take place, several lines of evidence suggest that the progress towards full malignancy, of cells that bear potentially oncogenic mutations, requires a permissive tissue microenvironment [Wright and Shay, 2002; Bissell *et al.*, 2005; Parrinello *et al.*, 2005; Hu and Polyak].

As focused earlier, fibroblasts are known to be part of the connective tissue, with supportive and feeder function towards the epithelial cell layer. Fibroblasts have the ability to secrete various ECM components namely collagen type IV, dystroglycan and EGF, as well as metalloproteinases (MMPs) and cytokines, contributing to the homeostasis of the cells [Junqueira and Carneiro, 2008; Krtolica and Campisi, 2002; Parrinello *et al.*, 2005]. Mutational events and the existence of genetic polymorphisms on fibroblasts can induce gene function gain or loss and consequently changes in protein expression [Bissell *et al.*, 2005].

For the formation of tumours, there is a great contribution from the stimuli resulting from the ECM [Krtolica and Campisi, 2002; Bissell *et al.*, 2003; Ghajar and Bissell, 2008]. It is increasingly apparent that crosstalk between cancer cells and cells of the neoplastic stroma is involved in the acquired capability for invasive growth and metastasis. Such signalling may impinge on carcinoma cells and act to alter their hallmark capabilities. For example, mesenchymal stem cells (MSCs) present in the tumour stroma have been found to secrete Chemokine (C-C motif) ligand 5 (CCL5), also known as RANTES, in response to signals released by cancer cells; CCL5 then acts reciprocally on the cancer cells to stimulate invasive behaviour [Hanahan and Weinberg, 2011]. Published results revealed that in epithelial cells, particularly in breast tissue, there is an increased cell polarization due to changes in the microenvironment induced by fibroblasts [Ghajar and Bissell, 2008].

It has been shown that the histological appearance of the epithelial cells can vary according to the type of cells that surround them [Olumi *et al.*, 1999]. In a prostate carcinoma study, it has been observed that epithelial cells combined with CAFs formed an epithelial ductal structure lined with an abnormal stratified squamous epithelium, poorly differentiated. In contrast epithelial cells in the presence of normal fibroblasts formed ductal structures lined by tall columnar epithelial cells that expressed prostate-specific antigen (Figure 1.9) [Olumi *et al.*, 1999].

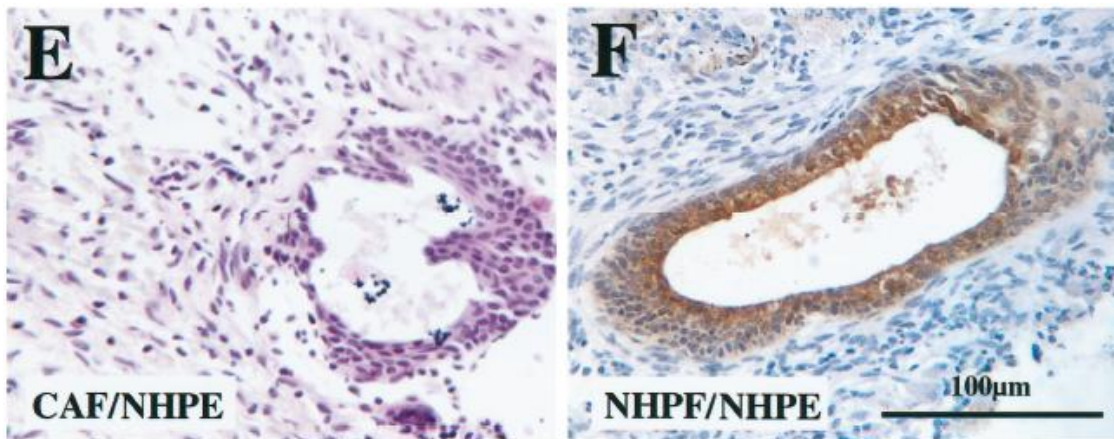


**Figure 1.9:** Histological images of tissue recombinants of Carcinoma-Associated Fibroblasts (CAF) in a human prostate Epithelium (E); Normal Human Prostate Fibroblasts (NHPF) in a normal in a human prostate Epithelium (F) (adapted from Olumi *et al.*, 1999).

Aging can give way to accumulation of genetic mutations and/or unfavourable conditions for cells, prone to the stage of senescence [Wright and Shay, 2002]. These changes, both on fibroblasts and epithelial cells, render cells vulnerable to changes in the microenvironment [Hu and Polyak, 2008]. However, phenotypic changes on epithelium require less mutations than on fibroblasts to occur [Krtolica and Campisi, 2002; Parrinello *et al.*, 2005].

## 1.6. SENESCENCE

Senescence frequently appears as a strategy organisms develop to expand their lifespan by inhibiting several death causes, namely in cancer [Campisi, 2005]. However, the fact that aging favours the emergence of carcinomas leads to the hypothesis that traits selected to maintain early life fitness can have unselected deleterious effects late in life, a phenomenon termed antagonistic pleiotropy [Krtolica *et al.*, 2001; Krtolica and Campisi, 2002; Campisi, 2005].

Cellular senescence is the ultimate and irreversible loss of replicative capacity and, consequently, although growth arrested cells maintain their viability [Krtolica *et al.*, 2001; Krtolica and Campisi, 2002; Wright and Shay, 2002; Cooper and Haussman, 2009]. At the cellular level cellular senescence is characterized by an arrest in G1 cell-cycle phase, altered gene expression, resistance to apoptosis and changes in the cellular differentiation status [Goodwin *et al.*, 2000; Krtolica and Campisi, 2002; Wright and Shay, 2002]. Mechanistically,

cellular senescence is related to shortening of telomeres, which are repetitive sequences of DNA at the chromosomal ends. Telomere functions comprehend the protection of chromosomes' wealthy regions on genetic information, the maintenance of chromosomes integrity, avoiding chromosomal fusion and maintenance of DNA replication ability [Lodish *et al.*, 2004]. Immediately after cellular differentiation, there is loss of telomerase activity, which results in telomere shortening and increased probability of DNA loss at sub-terminal level [Krtolica *et al.*, 2001; Krtolica and Campisi, 2002; Wright and Shay, 2002; Campisi, 2005].

Another type of senescence is the stress-induced senescence and has nothing to do with telomeres shortening. This process is triggered in still healthy young cells by external agents that induce DNA damage, reactive oxygen species (ROS) or gain of function of oncogenes or loss of tumor suppressor genes, [Coppé *et al.*, 2008a; Campisi, 2005]. In the specific case of cancer, it can also be triggered by other forms of intracellular deregulation that can affect mitosis control [Krtolica *et al.*, 2001; Krtolica and Campisi, 2002; Wright and Shay, 2002; Campisi, 2005].

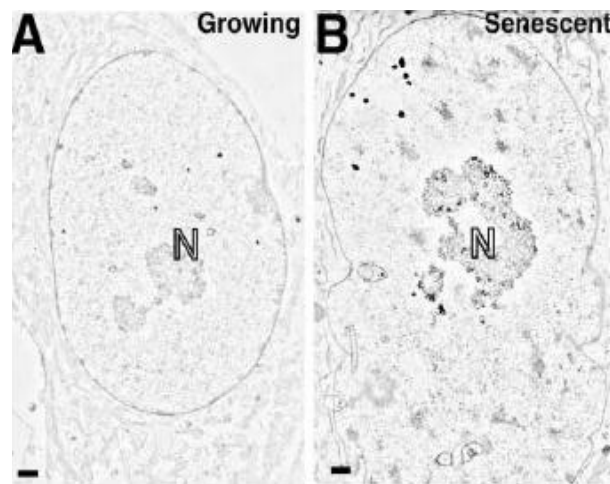


**Figure 1.10:** Morphologic images of normal fibroblasts (A) and senescent fibroblasts (B) (adapted from Narita *et al.*, 2003).

There are different senescence sub-phenotypes depending on the cell type [Krtolica and Campisi, 2002; Parrinello *et al.*, 2005]. The senescence-associated phenotypic changes in fibroblasts derive from a series of molecular events at cellular level that can be used as markers. In fibroblasts, senescence is associated with an increased neutral  $\beta$ -galactosidase activity (SA- $\beta$ gal), although SA- $\beta$ gal involvement in tumour onset and progression remains unknown [Dimri *et al.*, 1995; Krtolica and Campisi, 2002; Parrinello *et al.*, 2005]. Senescent fibroblasts are also characterized by the emergence of unique structures on their heterochromatin, named as senescent-associated heterochromatic foci [Narita *et al.*, 2003], as

well as an increased secretion of factors as EGF [Krtolica and Campisi, 2002; Parrinello *et al.*, 2005], heregulin [Krtolica and Campisi, 2002; Parrinello *et al.*, 2005] or HGF [Coppé *et al.*, 2008b]. These changes, capable of triggering proliferative responses on other cell types, are TGF- $\beta$ -dependent, even though TGF- $\beta$  expression can vary from phenotype to phenotype [Bissell *et al.*, 2005; Littlepage *et al.*, 2005; Parrinello *et al.*, 2005; Skibinski *et al.*, 2007; Hu and Polyak, 2008]. It has been reported that up to 40 different factors present increased secretion in senescent fibroblasts [Laberge *et al.*, 2011]. Morphologically senescent fibroblasts are larger and more planar-like (Figure 1.10) [Krtolica and Campisi, 2002].

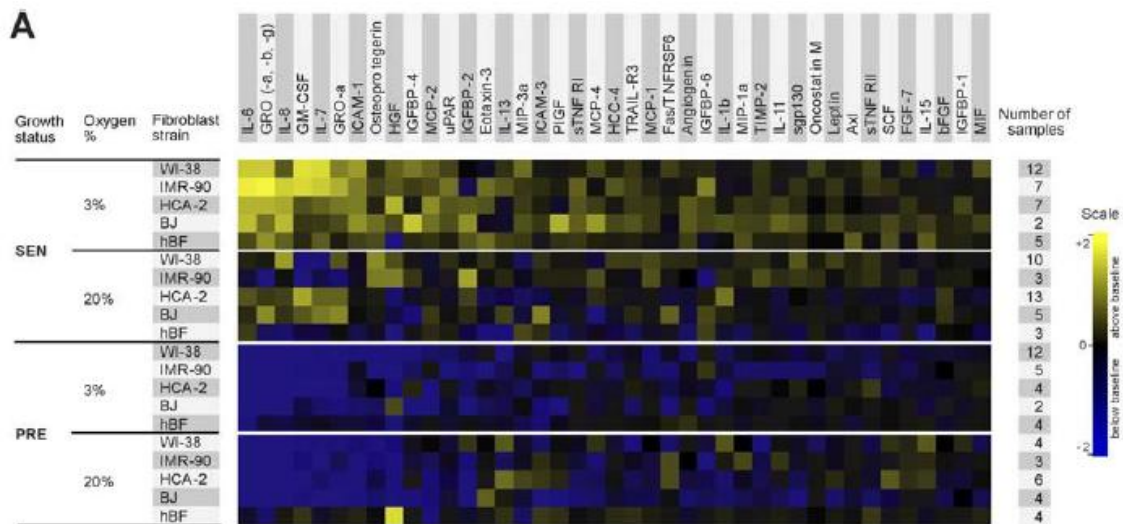


Figure 1.11: Soluble factors secreted by different strains of fibroblasts, both senescent and presenescent (adapted from Coppé *et al.*, 2008b).

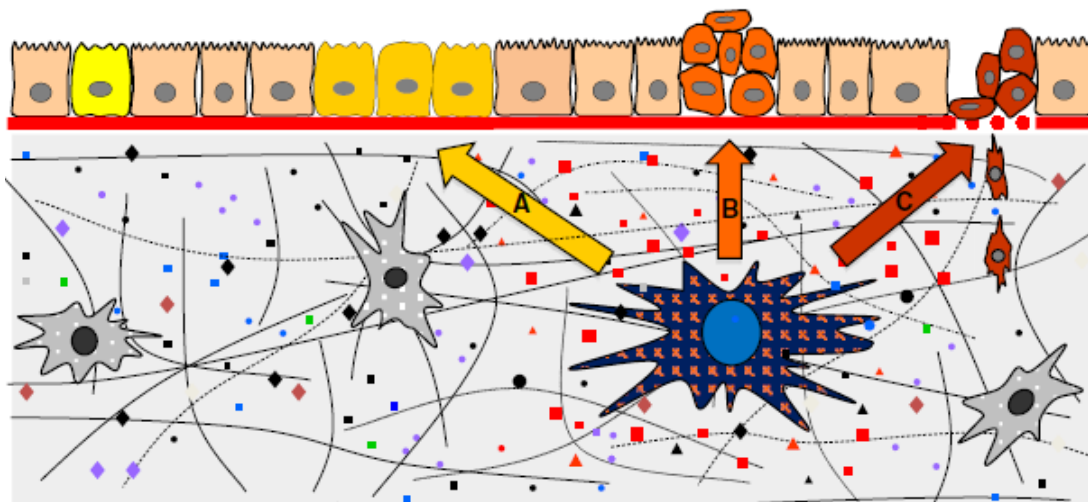


Figure 1.12: Senescent fibroblast (blue nucleus) in the stroma secretes various factors that stimulate pre-neoplastic epithelial cells (yellow cells) to proliferate (A). Further, the SASP stimulates transformed cells to undergo an EMT (orange cells). (B) Finally, the SASP promotes the invasion of mesenchymal-like cells (red cells) through the surrounding stroma (C) (adapted from Laberge *et al.*, 2011).

Recently, senescent fibroblasts were demonstrated to induce proliferation of epithelial cells with pre-malignant and malignant mutations without, however, affecting the proliferation of normal cells [Krtolica *et al.*, 2001]. The increase on cells' proliferation was achieved either by direct contact with senescent fibroblasts or indirectly by factors secreted by fibroblasts [Krtolica *et al.*, 2001; Krtolica and Campisi, 2002; Coppé *et al.*, 2008a; Hu and Polyak, 2008]. In mice, senescent fibroblasts, much more than pre-senescent fibroblasts were reported to induce pre-malignant and malignant epithelial cells to form tumours [Krtolica and Campisi, 2002]. This result evidenced what is considered evolutionary antagonistic pleiotropy because cellular senescence suppresses tumourigenesis early in life and promotes cancer in aged organisms [Krtolica *et al.*, 2001].

Senescent fibroblasts secrete certain metalloproteinases [Krtolica and Campisi, 2002; Bissell *et al.*, 2005; Parrinello *et al.*, 2005], as collagenase I (MMP1), collagenase III (MMP3) [Krtolica and Campisi, 2002; Parrinello *et al.*, 2005] and stromelysin-1 [Krtolica and Campisi, 2002], and interleukins (IL) [Krtolica and Campisi, 2002; Bissell *et al.*, 2005; Parrinello *et al.*, 2005; Coppé *et al.*, 2008b], as well as increased amounts of fibronectin [Krtolica and Campisi, 2002]. The expression of metalloproteinases, is directly accountable for collagen stability and degradation [Bissell *et al.*, 2003; Bissell *et al.*, 2005; Ghajar and Bissell, 2008], and consequent structural disorganization of the ECM, which will induce loss of epithelial cells stability [Bissell *et al.*, 2005] and changes in the differentiation pattern in order to survive [Bello-DeOcampo *et al.*, 2001; Bissell *et al.*, 2005]. Increased levels of metalloproteinases and ILs were also reported to induce increased levels of ROS in epithelial cells that, in turn, will induce changes on oxidative metabolism [Bissell *et al.*, 2005]. Under this microenvironment, as fibroblast and epithelial cells co-evolved, the malignization of one of these cell types becomes a probable event, possibly as the result of certain oncogenes expression [Krtolica and Campisi, 2002]. Under appropriated conditions, newly transformed cells can stimulate, through paracrine mechanisms, another cell type proliferation. The latter, in turn, will express growth factors that will affect the former cells, giving way to an ascendant stimuli-response-stimuli cascade, increasing exponentially the proliferation of the tumoral mass [Bissell *et al.*, 2005; Campisi, 2005].

From the various genes that induce phenotypic changes it should be emphasized that, as they are involved in checkpoints, tumour-suppressor genes don't allow the proliferation of potentially neoplastic cells [Campisi, 2005]. Thus, the senescent phenomenon is, in part, similar to apoptosis, with the big difference that apoptosis results in cells' death while senescence only prevents cells' replication [Krtolica *et al.*, 2001]. In this process the

microenvironment has a controller and determinative role, deciding between survival or death pathways, therefore being able to seal the cell's fate.

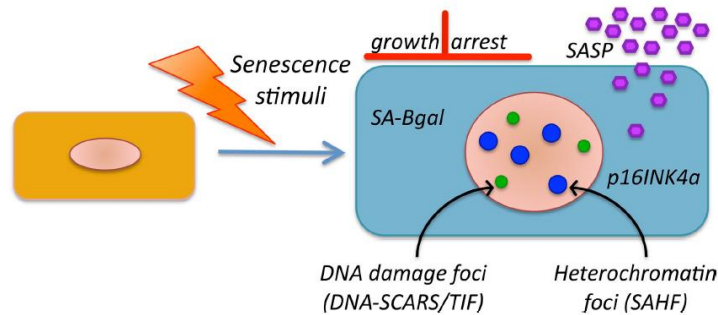


**Figure 1.13:** Representation of hallmarks of senescent cells. Senescent cells differ from other nondividing (quiescent, terminally differentiated) although, no single feature of the senescent phenotype is exclusively specific. Hallmarks of senescent cells include an essentially irreversible growth arrest, expression of SA-βgal and  $p16^{INK4a}$ , robust secretion of numerous growth factors, cytokines, proteases, and other proteins, and nuclear foci containing DNA damage response proteins (DNA-SCARS/TIF) or heterochromatin (Senescent Associated Heterochromatin Foci (SAHF)). The pink circles in the nonsenescent cell (left) and senescent cell (right) represent the nucleus (**adapted from Rodier and Campisi, 2011**).

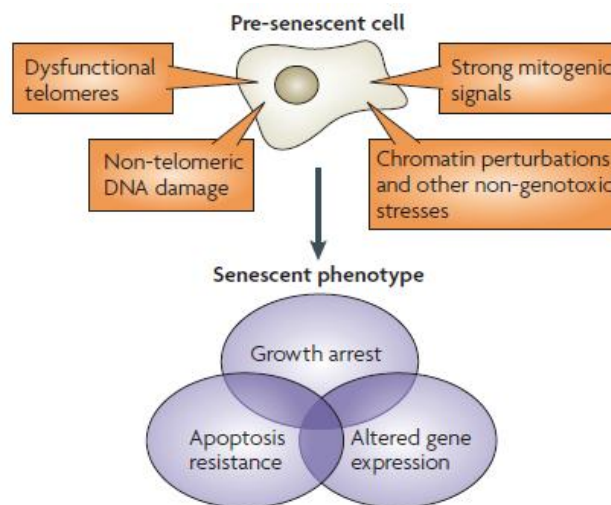


**Figure 1.14:** The senescent phenotype induced by multiple stimuli. Mitotically competent cells respond to various stressors by undergoing cellular senescence. These stressors include dysfunctional telomeres, non-telomeric DNA damage, excessive mitogenic signals including those produced by oncogenes (which also cause DNA damage), non-genotoxic stress such as perturbations to chromatin organization and, probably, stresses with an as-yet-unknown etiology. The senescence response causes striking changes in cellular phenotype. These changes include an essentially permanent arrest of cell proliferation, development of resistance to apoptosis (in some cells), and an altered pattern of gene expression (**adapted from Campisi and d'Adda di Fagagna, 2007**).

### 1.6.1. MOLECULAR MECHANISMS OF SENESCENCE

P53 pathway is activated in response to the DNA damage that results from extremely short or dysfunctional telomeres or from the excessive production of ROS [**Campisi, 2005; Feng et al., 2007; Rodier et al., 2007**]. As a consequence, p21 is activated by p53 and changes

in gene transcription are triggered. The ultimate result can be cellular senescence [Campisi, 2005; Rodier *et al.*, 2007; Lisanti *et al.*, 2010]. In fact, the senescent response is dependent upon p53 and pRb-associated pathways, even though the major mechanistic features underlying the process are still unknown [Krtolica and Campisi, 2002; Campisi, 2005]. With aging, the loss of heterochromatin allows certain genes, previously silenced, to be expressed by activation through pRb/E2F pathway, potentiating cell proliferation and consequently tumour formation [Campisi, 2005]. In addition, loss of p53 activity induces uncontrolled proliferation due to loss of cell-cycle control, allowing previously senescent cells to no longer be such [Bissell *et al.*, 2005; Campisi, 2005].

Regarding pRb pathway, the activation of RAS signal transduction pathway, due to intracellular stress and oncogenes, induces the activation of p16, inhibiting the cell-cycle which, in turn, will activate pRb. The chromatin reorganization, due to the activation of pRb affects E2F-dependent-gene transcription, as well as other genes associated with proliferation [Goodwin *et al.*, 2000; Campisi, 2005].

Finally, p53 and pRb pathways are inter-connected by the fact that active p53 leads to p21 activation, and consequent inhibition of cyclin-dependent-kinases (CDK4, CDK6) thus, promoting pRb hyperphosphorylation and subsequent activation, resulting in the emergence of an apparently irreversible senescence state [Campisi, 2005]. Even inactivating p53, supposedly reversing the senescent state, the pRb activation via p53-independent pathways would not reverse the senescent phenotype [Campisi, 2005; Coppé *et al.*, 2008b]. Due to the fact that few cells are capable of expressing both p21 and p16, the predicted simultaneous activation cascade of p53 and pRb pathways is not viable in most tissues [Campisi, 2005]. On the other hand, the silencing or reduction of p16 expression, by the respective promoter hypermethylation, inhibiting the pRb pathway leads to senescent response through p53 pathway [Campisi, 2005; Rodier *et al.*, 2007]. However, posterior inhibition of p16, p53 or even pRb proteins does not reverse the senescent stage [Goodwin *et al.*, 2000; Campisi, 2005].

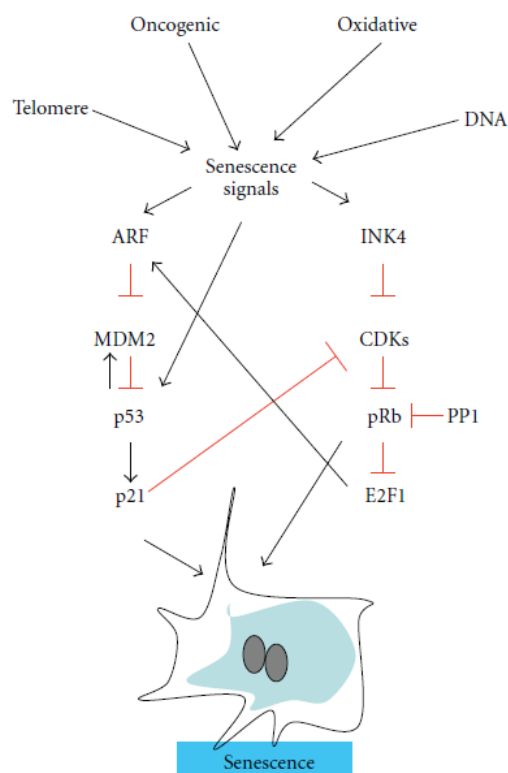


**Figure 1.15:** Representation of the senescence effector pathways crosstalk through p53 and pRb (adapted from Vergel *et al.*, 2010).

## 1.7. CHROMIUM, HEXAVALENT CHROMIUM AND CANCER

Chromium is a ubiquitous metal in nature, being present in soil, rocks and living organisms. The metal was discovered at the end of the XVII century by Nicolas-Louis Vauquelin on a plumb mineral, croicote ( $\text{PbCrO}_4$ ). It is a transition element, located at group IV of the periodic table, being a mixture of 4 stable isotopes:  $^{50}\text{Cr}$  (4.31%),  $^{52}\text{Cr}$  (83.76%),  $^{53}\text{Cr}$  (9.55%) and  $^{54}\text{Cr}$  (2.38%) [Cotton and Wilkinson, 1998]. This transition metal with incomplete  $d$  orbitals can present various oxidative states from  $2^-$  to  $6^+$  (VI) being the  $3^+$  (III) the more stable [Salnikow and Zhitkovich, 2008]. Chromium is widely used in textile, metallurgic and in stainless and chromed steel industries. Cr(II) oxidation state is a strong reducing agent and when exposed to air or water can, rapidly, generate the more stable trivalent state. Biologically, Cr(III) potentiates insulin activity, being indirectly involved on the glucose uptake. [O'Brien *et al.*, 2003; Barceloux, 1999]. Chemically, Cr(III) compounds are less soluble in water at a 4-11 pH, while in alkaline environment can be easily oxidized to the hexavalent form [Barceloux, 1999]. Cr(VI), obtained in nature from fossil combustion, can be found on Earth in the form of chromate ( $\text{CrO}_4^{2-}$ ) or dichromate ( $\text{Cr}_2\text{O}_7^{2-}$ ) salts, recognized respectively by yellow

and orange colours. It is biologically a very toxic agent mostly because its great reduction potential makes it a strong oxidative agent. It is easily inhaled, entering the organisms' respiratory tract and it is also quite soluble, being easily absorbed to the blood stream **[Barceloux, 1999]**.

Cr(VI) compounds are largely used in the production of stainless steel, textile dyes, wood preservation, leather tanning, anti-corrosive and conversion coatings. As a consequence, chromium industrial wastes released into the environment easily contaminate pristine waters and the atmosphere. Although Cr(III), in the form of chromium oxide, is the more abundant environmental contaminant, Cr(VI) can also appear in burned coal ashes **[Stern, Thomsen and Furst, 1984]**. However, the slow oxidation of Cr(III) to Cr(VI) renders accumulation of industrial wastes a huge health problem.

Cr(VI) compounds (chromates) can easily cross the biologic membranes, through anionic unspecific channels, as chromate salts have a tetrahedral geometry portraying structural similarities to sulphate and phosphate salts. Chromate salts carcinogenicity was revealed following epidemiologic studies on exposed miners and refinery workers **[Manahan, 2003; Barceloux, 1999; Salnikow and Zhitkovich, 2008]**. Exposure to environments contaminated with chromate can cause bronchogenic carcinoma, as the respiratory tract tissues are in direct contact with inhaled Cr(VI), with a latent period from 10 to 15 years **[Manahan, 2003; Barceloux, 1999]**. The International Agency of Research on Cancer (IARC) considers Cr(VI) as a group 1 carcinogenic lung agent **[Urbano *et al.*, 2008]**.

The carcinogenicity of Cr(VI) compounds has been explained by its easy intracellular accumulation and reduction to Cr(III) by glutathione, cysteine and ascorbate. During the reduction process, the very reactive Cr(V) and Cr(IV) intermediates can easily generate a variety of extremely reactive carbon, oxygen and sulphur centred radicals leading directly or indirectly to DNA and proteins damage **[Urbano *et al.*, 2008; Reynolds *et al.*, 2007]**. Cr(III) also reacts with DNA, generating binary and ternary Cr-DNA adducts, protein-Cr-DNA cross-links and bi-functional DNA-Cr-DNA inter-strand cross-links **[Zhitkovich, 2005]**. The ultimate result of Cr(VI) reduction process is DNA- single and - double strand breaks formation and a consequent activation of DNA repair systems which, when mutated or too slow to repair the extensive damage, may lead to chromosomic instability and cellular dysfunction **[Urbano *et al.*, 2008] (Figure 1.16)**.

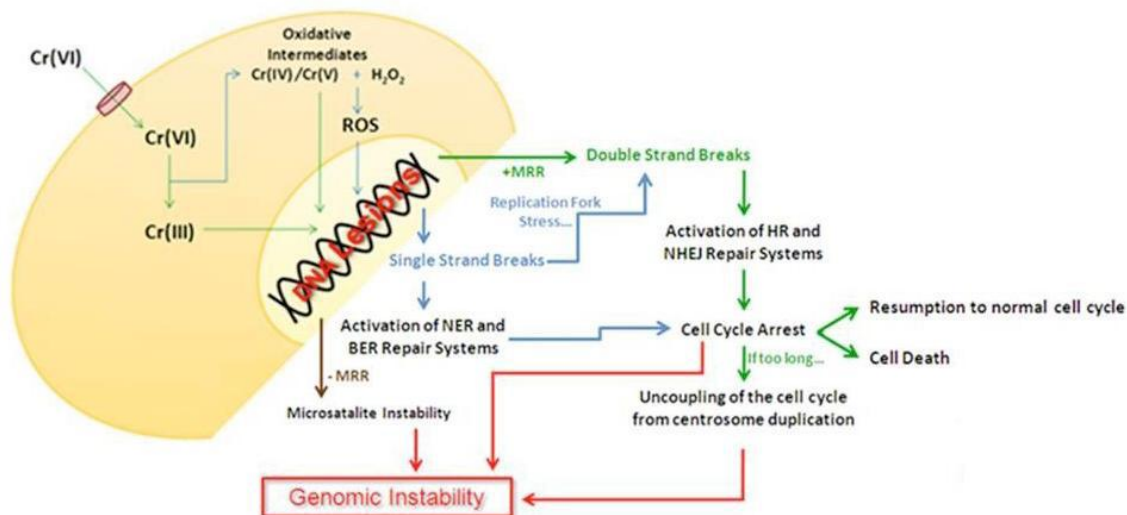


**Figure 1.16:** Schematic representation of possible pathways involved on Cr(VI)-induced carcinogenesis (adapted from Urbano *et al.*, 2008).

Exposure to Cr(VI) was reported to induce senescence, anchorage independence and mutations on human foreskin fibroblasts [Biedermann and Landolph, 1987]. The exposure regimen used in this study suggests that Cr(VI) may contribute to the development of cancer through its mutagenic effects, but also by ROS-mediated changes in stromal fibroblasts secretory phenotype. In fact, senescence is known to emerge in response to DNA damage and ROS formation [Campisi, 2005; Rodier *et al.*, 2007; Lisanti *et al.*, 2010].

A major drawback for the acceptance of most of the data obtained from *in vitro* studies relies on the fact that studies, that detected some of these mutagens and their DNA injuries, do not represent the *in vivo* events. The cell types used in most studies were not respiratory tract cells, the exposure regimens used were not representative of the carcinogenic process, and the results obtained were heavily dependent upon the system and experimental conditions employed [Urbano *et al.*, 2008; Rodrigues *et al.*, 2009]. However, very recently, it was successfully induced the malignant transformation of an SV40 immortalized human bronchial epithelial cells (BEAS-2B) following prolonged exposure to sub-cytotoxic Cr(VI) concentration [Rodrigues *et al.*, 2009].

To better depict the *in vivo* events occurring in Cr(VI) lung carcinogenesis a cellular model in which epithelial cells co-evolved together with bronchial fibroblasts will have to be established since, it is well documented that homeostasis of epithelial organs such as lung critically depends on interaction with the adjacent mesenchyme [Andriani *et al.*, 2003; Coppé *et al.*, 2008a; Hu and Polyak, 2008; Hyatt *et al.*, 2004; del Moral *et al.*, 2006]. But, the study of

the molecular mechanisms of these interactions *in vivo* is complicated by many variables and the lack of properly controlled experimental conditions. Epithelial–mesenchymal synergy has been frequently approached by using three-dimensional organotypic co-cultures of epithelial cells and fibroblasts embedded in different matrices. These complex culture models have provided valuable information on ultrastructural features of epithelial cells' differentiation and basement membrane formation [Andriani *et al.*, 2003] but are not amenable for detailed biochemical studies.

## 1.8. CELL CULTURE

Cell culture is a technique used in diverse fields of research. Its focus is the study of biological events in controlled conditions. Nowadays, cell culture importance is easily recognized as it allows a continuous analysis of multiple biological processes and properties in tissue cells that otherwise would be impossible to analyze in living organisms. Using such technique it has been possible to identify the genetic bases and phenotypic processes involved in cellular transformation and to compare, among other pathologies, normal and tumour cells' behaviour [Freshney, 2005; Bérubé *et al.*, 2010].

Cell culture was devised as a method to study the behaviour of animal cells, with the interference from systemic variable that frequently appear *in vivo* [Freshney, 2005]. As such, this *in vitro* technique, allows the controlled introduction of variables in the sample environment, increasing phenotype homogeneity proportional with passage number and observing their effects in the cells. Growth factors, nutrients needed and dosages, as well as pH and the presence of inorganic salts, CO<sub>2</sub> concentration and temperature, among others are major factors for the appropriate cell development. Therefore, it's very important to have an appropriate cell medium for each cell culture [Freshney, 2005]. The use of cell lines is extremely useful, as there is the production of an acceptable number of same type of cell, being able to be cryo-preserved. Unfortunately, they can lose a great deal of the original tissue phenotype [Sigma Cell Culture Manual Data Sheet, 2005].

Cell culture can be performed with cells in cellular suspensions or adherent plain surfaces forming monolayers [Freshney, 2002]. In suspension, cells grow in solution, forming small individualized aggregates, while in monolayers cells grow attached to the surface of the culture

flask. The culture type reflects the cells' origin, being that fluid tissue cells grow better in suspension, while solid tissue cells grow better in monolayer. In the latter case it is easy to classify cells according to their morphology as endothelial, epithelial, neuronal or fibroblasts, among others [Sigma Cell Culture Manual Data Sheet, 2005; Freshney, 2002].

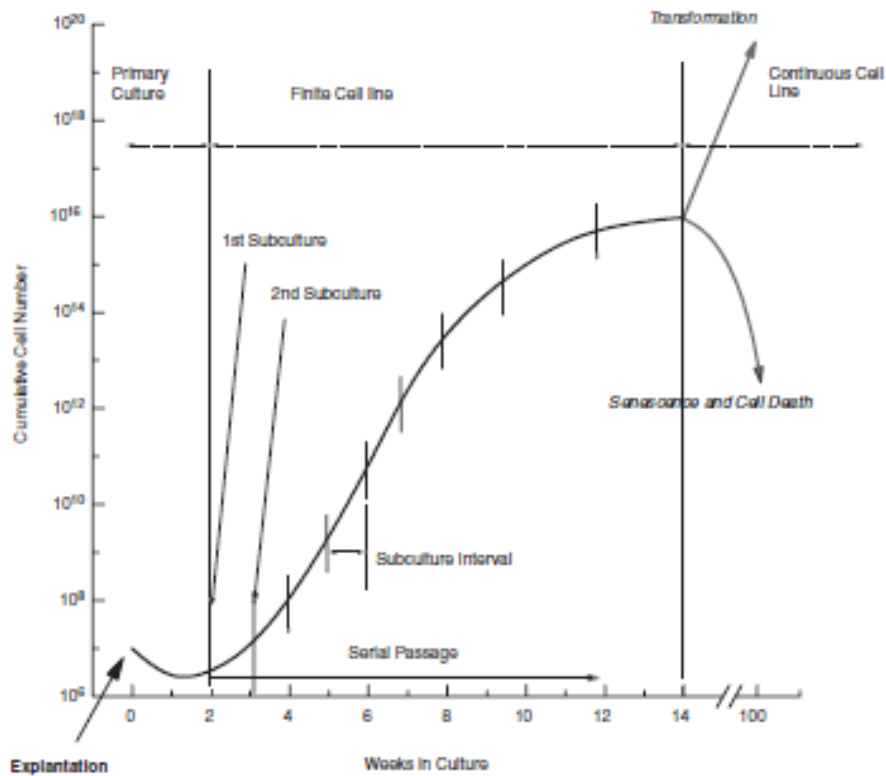


**Figure 1.17:** Evolution of a Cell Line. The vertical (Y) axis represents total cell growth (assuming no reduction at passage) for a hypothetical cell culture. Total cell number (cell yield) is represented on this axis on a log scale, and the time in culture is shown on the X-axis on a linear scale. Although a continuous cell line is depicted as arising at 14 weeks, with different cells it could arise at any time. Likewise, senescence may occur at any time, but for human diploid fibroblasts it is most likely to occur between 30 and 60 cell doublings, or 10 to 20 weeks, depending on the doubling time (adapted from Freshney, 2005).

### 1.8.1. PRIMARY CELL CULTURES

Cell cultures can be classified as primary and continuous cultures [Freshney, 2005]. Primary cultures are obtained directly from tissues, normally through biopsies. They are initially heterogeneous, and reflect the characteristics they had *in vivo*. However, its preparation and maintenance is exhaustive and cultures can only be kept *in vitro* for short periods of time [Sigma Cell Culture Manual Data Sheet, 2005]. This is due to the fact that, with aging, all tissues lose their ability to proliferate correctly. Depending on cell type the loss

of ability can vary. The turning point in time, in which cells stop normally proliferating and can go either through senescence or undergo transformation (possibly malignant), is called Hayflick Limit. This point is related to telomere shortening that occurs with aging, which can activate cell cycle arrest and therefore normal growth [Freshney, 2005]

Once in culture, primary cell lines grow to the confluence, stage at which they stop growing in a process called contact inhibition growth. If this primary culture is subjected to chemical or mechanical disaggregation and cells are re-plated in a lower density, a process called sub-culture or passage, a primary cell line is attained [Freshney, 2005]. Continuous cell culture, derive from primary cultures by a process of sub-culture or passage. These cultures are usually called cell lines. The cells' variety in each cell tends to diminish along time and cultures can be propagated for a finite number of cell division, normally about 30. Finite cell lines are generally diploid and present a certain degree of differentiation. In these cell lines it should be considered the emergence of senescent phenotype on latter passages, in order to maintain a proper culture [Freshney, 2005; Sigma Cell Culture Manual Data Sheet, 2005].

### 1.8.2. BEAS-2B CELL LINE

BEAS-2B cell line is a commercialized and transformed bronchial epithelial cell line. The cell line was initially isolated from normal human bronchial epithelium, obtained from autopsy of non-cancerous individuals. The cells were immortalized through infection with an adenovirus 12-SV40 virus hybrid. They are normally used in screening from chemical and biological agents for their ability to induce and affect differentiation or carcinogenic development.

This cell line was produced in 1988 at the National Cancer Institute, USA, by a group lead by Curtis Harris. [Reddel *et al.*, 1988] It is capable to be maintained up to a year in culture, a big advantage compared to primary cultures. Although not tumorigenic it can suffer genomic alterations that can induce a change in phenotype. Recently, it has been shown that Cr(VI) exposure can induce malignant transformation. [Rodrigues *et al.*, 2009; Costa *et al.*, 2010] Therefore, in alternative to the HBEC primary cultures due to difficulty in establishment a stable and long-term culture, BEAS-2B present themselves, due to their already known

characterization and increased stability in culture, as the best way to study the effect of senescent fibroblasts on bronchial epithelial cells.

### **1.8.3. CO-CULTURES**

As mentioned earlier, EMT and subsequent mesenchymal-epithelial (MET) transitions associated with alterations in E-Cadherin expression and are among the most dramatic examples of cells' plasticity in response to their microenvironment. In addition, they represent critical steps in tumour progression. Among the crucial signals that govern cell behaviour are those generated locally by neighbouring cells. Understanding how fibroblasts and epithelial cells interact with and modulate their microenvironment can provide insights into the molecular mechanism(s) involved with malignant transformation. To study these signalling mechanisms in a controlled setting, several co-culture systems have been developed.

Co-cultures have been especially useful in understanding the interactions between epithelial cells and stromal fibroblasts during normal development and neoplastic transformation, having shown that stromal fibroblasts are essential regulators of normal epithelial cell phenotypes and the malignant phenotypes of pre-neoplastic or neoplastic epithelial cells [Martinez-Outschoorn *et al.*, 2010].

#### **1.8.3.1. CO-CULTURE OF LUNG FIBROBLASTS AND BRONCHIAL EPITHELIAL CELLS**

Normal human bronchial epithelial (NHBE) cells have the ability to strongly develop a mucociliated morphology in air-liquid interface, similar to what is observed *in vivo* [Wiszniewski, Jornot, Dudez *et al.*, 2006]. However, NHBE primary cultures have a very short lifespan and can contain different cell types. Although, minor cell populations can be removed through cell passage, primary cultures are rather prone to phenotypic changes, and the proliferation rate is very small due to the lack of the ECM supporting layer which, in addition to

fibroblasts, contains other factors e.g., growth factors and hormones, needed for phenotype maintenance [Freshney, 2002]. The mutual regulation between the matrix and the epithelium is required for phenotype maintenance and normal development, playing also a crucial role in cellular (de)differentiation and transformation [Freshney, 2002; Wiszniewski, Jornot, Dudez et al., 2006; Pohl et al., 2009].

Immortalized or tumorigenic fibroblast cell lines rather than normal fibroblasts have been used to study fibroblast/epithelial interactions during tumour growth and development. These studies revealed that fibroblast cell lines that have been altered by viral or chemical carcinogens can enhance tumor growth when co-inoculated with carcinoma cells [Olumi et al., 1999].

Recently, Chanson's group [Wiszniewski et al., 2006], using transwells, successfully implemented a bronchial epithelial cell culture method, that keeps cells without any phenotypic change for extended periods of time (as long as 6 months) [Wiszniewski et al., 2006; Pohl et al., 2009]. In Chanson's co-cultures method, fibroblasts were seeded on a bottom layer of a multiwell, without being in direct contact with the epithelial layer present in the transwell compartment (Figure 1.17). Nevertheless, although the fibroblasts were not in direct contact with the epithelial cells, their secretion products (chemokines and cytokines) were able to reach the epithelial compartment through the porous membrane, mimicking the supportive and reciprocal connection between both cell layers. As the porous membrane separates the two compartments, it was impossible the contact between different cell layers, avoiding any possible cell invasion. Additionally, the porous membrane also allowed the use of different cell type specific medium [Wiszniewski, Jornot, Dudez et al., 2006; Pohl et al., 2009].

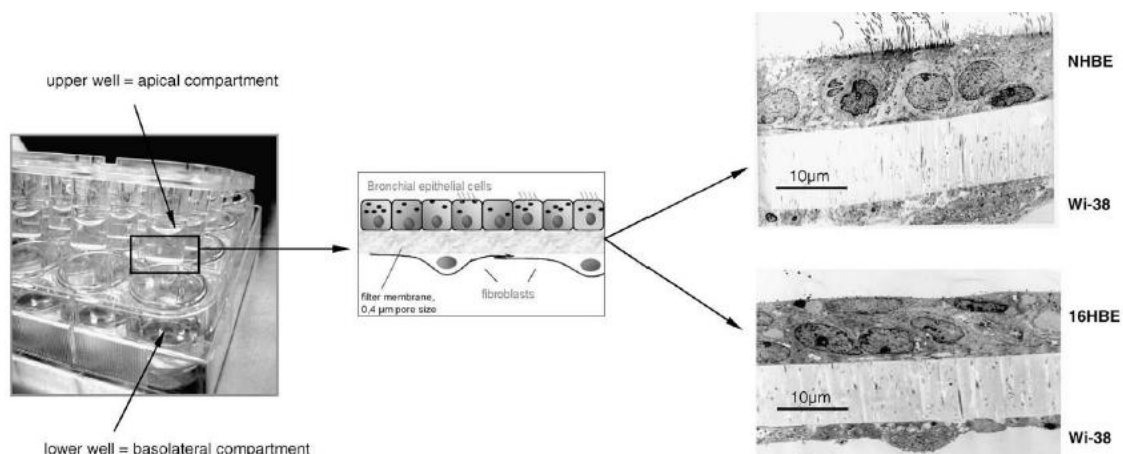


**Figure 1.18:** Co-culture *in vitro* system with NHBE and fibroblasts (adapted from Pohl et al., 2009). Fibroblasts are cultured on the bottom compartment, with the culture medium in direct contact with a filter membrane with 0.4 µm pores, on the base of transwell, allowing growth factors and other molecules to pass to the upper compartment, being in contact with NHBE cells, leading to a condition resembling the *in vivo* situation where NHBE proliferation and differentiation is modulated by the ECM.

Using a similar methodology Chanson demonstrated that the epithelial phenotype depends on the origin of fibroblasts feeder layer. Therefore, co-cultivating nasal polyps' epithelial cells in the presence of a feeder layer of bronchial fibroblasts it was possible to obtain ciliated epithelia, following epithelial proliferation and subsequent removal of the epithelial cell culture medium (Figure 1.18) [Wisniewski *et al.*, 2006].

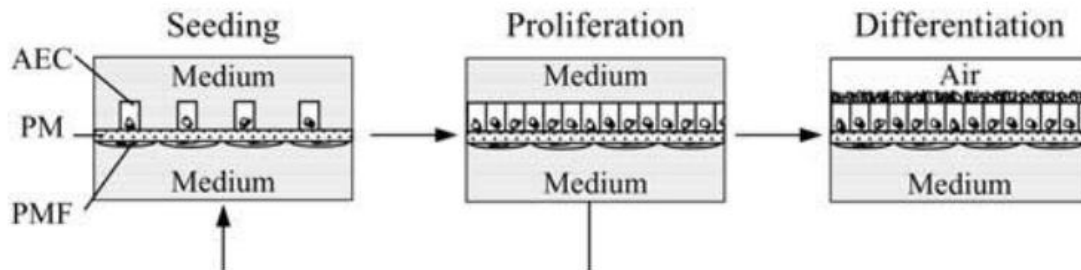


Figure 1.19: Representation of the proliferation and differentiation process in co-culture of NHBE and fibroblasts (adapted from Wisniewski, Jornot, Dudez *et al.*, 2006).

## 1.9. OBJECTIVE

Most studies on the mechanisms leading to cells' malignant transformation that use epithelial cell monocultures assumed that tumour microenvironment was a passive and inert entity. However, the behaviour of epithelial cells is easily modulated by extracellular microenvironment and culture conditions. Consequently, it is not surprising that gene expression changes observed in cancer cells from epithelial cell monocultures, often cannot be validated in clinical specimens and the screening of drugs for cancer treatment has rarely resulted in the identification of a clinically successful chemotherapeutic agent.

Understanding how epithelial cells and fibroblasts interact with and modulate their microenvironment can provide insights into the molecular mechanism(s) involved with malignant transformation and progression. Aiming to implement an *in vitro* model of Cr(VI)-induced carcinogenesis that better depicts what is observed *in vivo*, co-cultures of Cr(VI)-induced senescent fibroblasts and Cr(VI)-exposed human epithelial cells will be established. Through the implementation of this model it is expected to shed some light on the role of cellular senescence on the malignant transformation of human bronchial epithelium.

**Material**

**&**

**Methods**



In the course of this project several techniques were used ranging from basic biochemical laboratory procedures and cell culture, to molecular techniques as immunological staining. In this section all the experimental protocols used in this work will be presented, as will all the materials and equipment used, and their respective manufacturers.

## **2.1. REAGENTS AND MATERIAL**

Whenever necessary, ultrapure water obtained from a Simplicity™ (Millipore S.A., Molsheim) water purification system was used.

### **Reagents purchased to Sigma-Aldrich Química S.A., Sintra, Portugal:**

- Different salts for Phosphate Buffer Solution (PBS) preparation, namely KCl, NaCl,  $\text{KH}_2\text{PO}_4$  and  $\text{Na}_2\text{HPO}_4$ ;
- NaOH used for the preparation of the pH adjustment solution;
- Trypan Blue 0,4% solution (m/v) in PBS, used in cell counting;
- Potassium dichromate used for preparation of hexavalent chromium [Cr(VI)] solutions;
- Dimethyl sulphoxide (DMSO) used for cell culture cryopreservation;
- 3-(4,5-Dimethylthiazol-2-yl)-2,5-diphenyltetrazolium bromide (MTT) powder used for cell viability assays;
- Senescent cells staining kit used in the senescence evaluation assays;
- 2 % gelatine from bovine skin used to prepare the coating solution;
- Ammonia hydroxide used in the preparation of the type I collagen coating solution;
- Bovine serum albumin for the preparation of the 1 % gelatine solution.

**Reagents purchased to Gibco, CA, USA, through Alfacene, Lisbon, Portugal:**

- TrypLE Express 0,25 % trypsin solution to detach cells;
- Transferrin, sodium pyruvate and L-glutamine, used as medium supplement for bronchial epithelial primary cells cultures;
- Foetal bovine serum (FBS), used in fibroblasts primary cell culture;
- Dulbecco's Modified Eagle Medium (DMEM) and F12 cell culture mediums, used in fibroblasts primary cell cultures;
- LHC-9 cell culture medium, used for epithelial cell cultures
- Type I collagen, used in the preparation of a coating solution for primary bronchial epithelial cells;
- Penicillin and streptomycin used in the preparation of some cell culture mediums.

**Reagents purchased to Invitrogen, CA, USA, through Alfacene, Lisbon, Portugal:**

- Epidermal growth factor, used as a medium supplement for primary bronchial epithelial cells cultures.

**Reagents purchased to Panreac Química S.A., Barcelona, Spain:**

- Absolute ethanol used for cell fixation protocol during the immunocytochemistry analysis.

**Reagents purchased to Merck, Darmstadt, Germany, through VWR International, Lisbon, Portugal:**

- Hydrochloric acid and isopropanol, used in the MTT assay;
- Acetic acid, used for type I collagen coating solution preparation.

**Reagents purchased to Lonza, MD, EUA, through VWR International, Lisbon, Portugal:**

- Bronchial Epithelial Growth Medium (BEGM) used for bronchial epithelial primary cells culture.

**Reagents purchased to Roche, Sistemas de Diagnosticos Lda., Amadora, Portugal:**

- Pronase utilized during the establishment of primary bronchial epithelial cultures.

**From European Collection of Cell Cultures (ECACC), were purchased:**

- BEAS-2B cell line as a cryopreserved cellular suspension, used in the co-cultures.

**From Orange Scientific, Braine-l'Alleud, Belgium, through Frilabo, Porto, Portugal:**

- 96-wells tissue culture test plates, used for the MTT assay;
- 15 and 50 mL centrifuge tubes.

**From Corning Incorporated, NY, EUA, through Sigma-Aldrich Química S.A., Sintra, Portugal:**

- 12-wells tissue culture test plates, used for cell culture;
- T25 and T75 tissue culture flasks with vent cap, used for cell culture
- 6-well tissue culture transwells (3450), used in the co-cultures

**Reagents purchased to Lab Vision Corporation, Fremont, CA, USA,**

- UltraVision Large Volume Detection System Anti-Polyvalent, HRP (Ready-To-Use) Kit, for cell immunocytochemistry analysis.

**Reagents purchased to Novocastra DakoCytomation, Glostrup, Denmark,**

- Monoclonal mouse anti-human cytokeratin antibody, clone MNF116, used for cell immunocytochemistry analysis;
- Monoclonal mouse anti-human vimentin, clone Vim 3B4, used for cell immunocytochemistry analysis;
- Monoclonal mouse anti-human smooth muscle actin, clone 1A4, used for cell immunocytochemistry analysis.

**Reagents purchased to Novocastra Laboratories Ltd, Newcastle, United Kingdom,**

- Monoclonal mouse anti-human E-Cadherin antibody, clone 36B5 and 3,3-diaminobenzidine tetrahydrochloride (DAB), both used during the immunocytochemistry procedure.

**Reagents purchased to Hanna Instruments, Woonsocket, USA, through Hanna Instruments Portugal, Póvoa do Varzim, Portugal:**

- pH meter calibration solutions.

**Material purchased to Sarstedt Lda., Rio Mouro, Portugal:**

- 6 and 24-well tissue culture plates, used for cell culture;
- 25 mL serological pipettes;
- Petri dishes used for cell culture;
- Cryogenic vials utilized in cells' cryopreservation;
- 2 mL microcentrifuge tubes.

**Material purchased to Frilabo, Porto, Portugal:**

- 2, 5, 10 mL serological pipettes.

**Material purchased to Menzel-Gläser, Braunschweig, Germany, through VWR International, Lisbon, Portugal:**

- Coverslips and slides, used for immunocytochemistry analysis.

**Material purchased to Schleicher & Shuell, Microscience, Dassel, Germany, through Reagente 5, Porto, Portugal:**

- 0.2 µm filters, model FP30 utilized in the sterilization of small volume solutions.

## **2.2. EQUIPMENT AND SOFTWARE**

- Bench autoclave, model Omega Media from Prestige Medical, Blackburn, UK, distributed by Ezequiel Panão Jorge, Electromédica, Coimbra, Portugal;
- Water purification system, model Simplicity™ from Millipore S.A., Molsheim, France, distributed by Interface, Equipamento e Técnica Lda, Amadora, Portugal;
- Automatic pipetting aid, model ComfoPette from Orange Scientific, Braine-l'Alleud, Belgium, distributed by Frilabo, Porto, Portugal;
- Haemocytometer from Marienfeld, Germany, distributed by Reagente 5, Porto, Portugal;
- Laboratory hotte from Ibérica Industrial Laborum, distributed by the same company;
- Heating plate with magnetic stirrer, model Monotherm from Variomag, Daytona Beach, Florida, USA;

- pH meter, model HI 110 from Hanna Instruments, Woonsocket, USA, distributed by Hanna Instruments Portugal, Póvoa do Varzim, Portugal;
- Precision weight balance, model Sartorius B P210 S from Sartorius AG, Goettingen, Germany, distributed by Sartorius Lda, Lisbon, Portugal;
- Centrifuge model Heraeus Instruments, Labofuge 400e from Thermo Scientific, Waltham, Massachusetts, USA, distributed by SupplyLab, Cacém;
- Flux cabinet model VBH Compact Cabinet from Steril Manufacturing Division, Milan, Italy;
- Inverted microscope, model Nikon Eclipse TS100 from Nikon, USA, distributed by Nikon Portugal, Lisbon, Portugal;
- CO<sub>2</sub> Incubator, model CB150 from Binder-World, New York, USA;
- 96-well multiplate reader spectrophotometer, model SLT Spectra, from Alliance Analytical Inc.;
- Liquid nitrogen storage containers model Forma Cryoplus I from Thermo Scientific, Waltham, Massachusetts, USA;
- Ultra-low freezer, model -86C ULT Freezer from Thermo Scientific, Waltham, Massachusetts, USA;
- Graphpad QuickCalcs and Graphpad Prism 5, from Graphpad Software, La Jolla, California, USA, available free online at the website <http://www.graphpad.com/quickcalcs/index.cfm>;
- Nikon ACT-1 Software, from Nikon, USA, distributed by Nikon Portugal, Lisbon, Portugal;
- Microscope Photographic Camera, model Nikon Digital Camera DXM 1200F, attached to inverted microscope Nikon Eclipse 80i, both from Nikon, USA, distributed by Nikon Portugal, Lisbon, Portugal;
- Digital photographic camera, model T-100, from Olympus, USA, distributed by Olympus Portugal, Lisbon, Portugal;

## 2.3. SOLUTIONS AND NUTRIENT MEDIUM PREPARATION

- **Dulbecco's Modified Eagle Medium (DMEM) : F12 medium (1:1) preparation:**

To prepare 500 mL of DMEM:F12 (1:1) growth medium, 222.5 mL of DMEM should be mixed with the same volume of the F12 nutrient mixture. 50 mL of FBS are then added to the mixture in order to attain 10 % of the total volume. Finally, 5 mL (1 % of the total volume) of a penicillin and streptomycin mixture, containing penicillin at 100 U/mL activity and streptomycin at 100 µg/mL concentration, was added to avoid microbial contaminations.

- **Phosphate buffer solution 10x concentrated (10x PBS) preparation:**

The 10x PBS stock solution contained 2.68 mM of KCl, 4.15 mM of  $\text{KH}_2\text{PO}_4$ , 145 mM of NaCl and 8,1 mM of  $\text{Na}_2\text{PO}_4$  dissolved in ultrapure water. The pH of the solution was adjusted to 7.4.

The 1x PBS solution was obtained by diluting the 10x PBS stock solution with ultrapure water. This solution was sterilized prior to use using an autoclave.

- **Bronchial Epithelial Growth Medium (BEGM) Preparation:**

This growth medium, commercialized by Lonza, is available in the form of BulletKit®, made of Bronchial Epithelial Cell Basal Medium (BEBM) and 9 aliquots of medium supplements, that when added to the basal medium, guaranteed optimum growth conditions for epithelial cells. The supplements are: epinephrine, retinoic acid, thiiodothrionine (T3), hydrocortisone, transferrin, a mixture of gentamicin sulphate and amphotericin-B (GA-1000), human recombinant epidermal growth factor (rhEGF), human recombinant insulin and bovine pituitary extract (BPE). The preparation of the final bronchial epithelial growth medium (BEGM) only requires the unfreezing of the aliquots and their addition to the BEBM.

- **2 % (w/v) Bovine serum albumin (BSA) solution preparation:**

The 2 % BSA solution was obtained by dissolving 2 g of BSA on 100 mL of ultrapure water. The solution was then homogenized using a magnetic stirrer and subsequently sterilized by filtration.

- **1 % Gelatine solution preparation:**

To prepare 50 mL of 1 % gelatine solution from the commercial 2% gelatine solution, 50 mL of the commercial solution were efficiently mixed with 45 mL of 1x PBS and 5 mL of a 2% BSA solution.

- **Collagen type I solution preparation:**

The type I collagen solution was prepared from the commercial type I collagen solution. To this end, an initial volume of 25  $\mu$ L of acetic acid was successively diluted in ultrapure water, in a total volume of 25 mL. 287  $\mu$ L of this acetic acid diluted solution were diluted in a total volume of 50 mL. 800  $\mu$ L this solution were added to a 200  $\mu$ L solution of commercialized type I collagen solution. This solution was then added to 20 mL of 1x PBS and preserved at 4 °C.

- **Laminin 50  $\mu$ g/mL solution preparation:**

From a 200  $\mu$ g/mL laminin stock solution, stored in the freezer for conservation purposes, a 50  $\mu$ g/mL solution was prepared by diluting 1:3 (laminin solution:water) in ultrapure water.

- **Fibronectin 5  $\mu$ g/mL solution preparation:**

From a 100  $\mu$ g/mL fibronectin stock solution, a 5  $\mu$ g/mL was prepared by dilution in ultrapure water, in a ratio of 1:19 (fibronectin solution:water).

- **500  $\mu$ M hexavalent chromium [Cr(VI)] stock solution preparation:**

A 500  $\mu$ M Cr(VI) solution was prepared by dissolving 0.0037 g of potassium dichromate ( $K_2Cr_2O_7$ ) in 50 mL of ultrapure water.

- **5  $\mu$ M hexavalent chromium solution preparation:**

A 5  $\mu$ M Cr(VI) solution was prepared by dilution of the previously prepared 500  $\mu$ M Cr(VI) solution in a 1:100 ratio with ultrapure water.

- **3-(4,5-Dimethylthiazol-2-yl)-2,5-diphenyltetrazolium bromide (MTT) 0.5 mg/mL solution preparation:**

The MTT 0.5 mg/mL solution was prepared by dissolving 75 mg of MTT in 10% 10x PBS (15 mL) and 90% ultrapure water (135 mL) under magnetic agitation. The volume was then divided in 15 mL aliquots and the aliquots frozen.

- **Acid isopropanol crystal dissolving solution preparation:**

In the MTT assay, for absorbance reading, the solution used for crystal dissolution was prepared adding 0.5 mL of 37% HCl to 49.5 mL of isopropanol, attaining this way an isopropanol solution in 0.1 M HCl.

## **2.4. METHODS**

- **Statistical analysis**

Statistical analysis was performed using an unpaired t-test through the GraphPad Prism program (GraphPad Software, San Diego, CA).

- **Digital images**

Throughout this study, cells' morphology and growth pattern were continuously monitored by microscopic observation. Photographs were obtained using an Olympus T-100 digital camera.

#### **2.4.1. CELL CULTURE**

For the purpose of this work, both bronchial epithelial cells and bronchial fibroblasts were cultured using the appropriated cell medium. All cell cultures were implemented in aseptic conditions, preventing contamination with microorganisms, and the cells were incubated, unless noted, at 37°C in an atmosphere with 5% CO<sub>2</sub>.

- **Conditions and asepsis**

To ensure asepsis conditions, cell culture was done in a culture room with proper ventilation, constant temperature and no direct contact with the outside, as well as presence of UV lighting. The flux chamber used was of safety level 2 and was exposed to UV radiation, before and after proceedings.

All the equipment used in the culture room was previously sterilized by means of autoclaving, bleaching or 70% alcohol washing. All the solutions were filtered with 0.2 µM-sized porous filters before usage while all proceedings were performed with gloves.

- **Primary cell cultures**

Primary cell cultures were obtained from lung biopsies obtained at Hospitais da Universidade de Coimbra (HUC). Different protocols were used to obtain viable cell cultures from the biopsies.

Primary cultures of human bronchial fibroblasts and human bronchial epithelial cells were obtained from lung biopsies using both mechanical and chemical procedures. Care was taken to avoid biopsies containing alveolar parts (pneumocytes) as it is impossible to implement epithelial cell cultures from pneumocytes.

#### **2.4.1.1. HUMAN BRONCHIAL FIBROBLASTS (HBF) PRIMARY CULTURES**

**Mechanical method:** tissue biopsies were washed with 1x PBS and dissected, under sterile conditions, with the help of a scalpel, into tiny bits (about 1 mm<sup>2</sup>). The tissue pieces were homogeneously placed in the surface of a T25 cell culture flask and a drop of FBS was placed on the top of each tissue sample to facilitate the attachment to the cell surface and to provide nutrients for attachment period. With a Pasteur pipette, the excess of serum was removed from the neighbours of the tissue fragments and the flask was turned upside down and placed in the CO<sub>2</sub> incubator overnight. After this incubation period, 5 mL of DMEM/F12 medium were added to the top of the flask and the flask was gently turned to its correct position allowing the tissue fragments to contact with the medium. Cells were expected to migrate from these explants in the next two weeks.

**Chemical method:** also required biopsies dissection to obtain small pieces of tissue. The tiny tissue pieces were placed into a 15 mL centrifuge tube containing pronase, a protease capable of cleaving cell-cell interactions, and left at 4°C temperature overnight to allow pronase to act. After the digestion, the tissue left unfragmented was removed with the help of a Pasteur pipette and the remaining cell suspension centrifuged for 5 minutes at 1200 rpm. The supernatant containing dead cells and pronase was removed and the pellet re-suspended in 5 mL DMEM/F12 medium. This cellular suspension was placed in a new T25 cell culture flask and fibroblasts were allowed to attach to the surface for 4 hours. The supernatant containing epithelial cells (didn't attach under such culture conditions) was removed and used to establish the human bronchial epithelial primary cell cultures. To the flask containing the attached fibroblasts, 5 mL of fresh DMEM/F12 were added and the cells allowed growing for approximately two weeks. Once a week half the volume of medium was replaced by fresh medium to give the cells fresh nutrients but avoiding the deprivation of cell-secreted growth factors.

Once established, the cultures were maintained as described below in section 2.4.1.4.

#### **2.4.1.2. HUMAN BRONCHIAL EPITHELIAL CELLS (HBEC) PRIMARY CULTURES**

Just like HBF, primary cultures of HBEC were established out of the same biopsies using either mechanical or chemical protocols.

The mechanical method was very similar to the one used to establish the primary cultures of fibroblasts, except that BEGM medium was used instead of the DMEM/F12 medium.

The chemical method used to establish the epithelial cultures profited the supernatant containing the cells that didn't attach to the flask surface in DMEM/F12 after the 4 hours incubation. This supernatant was collected into a centrifuge tube and centrifuged for 5 minutes at 1200 rpm to remove any dead cells. The pellet was re-suspended in BEGM and the mixture placed into T25 culture flasks previously coated with a matrix solution.

To look for the best matrix, several experiments were performed. In the case of gelatine, 1 mL of a 1 % gelatine solution was added to the T25 flask 2 to 72 hours prior the passage. During this period gelatine was allowed to polymerize in the CO<sub>2</sub> incubator and the excess of gelatine solution was removed from the flask right before the addition of cells.

For type I collagen coating, 1 mL of type I collagen solution was added to a T25 flask and 200 µL for 24-well multiplate. The flasks or the multiwall plates were incubated for 30 minutes at room temperature, and the excess of collagen solution removed. The recipient was then transferred to an isolated box, with a piece of paper embedded in ammonia hydroxide to sterilize the recipient, for 15 minutes. The recipient was then washed with 1x PBS and cells were plated in its surface.

The laminin and fibronectin coatings were done similarly to gelatine coating, with the addition of the laminin and fibronectin solutions previously prepared to the surface of the cell culture flasks. The flasks were incubated at 37°C for a minimum of 6 hours and the excess solution removed before cells were plated on the coated surfaces.

A mixture of the three supportive materials was also tested to mimic as much as possible the ECM. Once established the cultures, culture maintenance was performed as described below in section 2.4.1.4.

### **2.4.1.3. BEAS-2B CELL LINE CULTURES**

BEAS-2B cells were defrosted from stock quantities of this cell line and plated, on previously coated with gelatine 1% for a minimum of 2 hours, T75 flasks containing 13 mL of LHC-9 at 37°C. The medium was changed 24h after plating and cells were incubated at 37°C in an atmosphere with 5% of CO<sub>2</sub> for a week until reaching confluence. Once reached, culture maintenance was performed as described below in section 2.4.1.4.

### **2.4.1.4. CELL PASSAGE**

To guarantee the healthy preservation of the cultures, considering their growth rate and the fact that the cells' phenotype can change once confluence is attained, any cell culture must be sub-cultured when they reach about 80% confluence. The minimum initial cell density used was 4000 cells/cm<sup>2</sup>.

In anchorage-dependent cell cultures, once the ideal confluence was reached, the proceeding was straightforward. The cell medium was discarded and the flask washed with 1x PBS in order to remove the remnants of the cell medium. Following PBS removal, trypsin was added to detach cells' from the supporting matrix, allowing cells to be collected. For trypsin's maximum effect, the flask containing the cells and trypsin was incubated at 37°C for 10 minutes, assuring that all cells were detached.

After trypsinization, 5 mL of PBS were added to the flask to detach and collect cells and the suspension was then transferred to a centrifuge and centrifuged for 5 minutes at 1200 rpm. The supernatant was discarded and the pellet resuspended in the cells' specific medium. A 10 µL aliquot of the cells' suspension was used for cell counting with trypan blue. Once

evaluated the cell's density, the volume containing the desired number of cells was transferred to a new flask and medium was added to get a total volume of 5 mL.

#### **2.4.1.5. CELL COUNTING**

0.4% Trypan blue was used to assess the correct suspension cells' density in order to transfer, to the culture flask, the exact number of cells. Trypan blue dye quickly enters the cells when the cell membrane is fragile. Inside the cells trypan blue gives the intracellular space a strong blue colour, allowing the assessment of the number of dead cells in the sample. Simultaneously, it is possible to evaluate the number of viable cells as they will not be stained and their cytoplasm is brighter.

From the total cell suspension, a 10  $\mu\text{L}$  sample was collected and mixed with a 10  $\mu\text{L}$  sample of 0.4% trypan blue solution. From the 20  $\mu\text{L}$  homogenous solution, 10  $\mu\text{L}$  were collected and transferred to the haemocytometer. The number of viable cells was counted in each quadrant (in red in the Figure 2.1) and the average number of viable cells per quadrant was determined.

Each haemocytometer quadrant has the virtual volume of  $0.1 \text{ mm}^3$  or 0.0001 mL and the haemocytometer contains only half of the cells' volume removed from the original cell suspension as half of the volume is the trypan blue solution. Therefore, to calculate the viable cells' concentration expressed as number of cells/volume (mL), the average number of cells were multiplied by 2 (due to concentration) and by 10000 (due to the solution volume in each quadrant). With this information it was possible to estimate the cells' concentration in the original cell suspension and afterwards to calculate the volume to be transferred according to the number of cells required for each experiment.

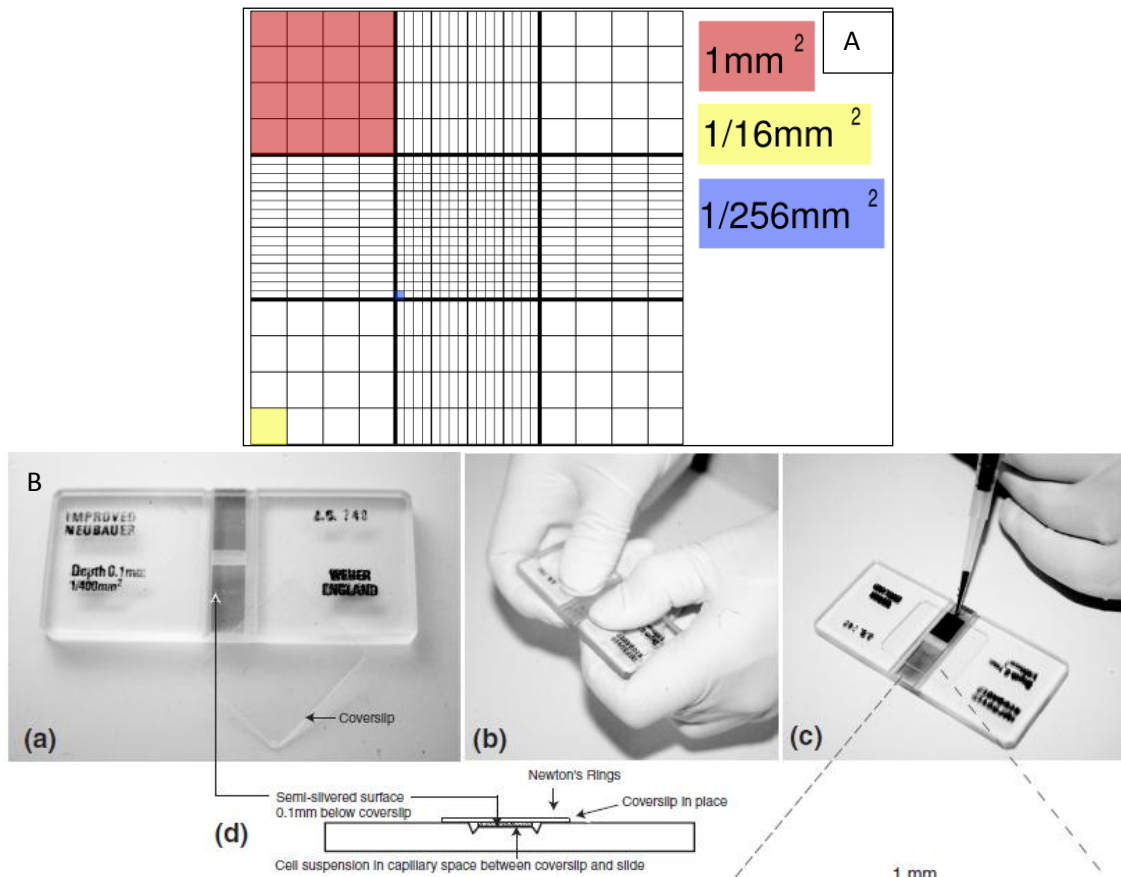


**Figure 2.1:** Representation of haemocytometer relation of area/volume (A) and cell counting proceeding (B) (adapted from [http://en.wikipedia.org/wiki/File:Haemocytometer\\_Grid.png](http://en.wikipedia.org/wiki/File:Haemocytometer_Grid.png)).

## 2.4.1.6. CELL FREEZING/UNFREEZING

### 2.4.1.6.1. CELLS' FREEZING

Cells were preserved by freezing. In order to freeze cells, confluent T75 cell culture flasks (about 4 million cells) were used. Once obtained a confluent culture (see section 2.4.1.4), the cells' suspension in medium:FBS:DMSO ( 7:2:1 ratio) were placed in a cryogenic vial. The vials were subsequently transferred to an isopropanol-containing recipient at  $-80^{\circ}\text{C}$

for at least 4 hours, to allow a gradual decrease in temperature and, as such the cells' gradual freezing, avoiding the formation of ice crystals due to the presence of DMSO. The vials were later transferred to a liquid nitrogen container at -120°C, where they were cryopreserved until needed.

#### **2.4.1.6.2. CELLS' UNFREEZING**

Frozen cells can be reused in cell culture. To obtain cells, the frozen vials were removed from the container and unfrozen by manual friction. The vials content was then added to a previously warmed (37°C) T75 culture flask (pre-coated with gelatine in the case of epithelial cells) containing the appropriate cell culture medium. The flask was placed in the incubator and 24 hours after cells' plating, medium was changed to remove the DMSO, which is toxic for cells at 37°C. Once the culture reached 80% confluence, cells were sub-cultured as indicated in section 2.4.1.4.

### **2.5. ESTABLISHMENT OF Cr(VI) EXPOSURE CONDITIONS THAT INDUCED SENESENCE ON HBF**

Aiming to establish the Cr(VI) exposure conditions (concentration and time) that would induce the emergence of a stable and irreversible senescent HBF phenotype, HBF cultures were only sub-cultivated till passage 13 to avoid replicative senescence and to mimic the fibroblasts in an adult lung. These cells were then regularly exposed, for extended periods of time, to different concentrations of Cr(VI), by adding different volumes of a 5 µM K<sub>2</sub>Cr<sub>2</sub>O<sub>7</sub> solution to the cells' suspension in DMEM/F12. Cell medium was also regularly removed and new medium containing Cr(VI) was added. The protocols varied in initial cell density, Cr(VI) concentration, frequency of medium change, interval of time to start the exposure and ability to undergo further cell passages until reaching the senescence, without compromising viability. In parallel, control experiments were performed but in the absence of Cr(VI).

To evaluate Cr(VI) exposure effects, the cells growth kinetics, morphologic and phenotypic change and senescent-associated- $\beta$ -Galactosidase (SA- $\beta$ -Gal) activity were monitored in control and Cr(VI) exposed cells using the MTT cell viability/proliferation assay, trypan blue, microscopic observation, immunocytochemistry, and the senescent-staining kit.

## **2.6. CO-CULTURES**

To perform the co-cultures, 6-well multiwall plates were used. In each well, fibroblasts were seeded at an initial cell density of  $2 \times 10^4$  cell/cm<sup>2</sup> in DMEM/F12, in a total volume of 2 mL per well. For 4 weeks the cells were treated with either 0.25 or 0.5  $\mu$ M Cr(VI), changing the medium every two days until cells' reached the senescent state. Afterwards, 1% gelatine coated transwells were placed on each well, allowing the fibroblasts' cell medium to be in direct contact with the bottom part of the transwell. This allowed the cells' secreted factors to be in contact with the BEAS-2B cultivated on the upper compartment of the transwells, previously coated with gelatine. LHC-9 medium was used to cultivate the BEAS-2B plated at an initial cell density of  $4.5 \times 10^4$  cell/cm<sup>2</sup> in the transwell compartment, as was done by Chanson's group, as well as other groups [Wiszniewski *et al.*, 2006; Pohl *et al.*, 2009]. Total volume of medium of each specific compartment was changed every three days for three to four weeks

Control experiments were performed using Cr(VI)-untreated HBF and BEAS-2B seeded in their respective compartments in the absence of Cr(VI) insults. Additionally, Cr(VI) senescent fibroblasts and BEAS-2B were cultivated in presence of 0.25  $\mu$ M and 0.5  $\mu$ M concentration of Cr(VI), with the medium changed every 3 days.

## **2.7. CELLS' VIABILITY EVALUATION – MTT ASSAY**

The MTT assay is a colorimetric assay that quantifies the presence of mitochondrial dehydrogenases in cells. In this assay cleavage of the MTT structure by mitochondrial dehydrogenates and cellular reductases allows the quantification of cells' viability by

measuring the absorbance in a 96-well multiplate reader of the purple formazan solutions, obtained following solubilisation of formazan crystals.

In order to fulfil this objective, the cell medium was removed and the 0.5 mg/mL MTT solution was placed in contact with the cells. The volume of MTT solution needed for any result is 75% of the cell culture medium. The cells were incubated for 3 hours at 37 °C at 5% CO<sub>2</sub> and, afterwards, the solution was removed from the wells, leaving the formazan crystals intact. The crystals were then dissolved with acidic isopropanol, using half of original cell medium volume (e.g. in case of 1 mL of DMEM/F12, 0.5 mL of medium was preserved). The resultant coloured solution was transferred to a 96-well multiwell, using 100 µL per well, with the absorbance being read in a multiplate reader, with a reference wavelength of 620 nm and a reading wavelength of 570 nm. The experiments were always done in comparison to a standard curve considering the initial cell density in order to obtain an estimative of cells' proliferation.

## **2.8. CELL'S MORPHOLOGY AND GROWTH PATTERN EVALUATION**

Cells' morphology and growth pattern were continuously monitored by microscopic observation. Photographs were obtained using an Olympus T-100 digital camera.

## **2.9. SENESCENT PHENOTYPE EVALUATION**

To this end a senescent cell staining kit was used. The cells, in 12-well plates were fixed for 6-7 minutes in the 1x fixation buffer solution, prepared from the 10x fixation buffer solution by dilution with ultrapure water. Following removal of the fixation buffer, a mixture of 40 µL of the 10x staining solution, 5 µL of reagent B, 5 µL of reagent C, 10 µL of X-Gal solution and 340 µL of ultrapure water was added to each well. The plates were sealed with parafilm and incubated at 37°C for 5 hours. Cells were observed by microscopy and images were recorded with the aid of a Olympus T-100 digital camera.

## 2.10. IMMUNOCYTOCHEMISTRY

For immunocytochemistry analysis fibroblast were grown on top of slides under exposure conditions (0.25 or 0.50  $\mu\text{M}$  Cr(VI) and exposure time) used to induce fibroblasts' senescence. The cell medium was removed and cells were washed 3 times with 1x PBS and then fixed in 95% ethanol.

Afterwards, the endogenous peroxidase activity was quenched using 15 minutes incubation in 3% diluted hydrogen peroxide ( $\text{H}_2\text{O}_2$ ). For blocking the nonspecific binding with primary antibodies, slides were first dipped in Ultra V Block, from the Ultra Vision Kit, from 5 minutes. Primary antibodies against cytokeratin (MNF116) at a dilution of 1:50, Vimentin at a dilution of 1:200, anti-human smooth muscle actin ( $\alpha$ -SMA) at a dilution of 1/200, E-Cadherin at a dilution 1:25, were applied to the sections and incubated at room temperature for 30 minutes in the case of the first three antibodies and for 60 minutes E-Cadherin. The slides were then washed with 1x PBS from the Ultra Vision Kit, and incubated 15 minutes with biotin-labeled secondary antibody, commercialized as part of the Ultra Vision Kit. Primary antibody binding was localized using peroxidase-conjugated streptavidin (Ultra Vision Kit) and 3,3'-diaminobenzidine tetrahydrochloride (DAB) was used as chromogen, according to manufacturer's instructions. Hematoxylin was used to counter stain the slides which were then dehydrated and mounted.

For positive controls, different tissues were compared to, using smooth muscle for  $\alpha$ -actin staining, colon for vimentin, tonsils for E-Cadherin and epithelial cells for cytokeratin (MNF-116).



**Results**

**&**

**Discussion**



### 3.1. HUMAN BRONCHIAL FIBROBLASTS (HBF) PRIMARY CULTURES

During the course of this project several human primary cultures were established from lung biopsies. The efficiency of the protocols varied considerably, mainly due to impossibility of controlling the lung location from where the biopsies were extracted.

Using the mechanic protocol, after one week cells were able to outgrow from the explants. The primary cultures of HBF established with this protocol remained viable for one month and could stand viable following cryopreservation (**Figure 3.1**). However, the cultures were not homogeneous and it was possible to identify morphologically different cellular sub-populations. These findings emphasized the fact that HBF cultures greatly depend on the original tissue surrounding environment, as different cellular phenotypes can be present in biopsies acquired from the same patient.

As to the chemical protocol, after one week in culture cells were able to attach the flask surface and to form colonies. Culture confluence was obtained, in some cases, after two weeks, while in others was up to one month (**Figure 3.2**). This large variance was again related to the location of the tissue in the lung and the abundance of connective tissue.

Both protocols used to implement HBF cultures were equally effective, with the chemical protocol being slightly more efficient (one additional cell culture was established) (**Table 3.1**).

**Table 3.1:** Viable primary HBF cultures obtained by the mechanical and the chemical protocols.

Mechanical Protocol	Chemical Protocol
PN46-D3	Fibro.PN2
PN44-G	PN2
PN44-H	Fibroblastos-14
PT46-C2	Fibroblastos-13
PT44-B	Fibroblastos-11
PT44-B1	Fibroblastos-10
	Geneva1

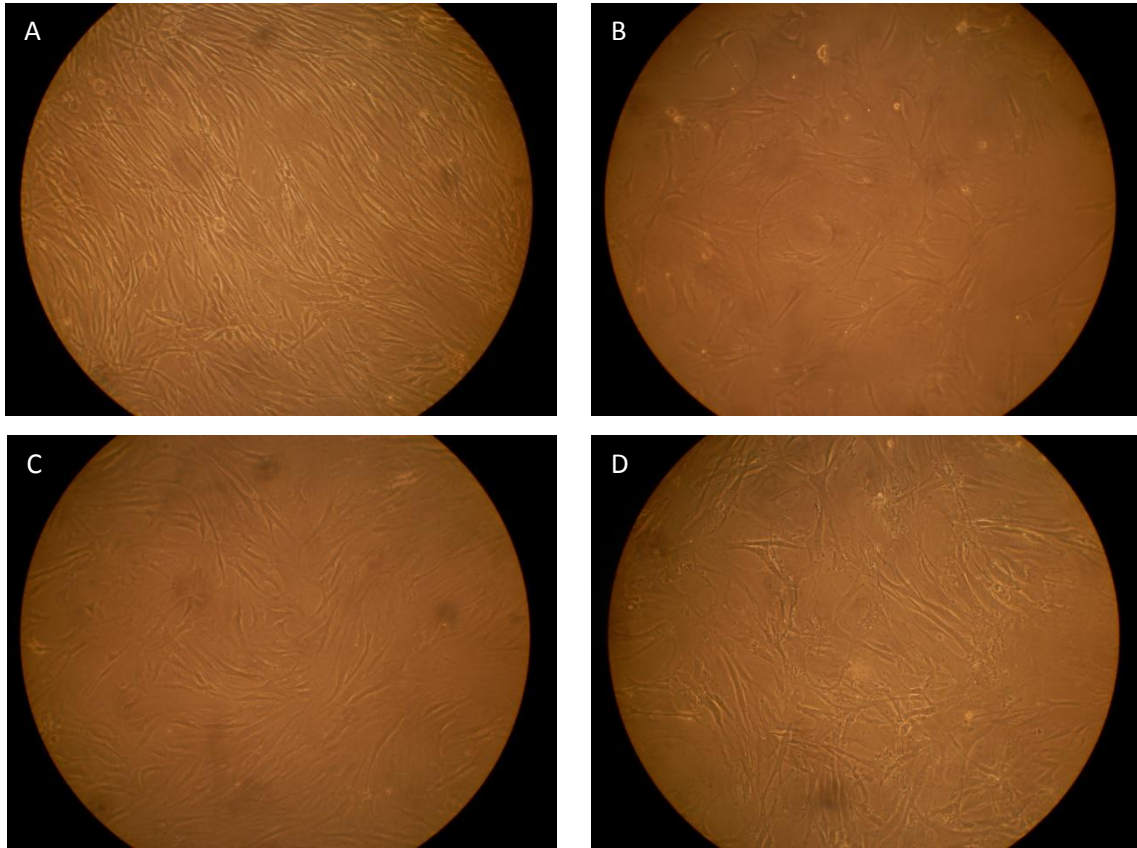


**Figure 3.1:** Representative images of the morphology of HBF cultures obtained using the mechanical protocol: PN44-G (A), PN46-D3 (B), PT44-B1 (C), PT44-B (D), all at passage 1 and magnified 100X.

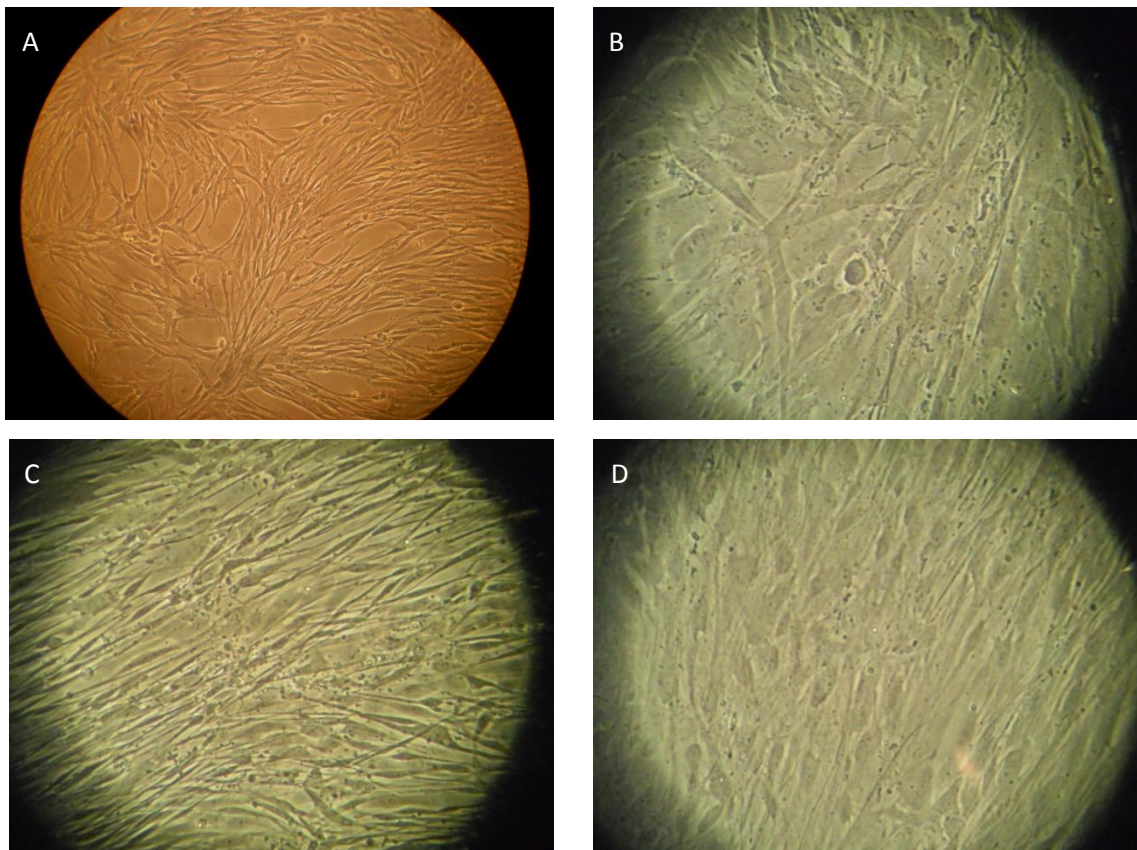


**Figure 3.2:** Representative images of the morphology of HBF cultures obtained using of chemical protocol: Geneva1 at passage 4 (A) and Fibro.PN2 (B), Fibroblastos-13 (C) and Fibroblastos-11 (D) at passage 1 and magnified 100X.

### 3.2. PRIMARY CULTURES OF HUMAN BRONCHIAL EPITHELIAL CELLS (HBEC)

Regarding the HBEC primary cultures, both protocols were tested but the chemical protocol was unsuccessful as no primary cultures were able to grow out of the pronase digested tissues.

Using the mechanical protocol it was possible to obtain some primary cultures of epithelial cells that grew out of the lung explants (**Figure 3.3**). The success of this protocol was far from 100% as only in one third of total number of flasks epithelial cultures were established. One possible explanation is the lung location from where the biopsies were collected as diversity of cell types and their respective abundance varies with the zone location in the lung. Regarding this, regions of alveolar sacs contain a great quantity of pneumocytes while in the primary bronchial segment a great deal of goblet cells can be found [**Figure 1.1**]. Overall, it was possible to establish six epithelial primary cultures.

**Table 3.2:** The attained HBEC cultures using the mechanical protocol.

Mechanical Protocol
3
4 A
7 A
10
11

Unfortunately, none of the HBEC cultures was able to be maintained after 4 weeks in culture. Confluence was never obtained even by keeping medium quality by changing frequently the medium. Additionally, following the trypsinization process, only one of the trypsinized cells was able to re-attach to the gelatin matrix-coated surface of the culture flasks. The remaining attempts to use different matrixes such as collagen type I, fibronectin and laminin, either isolated or combined, revealed unsuccessful. These results confirmed that the lack of a real supportive layer, such as fibroblasts, like happens *in vivo* in the bronchus,

rendered very difficult the development of a confluent epithelial layer, as the cells' proliferation was very reduced, being dependent of growth factors secreted from the connective tissue, namely integrins and collagen.

Thus, as the alternatives to obtain stable primary cultures of HBEC failed, the commercial human bronchial epithelial cell line BEAS-2B was used instead in the co-culture experiments with Cr(VI)-induced senescent fibroblasts.

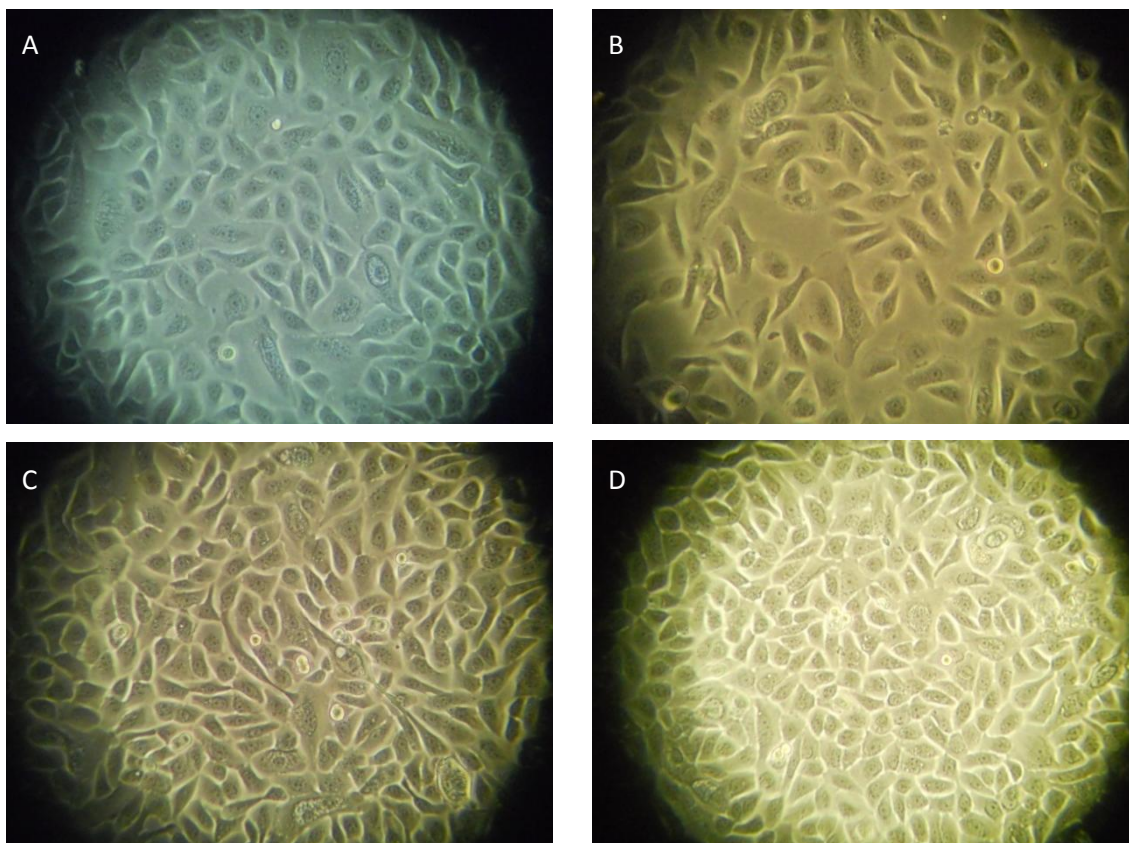


**Figure 3.3:** Representative images of the morphology of epithelial cell cultures obtained using the mechanical protocol: Culture 3 (A), 4A (B), 10 (C), 7A (D), all magnified 100X.

### **3.3. Cr(VI) EXPOSURE CONDITIONS THAT INDUCE SENESCENCE ON HUMAN BRONCHIAL FIBROBLASTS (HBF)**

Several experiments were performed to induce an irreversible state of senescence on fibroblasts. For this purpose several primary cultures of HBF were used and their respective passage number is illustrated in **Table 3.3**.

The primary cultures of HBF used were: HFP6, CBR, previously prepared and used from passage 8 and passage 3 onwards respectively, as well as Geneva1, used from passage 4 onwards.

**Table 3.3:** Primary HBF cultures used in the senescence experiments.

Primary Culture	Starting Passage	Final Passage
HFP6	8	17
CBR	3	12
Geneva1	4	6

### 3.3.1. DETERMINATION OF THE Cr(VI) EXPOSURE CONDITIONS THAT INDUCE GROWTH ARREST

Initially, the experiments with HFP6 bronchial fibroblasts were performed to evaluate: (i) time and Cr(VI) concentrations that would induced morphologic changes associated with the emergence of the senescent phenotype; (ii) the ideal cell density to start up the cultures in order to achieve, at the end of one week in culture, a cell density that would avoid quiescence as result of confluence; (iii) a cell density that would give rise to enough cells to cover the bottom of transwells to be used in the co-cultures.

Based on the work from the Lab [Rodrigues *et al.*, 2009; Costa *et al.*, 2011], the concentrations of Cr(VI) tested ranged from 0.1 to 4  $\mu$ M, as Cr(VI) exposures < 1  $\mu$ M induced proliferation of BEAS-2B, while 1  $\mu$ M Cr(VI) induced cells' malignant transformation. Conversely, concentrations > 1  $\mu$ M Cr(VI) induced BEAS-2B cells' death [Rodrigues *et al.*, 2009; Costa *et al.*, 2011].

**Table 3.4:** Experiments using HFP6 passage 9 and 10 fibroblasts. In the experiments with HFP6 passage 9, Cr(VI) was added on day 1 after plating, and cells were cultured for additional 3 days. In the experiments with HFP6 passage 10, Cr(VI) was added on day 3 after plating and cells were cultured for additional 4 days. Control experiments were performed similarly but in the absence of Cr(VI).

HFP6 Passage Number	Cell Density (cell/cm <sup>2</sup> )	[Cr(VI)] (μM)	Days							
			0	1	2	3	4	5	6	7
9	50000	0.1	Plating	Addition of Cr(VI)						
		0.5								
		1								
		2								
		2								
10	50000	0.1	Plating			Addition of Cr(VI)				
		0.5								
		1								
		2								
		4								

As illustrated in **Table 3.4** in the experiments using HFP6 passage 9, Cr(VI) was added one day after plating, and cells were cultivated for additional 3 days without changing the medium. In the experiments with HFP6 passage 10, Cr(VI) was added on day 3 after plating and cells were cultivated for additional 4 days without changing the medium.

**Figure 3.4** illustrates the morphological changes observed in HFP6 passage 9 cells, 3 days exposed to 2 μM Cr(VI). The images revealed that Cr(VI) induced changes on both the cells' number and morphology, as cells exposed to the oxyanion display a rounder shape. Lower Cr(VI) concentrations induced less visible effects as revealed in **Figure 3.4**.

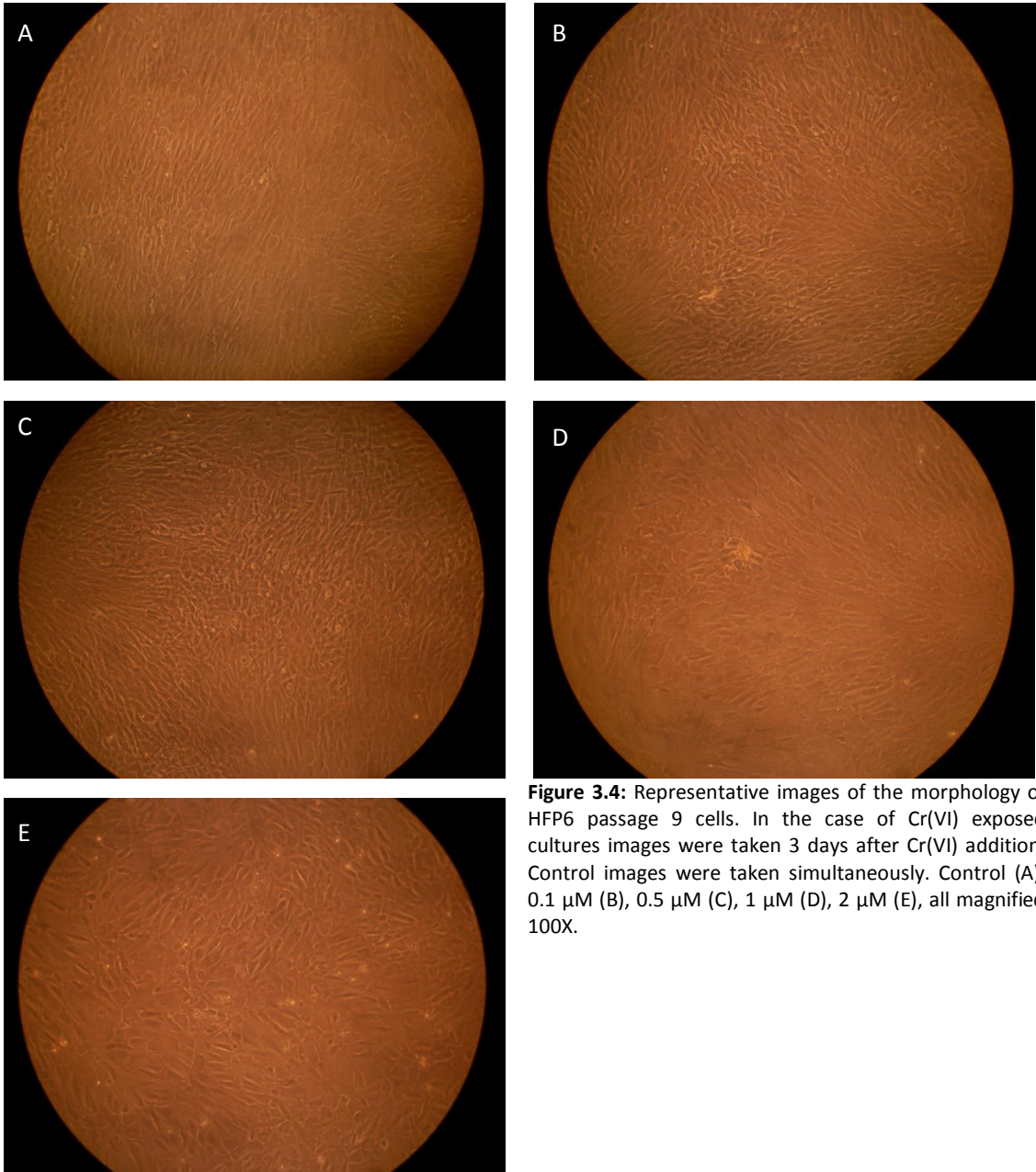


**Figure 3.4:** Representative images of the morphology of HFP6 passage 9 cells. In the case of Cr(VI) exposed cultures images were taken 3 days after Cr(VI) addition, Control images were taken simultaneously. Control (A), 0.1  $\mu$ M (B), 0.5  $\mu$ M (C), 1  $\mu$ M (D), 2  $\mu$ M (E), all magnified 100X.

As to the experiments performed with HFP6 passage 10, even though Cr(VI) was added when cells were already at the exponential growth phase and, as such, more resistant, the longer exposure time (4 days) to higher Cr(VI) concentrations (2 and 4  $\mu$ M) induced some cell death. The cell death can be seen by the increasing amount of floating round cells in cultures (brighter round spots on **Figure 3.5**), as well as a rounder and darker tone to the cells in the same figure. As illustrated in **Figure 3.5**, 4 days exposure to 1  $\mu$ M Cr(VI) induced, in HFP6 passage 10 fibroblasts, morphologic changes similar to the ones observed in HFP6 passage 9 fibroblasts exposed 3 days to 2  $\mu$ M Cr(VI) (**Figure 3.4**).

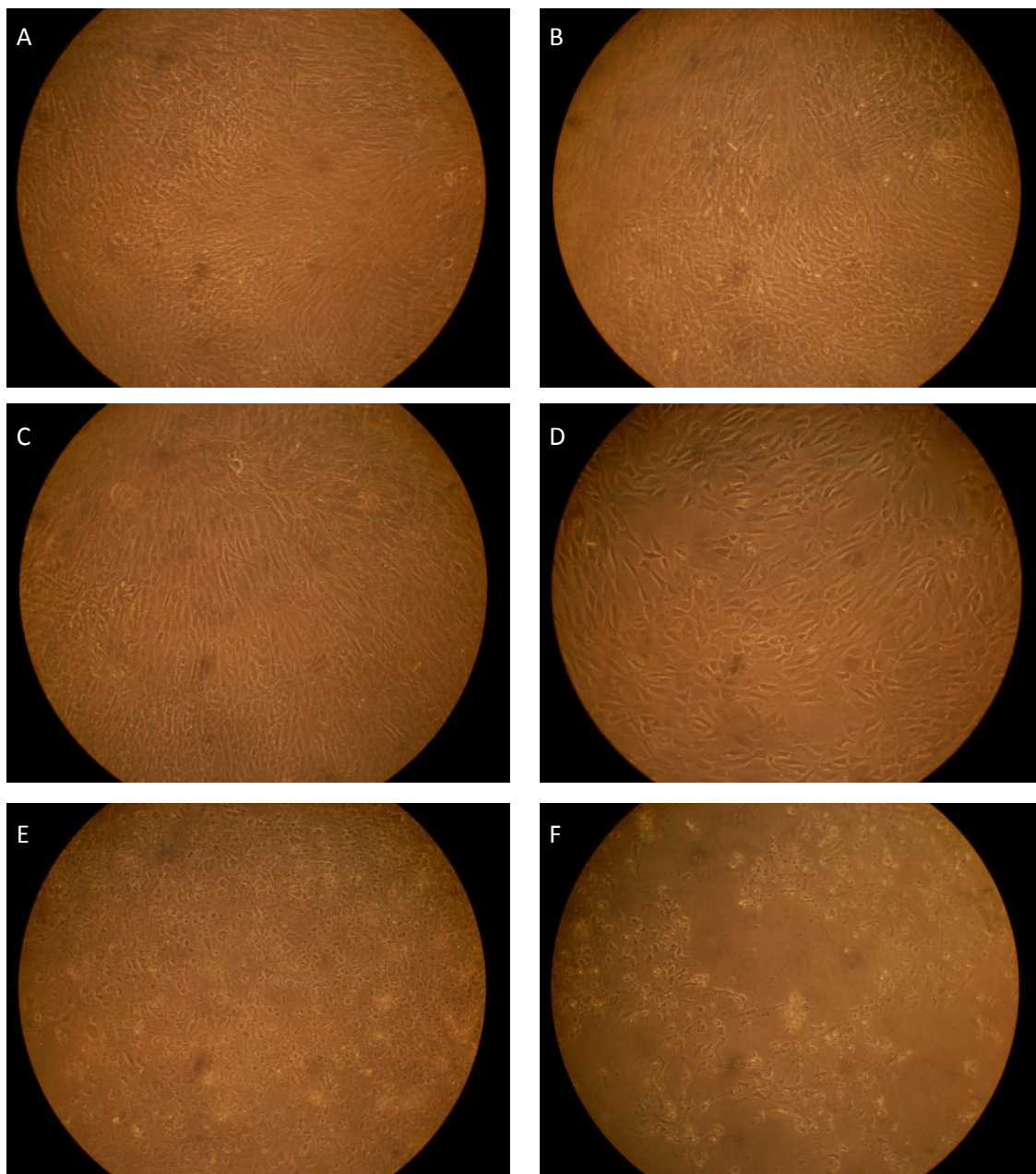


**Figure 3.5:** Representative images of the morphology of HFP6, passage 10 cells, at day 7 in culture. In the case of Cr(VI) exposed cultures images were taken 4 days after Cr(VI) addition. Control (A), 0.1  $\mu\text{M}$  (B), 0.5  $\mu\text{M}$  (C), 1  $\mu\text{M}$  (D), 2  $\mu\text{M}$  (E), 4  $\mu\text{M}$  (F), all magnified 100X.

As Cr(VI) concentration decreases along time in culture, due to Cr(VI) cellular uptake it was decided to frequently replace the medium by fresh one with Cr(VI). Doing so the main goal was to evaluate whether exposing cells to a more uniform Cr(VI) concentration would induce more distinct changes.

Additionally, the cell density was reduced to 20000 cells/cm<sup>2</sup>, as these would be the ideal cell density to be used in the co-cultures experiments accordingly to Chanson and

collaborators [Wiszniewski *et al.*, 2006]. Moreover, as results revealed, increasing the cell density would lead to early to confluence.

**Table 3.5:** Experiments using HPF6 fibroblasts, passage 11. In Condition 1 experiments, Cr(VI) was added just once at day 1. In Condition 2, experiments the medium containing Cr(VI) was replaced on day 2 by fresh medium with Cr(VI). In Condition 3 experiments the medium containing Cr(VI) was replaced on days 2 and 3, by fresh medium with Cr(VI). In Conditions 4-6 experiments the medium replacement schedule, after the first Cr(VI) addition, was as in previous Conditions 1-3 experiments. Control experiments were performed similarly but in the absence of Cr(VI). Morphological changes were observed at day 8.

Experiment	Passage Number	Cell Density (cell/cm <sup>2</sup> )	[Cr(VI)] (μM)	Days								
				0	1	2	3	4	5	6	7	
<b>Condition 1</b> (Cr(VI) was added once 24h after plating)	11	20000	<b>0.5</b> <b>1</b> <b>2</b>	Plating	Addition of Cr(VI)							
<b>Condition 2</b> (As in Condition 1 but medium was replaced once)	11	20000			Addition of Cr(VI)	Addition of Cr(VI)						
<b>Condition 3</b> (As in Condition 1 but medium was replaced twice)	11	20000			Addition of Cr(VI)	Addition of Cr(VI)	Addition of Cr(VI)					
<b>Condition 4</b> (Cr(VI) was added once 48 h after plating)	11	20000				Addition of Cr(VI)						
<b>Condition 5</b> (As in Condition 4 but medium was replaced once)	11	20000				Addition of Cr(VI)	Addition of Cr(VI)					
<b>Condition 6</b> (As in Condition 4 but medium was replaced twice)	11	20000				Addition of Cr(VI)	Addition of Cr(VI)	Addition of Cr(VI)				

In these experiments, cell death was observed in both 1 μM and 2 μM Cr(VI)-exposed HFP6 (passage 11). These results are easily explained considering that the cells' density was less than half the density used in previous experiments and, consequently, the Cr(VI) concentration each cell was exposed to, almost duplicate. The morphologic changes, more rounded shaped cells, and the decreased cellular proliferation ability (as evaluated by trypan blue) observed in 0.5 μM Cr(VI)-exposed HFP6 cells (passage 11), were similar to the changes observed in previous experiments with 1 μM Cr(VI)-exposed HPF6 passage 10 (**Figure 3.5 D**) (**Figure 3.6**).

Nevertheless, it could be observed that a single addition of 1 μM of Cr(VI), 48h after cells' plating (Condition 4), did not induce cell death but, morphologic changes similar to the ones observed 4 days after 1 μM Cr(VI) addition to HPF6 passage 10 cells (**Figures 3.5,D and 3.6, F,G**). Similar effects were observed in HPF6 passage 11 fibroblasts cultures, at day 7, following repetitive exposure to 0.5 μM Cr(VI) (Condition 3 experiments) (**Figure 3.6, C**).

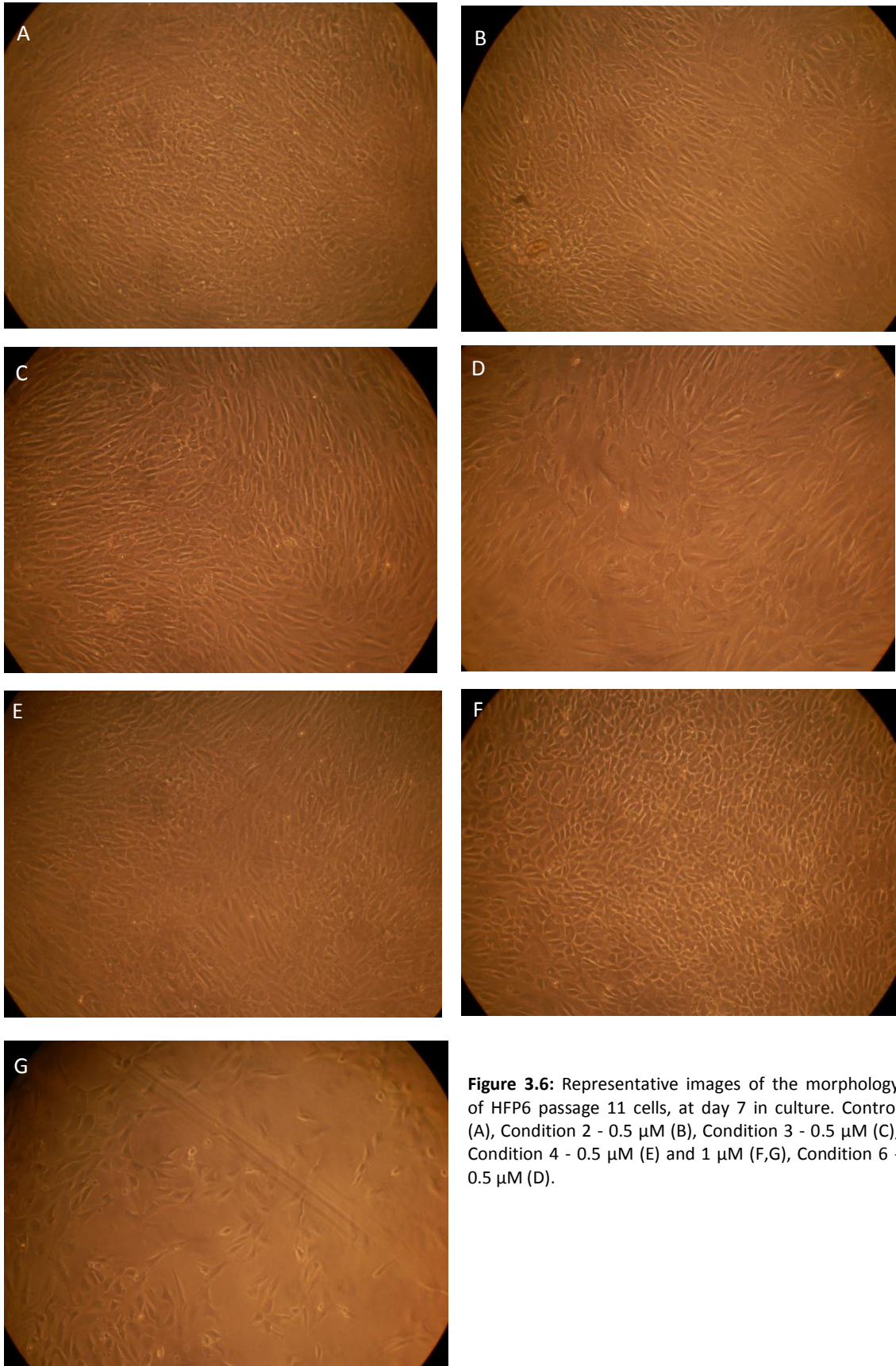


**Figure 3.6:** Representative images of the morphology of HFP6 passage 11 cells, at day 7 in culture. Control (A), Condition 2 - 0.5  $\mu\text{M}$  (B), Condition 3 - 0.5  $\mu\text{M}$  (C), Condition 4 - 0.5  $\mu\text{M}$  (E) and 1  $\mu\text{M}$  (F,G), Condition 6 - 0.5  $\mu\text{M}$  (D).

As revealed by the trypan blue assay and illustrated in **Figure 3.7**, HFP6 passage 11 cultures exposed to 0.5  $\mu\text{M}$  Cr(VI), except Condition 3 exposed cells, proliferate after a week in culture. Most important was the finding that for 1  $\mu\text{M}$  Cr(VI) Condition 4, the change in HFP6 passage 11 cells' morphology and the constant cell number along the 7 days cultivation suggested the emergence of a senescent-like phenotype (**Figure 3.6**).

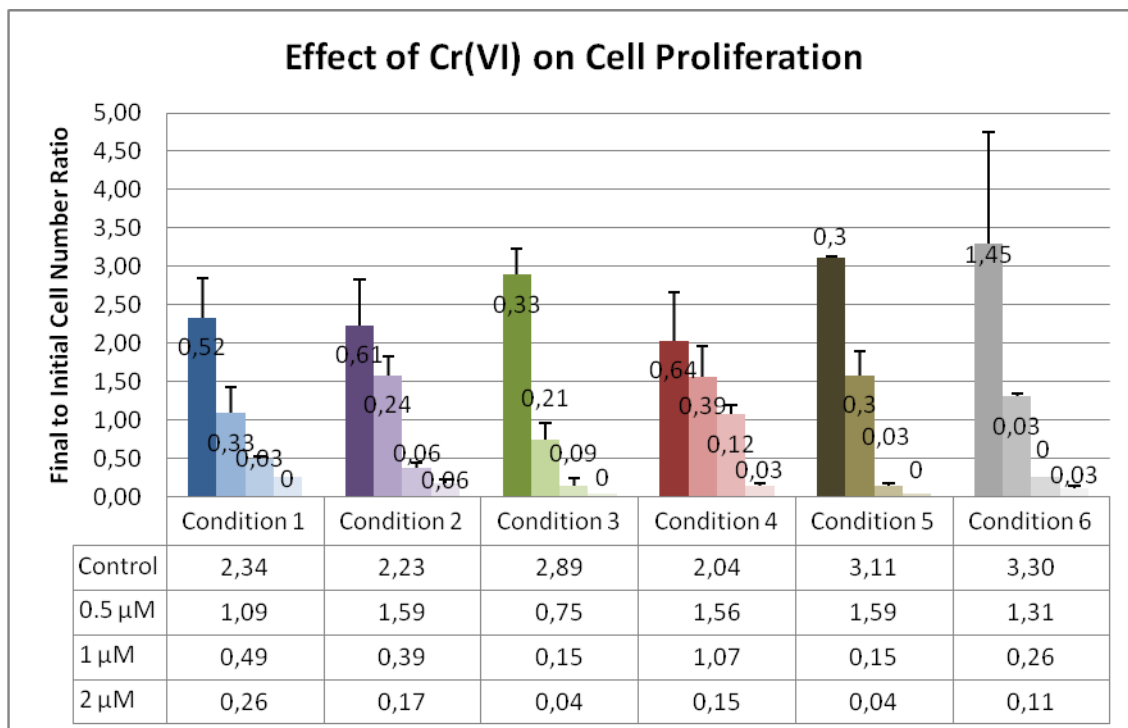


**Figure 3.7:** Cr(VI) effects on HFP6 passage 11 cells' proliferation. The number of cells, at day 7 in culture, was evaluated by trypan blue assay. The results, expressed as the ratio of final to initial cells' number in each culture, are the mean  $\pm$  SD of at least three experiments carried out in triplicate.

All these results have showed that there is a great dependence on cell density, resulting of which the Cr(VI)-exposure effect will vary. Also, the time of addition of Cr(VI) is also an important variable, as cell density will increase with time, therefore diminishing the Cr(VI) effect. Also, passage number is presented as a variable due to progressive loss of replication capacity as senescence is an aging-related process.

In order to evaluate whether the Cr(VI) effects were dependent upon HFP6 cells' passage number, the experiments were repeated [except conditions 5 and 6, as well as 2  $\mu\text{M}$  Cr(VI) exposures] using HFP6 passage 13 fibroblasts. Cells' counting was performed the day after the last Cr(VI) addition and at day 7 in culture (**Table 3.6**) using the trypan blue method.

**Table 3.6:** Experiments using HPF6 passage 13. In Condition 1 experiments Cr(VI) was added just once at day 1. In Condition 2 experiments the medium containing Cr(VI) was replaced on day 2 by fresh medium with Cr(VI). In Condition 3 experiments the medium containing Cr(VI) was replaced on days 2 and 3, by fresh medium with Cr(VI). In Conditions 4 experiments Cr(VI) was added just once at day 2. Control experiments were performed similarly but in the absence of Cr(VI). Morphological changes were observed at day 7.

Experiment	Passage Number	Cell Density (cell/cm <sup>2</sup> )	[Cr(VI)] (μM)	Days								
				0	1	2	3	4	5	6	7	
<b>Condition 1</b> (Cr(VI) was added once 24h after plating)	13	20000	0.5	Plating	Addition of Cr(VI)	Cell Count						Cell Count
<b>Condition 2</b> (As in Condition 1 but medium was replaced once)	13	20000			Addition of Cr(VI)	Addition of Cr(VI)	Cell Count				Cell Count	
<b>Condition 3</b> (As in Condition 1 but medium was replaced twice)	13	20000	1		Addition of Cr(VI)	Addition of Cr(VI)	Addition of Cr(VI)	Cell Count			Cell Count	
<b>Condition 4</b> (Cr(VI) was added once 48 h after plating)	13	20000				Addition of Cr(VI)	Cell Count				Cell Count	

The addition of Cr(VI) 24h after cells' plating (**Conditions 1 and 3**) lead to extensive cell death, more pronounced under Condition 3 experimental conditions (**Table 3.7**). The surviving cells gained rounded-like shape morphology 72h after being exposed to Cr(VI) (**Figure 3.8**). Under Conditions 4 experimental conditions (addition of Cr(VI) 48 hours after plating), decreased cell death was observed in HPF6 passage 13 fibroblasts exposed to 1 μM Cr(VI) and for 0.5 μM Cr(VI) exposures the number of cells remained constant since Cr(VI) addition (**Table 3.7**). In spite of the constant cell number cells lose their spindled-like shape and very quickly gained flat rounded shape morphology (**Figure 3.8**).

**Table 3.7:** Experiments using HFP6 passage 13. Control experiments were performed in the absence of Cr(VI). Cells' counting was performed 24 hours after Cr(VI) addition and at day 8 in culture. The results are expressed as the ratio of initial to final cells' number, and represent the mean  $\pm$  SD of at least three experiments carried out in triplicate.

Experiment	Passage Number	Cell Density (cell/cm <sup>2</sup> )	[Cr(VI)] ( $\mu$ M)	Ratio of Initial to Final Cells' Number				
				After Cr(VI) Exposure	SD value	One Week of Culture	SD value	$\Delta$ Ratio
<b>Condition 1</b> (Cr(VI) was added once 24h after plating)	13	20000	Control	2,71	0,38	5,93	0,80	3,22
			0.5	2,04	0,05	0,00	0,00	-2,04
			1	0,81	0,15	0,01	0,00	-0,80
<b>Condition 2</b> (As in Condition 1 but medium was replaced once)	13	20000	Control	3,57	0,33	5,62	0,83	2,05
			0.5	0,60	0,15	0,36	0,00	-0,24
			1	0,29	0,00	0,01	0,00	-0,28
<b>Condition 3</b> (As in Condition 1 but medium was replaced twice)	13	20000	Control	4,38	0,41	6,74	0,73	2,36
			0.5	0,48	0,11	0,19	0,15	-0,29
			1	0,14	0,00	0,07	0,00	-0,07
<b>Condition 4</b> (Cr(VI) was added once 48 h after plating)	13	20000	Control	3,40	0,15	5,24	0,69	1,84
			0.5	3,05	0,32	3,36	0,00	0,31
			1	2,88	0,22	2,33	0,30	-0,55

As illustrated in **Table 3.7**, the addition of Cr(VI) 24 hours after cells' plating lead to extensive cell death, while the addition of Cr(VI) 48 hours after plating lead to growth arrest, this one more pronounced in the 0.5  $\mu$ M exposures.

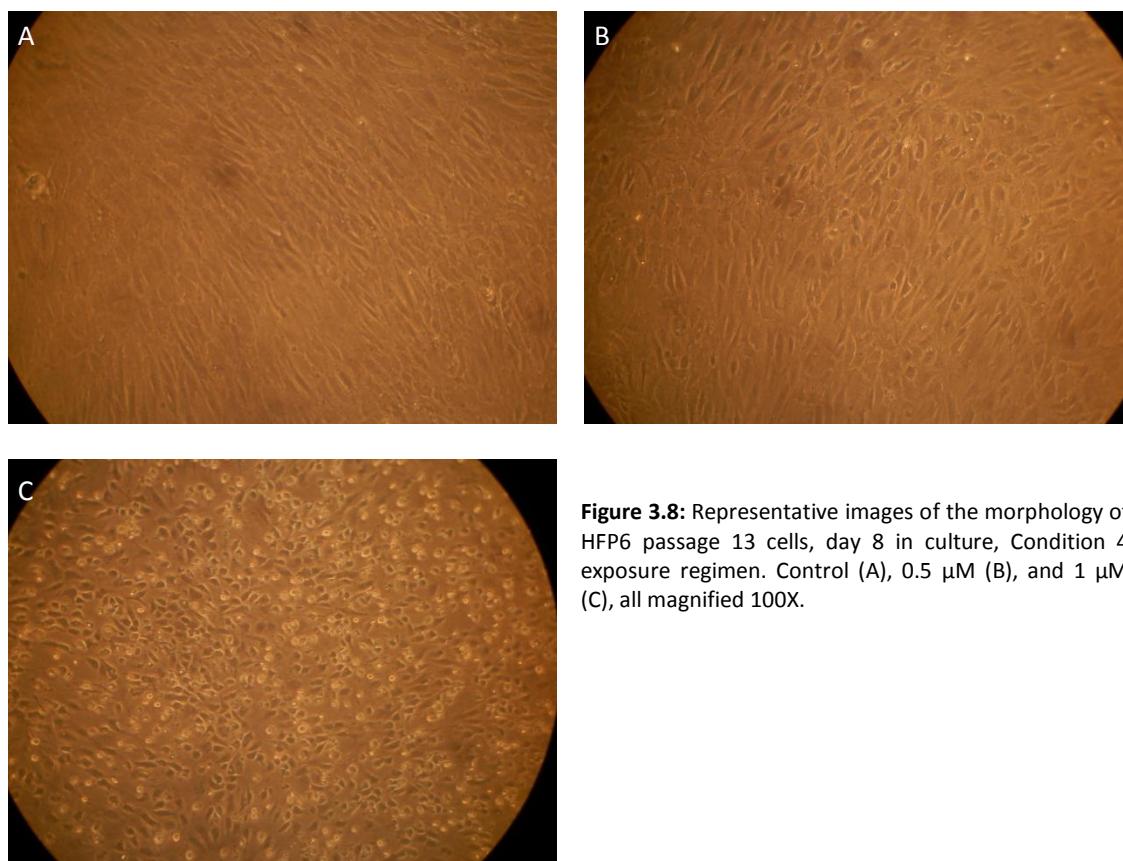


**Figure 3.8:** Representative images of the morphology of HFP6 passage 13 cells, day 8 in culture, Condition 4 exposure regimen. Control (A), 0.5  $\mu$ M (B), and 1  $\mu$ M (C), all magnified 100X.

These last results confirm that there was a great dependence on cell passage, as concentrations previously non-lethal had become lethal after just two cell passages, especially in conditions when Cr(VI) is added just 24h after plating. This particular result can indicate that cell-adhesion was the most affected process by passage number increase, as cells were easily detached and started floating after Cr(VI) exposure.

### **3.3.2. DETERMINATION OF THE Cr(VI) EXPOSURE CONDITIONS THAT INDUCED SENESENCE**

Accordingly to Chanson and collaborators [**Wiszniewski *et al.*, 2006**], human airway epithelial cells (HAEC) co-cultivated with HBF differentiate into ciliated cells. For this to happen, HAEC were grown for four weeks in transwells undercoated with fibroblasts under submerged conditions with the growth medium being refreshed every 2 days [**Wiszniewski *et al.*, 2006**].

To evaluate whether Cr(VI)-induced senescent HBF would induce transformation (and not differentiation) on bronchial epithelial cells it was imperative to find which Cr(VI) exposure conditions would induce HBF senescence and whether this senescent cells would be able to sustain continuous long-term exposure (four weeks) and remain senescent.

Having in mind that 0.5  $\mu\text{M}$  Cr(VI), added 48 hours after fibroblasts plating, induced growth arrest and morphologic changes that suggested the emergence of cells with senescence phenotype (section 3.3.1), primary cultures of HBF, identified as CBR (passage 4 and 5) were exposed, 48 hours after plating, to 0.05 to 0.75  $\mu\text{M}$  Cr(VI) with medium changed every two days for four weeks (**Tables 3.8 and 3.9**). Cells' viability and number, evaluated by the MTT and trypan blue assays, was determined every two or four days of culture to know whether cells' were able to sustain long-term Cr(VI) insults, without reversing the senescent phenotype or dying. Experiments were also performed with CBR passage 5 fibroblasts to evaluate whether passage number was interfering with the results (**Table 3.9**).

**Table 3.8:** Experiments using CBR passage 4 fibroblasts. In all experiments Cr(VI) was added 48 days after cells' plating and the medium renewed every two days. Control experiments were performed similarly but in the absence of Cr(VI). Cells' viability was evaluated by MTT every two days.

Experiment											
[Cr(VI)] ( $\mu\text{M}$ )	Passage Number	Cell Density (cell/cm <sup>2</sup> )	Days								
			0	1	2	3	4	5	6	7	8
Control	4	20000	Plating		Cell Viability		Cell Viability		Cell Viability		Cell Viability
0.05	4	20000			Addition of Cr(VI) Cell Viability		Addition of Cr(VI) Cell Viability		Addition of Cr(VI) Cell Viability		Cell Viability
0.1	4	20000			Addition of Cr(VI) Cell Viability		Addition of Cr(VI) Cell Viability		Addition of Cr(VI) Cell Viability		Cell Viability
0.25	4	20000			Addition of Cr(VI) Cell Viability		Addition of Cr(VI) Cell Viability		Addition of Cr(VI) Cell Viability		Cell Viability
0.5	4	20000			Addition of Cr(VI) Cell Viability		Addition of Cr(VI) Cell Viability		Addition of Cr(VI) Cell Viability		Cell Viability
0.75	4	20000			Addition of Cr(VI) Cell Viability		Addition of Cr(VI) Cell Viability		Addition of Cr(VI) Cell Viability		Cell Viability

**Table 3.9:** Experiments using CBR passage 5 fibroblasts. In all experiments Cr(VI) was added 48 days after cells' plating and the medium renewed every two days. Control experiments were performed similarly but in the absence of Cr(VI). Cells' viability and number were evaluated by MTT and trypan blue assays every two days.

Experiment											
[Cr(VI)] ( $\mu\text{M}$ )	Passage Number	Cell Density (cell/cm <sup>2</sup> )	Days								
			0	1	2	3	4	5	6	7	8
Control	5	20000	Plating		Cell Viability		Cell Viability		Cell Viability		Cell Viability
0.1	5	20000			Addition of Cr(VI) Cell Viability		Addition of Cr(VI) Cell Viability		Addition of Cr(VI) Cell Viability		Cell Viability
0.25	5	20000			Addition of Cr(VI) Cell Viability		Addition of Cr(VI) Cell Viability		Addition of Cr(VI) Cell Viability		Cell Viability
0.5	5	20000			Addition of Cr(VI) Cell Viability		Addition of Cr(VI) Cell Viability		Addition of Cr(VI) Cell Viability		Cell Viability

As illustrated in **Figures 3.9** and **3.10**, cells continuously exposed to 0.5  $\mu\text{M}$  did not proliferate, visibly delaying their growth when compared to lower Cr(VI) concentration exposures. Conversely, cell death was observed in cultures exposed to 0.75  $\mu\text{M}$  Cr(VI) (**Figure 3.9**). As shown in **Figures 3.9** and **3.10** low passage number cells' portrayed similar behaviour.

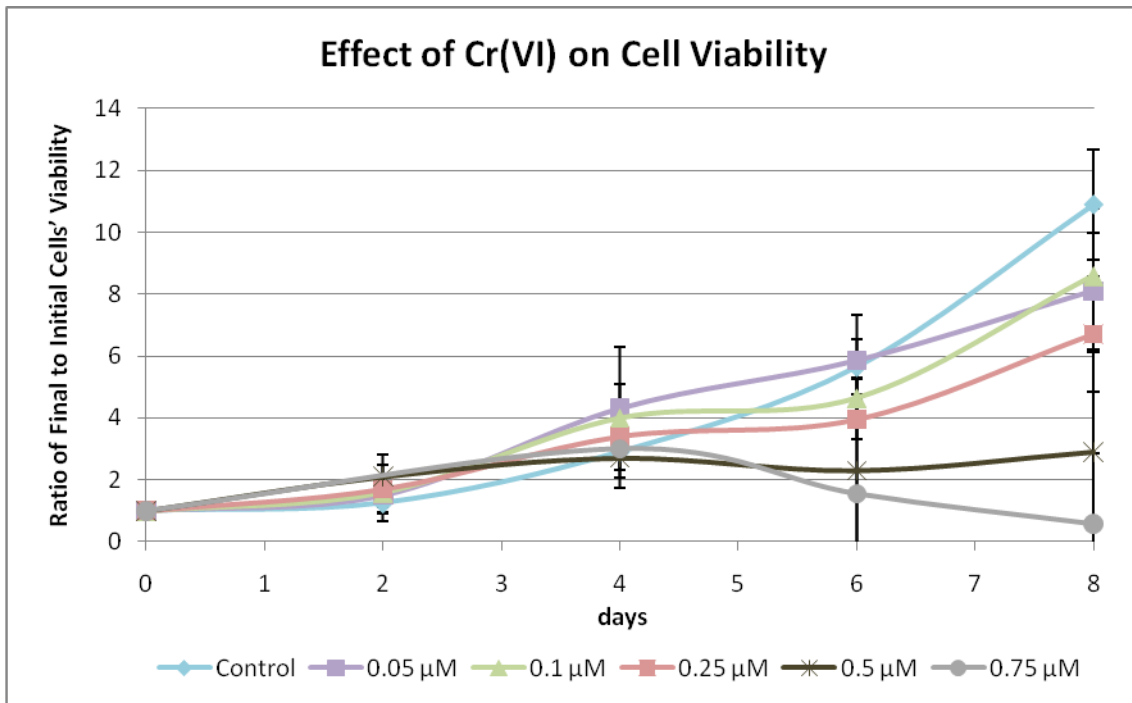


**Figure 3.9:** Cr(VI) effects on in CBR passage 4 cells viability. The cell viability in culture was evaluated by MTT assay every two days. The results, expressed as the ratio of final to initial cells' viability are the mean  $\pm$  SD of at least experiments carried out in triplicate.

**Table 3.10:** Cr(VI) effects on in CBR passage 4 cells viability. The cell viability in culture was evaluated by MTT assay every two days. The results, expressed as the Ratio of final to initial cells' viability are the mean  $\pm$  SD of at least experiments carried out in triplicate.

[Cr(VI)] ( $\mu$ M)	Passage Number	Cell Density (cell/cm <sup>2</sup> )	Days							
			2	SD Value	4	SD Value	6	SD Value	8	SD Value
Control	4	20000	1,25	0,58	2,90	0,27	5,65	0,89	10,90	1,79
0.05	4	20000	1,50	0,55	4,30	1,99	5,85	1,48	8,10	1,88
0.1	4	20000	1,60	0,48	4,00	1,08	4,65	0,65	8,60	2,16
0.25	4	20000	1,70	0,78	3,40	0,45	3,95	0,65	6,70	1,87
0.5	4	20000	2,10	0,69	2,70	0,65	2,30	2,96	2,90	3,21
0.75	4	20000	ND	ND	3,00	1,24	1,55	3,03	0,58	2,29

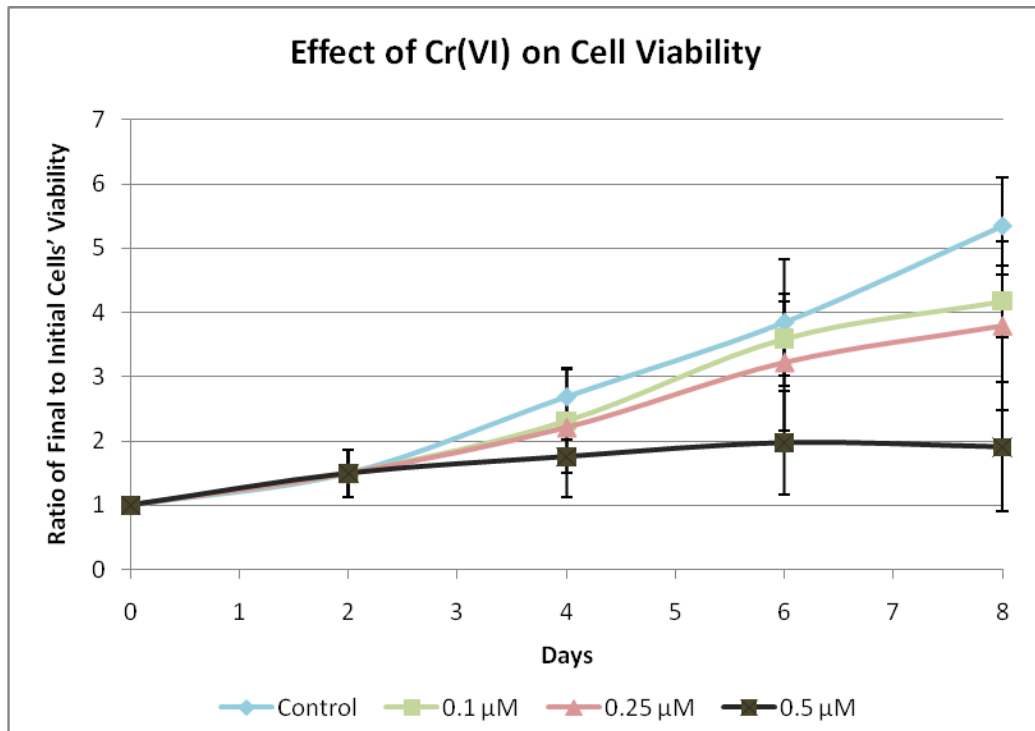


**Figure 3.10:** Cr(VI) effects on in CBR passage 5 cells viability. The cell viability in culture was evaluated by MTT assay every two days. The results, expressed as the ratio of final to initial cells' viability are the mean  $\pm$  SD of at least experiments carried out in triplicate.

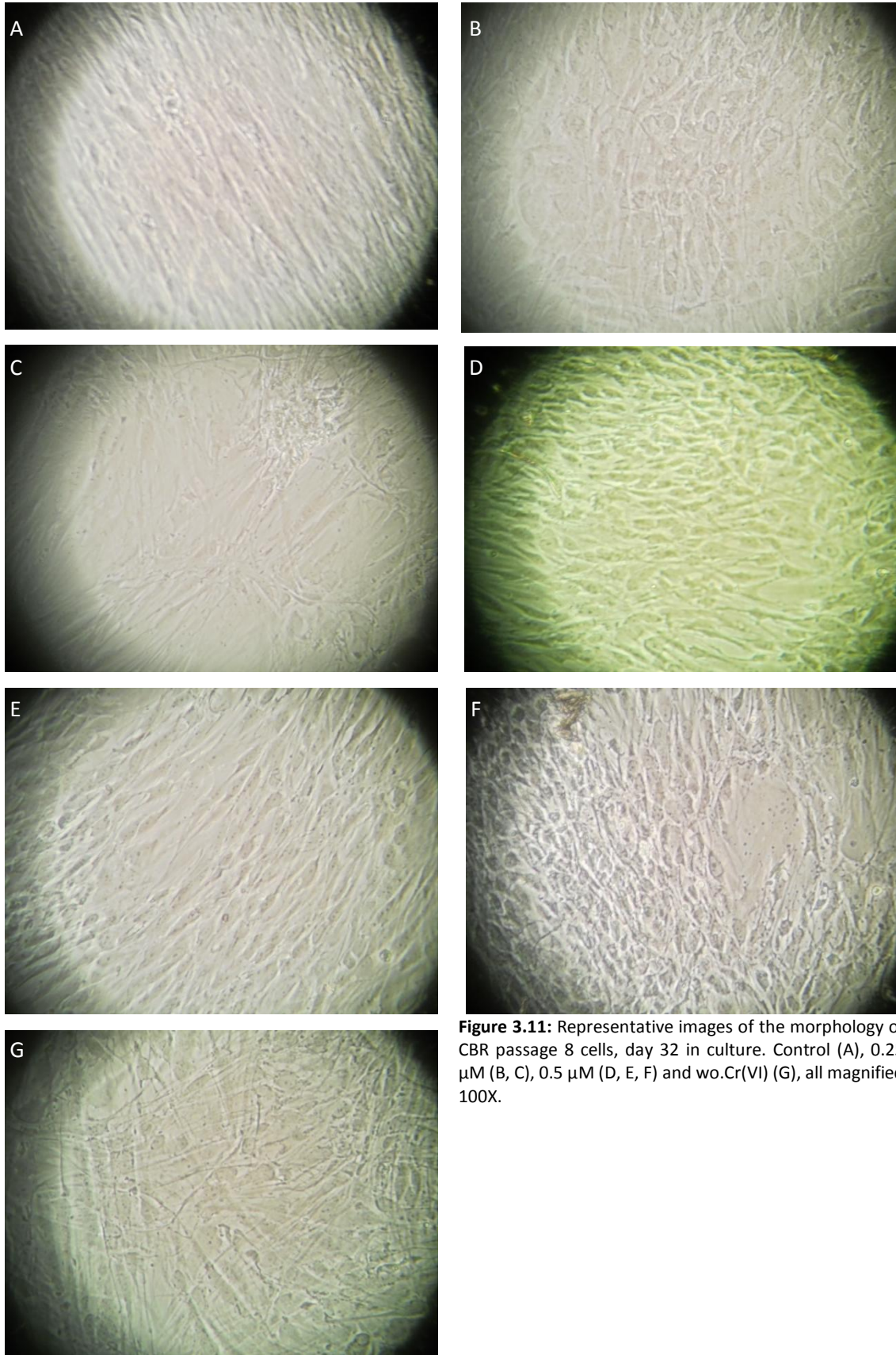
**Table 3.11:** Cr(VI) effects on in CBR passage 5 cells viability. The cell viability in culture was evaluated by MTT assay every two days. The results, expressed as the ratio of final to initial cells' viability are the mean  $\pm$  SD of at least experiments carried out in triplicate.

[Cr(VI)] ( $\mu$ M)	Passage Number	Cell Density (cell/cm <sup>2</sup> )	Ratio of Final to Initial cells' Viabilit y	Days							
				2	SD Value	4	SD Value	6	SD Value	8	SD Value
Control	5	20000		1,50	0,37	2,69	0,45	3,84	0,99	5,34	0,76
0.1	5	20000		1,50	0,37	2,31	0,80	3,59	0,57	4,18	0,56
0.25	5	20000		1,50	0,37	2,21	0,18	3,22	1,07	3,79	1,31
0.5	5	20000		1,50	0,37	1,75	0,63	1,97	0,80	1,90	1,00

Finally, four week-long experiments were performed using 0.25 and 0.5  $\mu$ M Cr(VI) concentrations and CBR passage 8 cells. Cr(VI) containing medium was renewed every two days (Table 3.12). Additionally, experiments without Cr(VI) [wo.Cr(VI)] were carried out to evaluate if in the absence of a continuous Cr(VI) insult the emergent phenotype would reverse. To this end, cells were exposed to 0.5  $\mu$ M Cr(VI), with constant Cr(VI) containing medium renewal every two days for a week. Thereafter, medium without Cr(VI) was added and renewed every two days for the next three weeks (Table 3.12). Senescence-associated  $\beta$ -galactosidase staining kit was used to evaluate the emergence of senescence phenotype along cultures and the senescence levels.

**Table 3.12:** Experiments using CBR passage 8 cells. In all experiments Cr(VI) was added 48 hours after cells' plating and the medium renewed every two days along four weeks except in wo. Cr(VI) cultures which were exposed to Cr(VI) just one week as described in Materials and Methods.

Passage Number	8	8	8	8	
Cell Density (cell/cm <sup>2</sup> )	20000	20000	20000	20000	
[Cr(VI)] (μM)	Control	0.25 μM	0.5 μM	wo. Cr(VI)	
Days	0	Plating			
	1				
	2		Addition of Cr(VI)	Addition of Cr(VI)	Addition of Cr(VI)
	3				
	4		Addition of Cr(VI)	Addition of Cr(VI)	Addition of Cr(VI)
	5				
	6		Addition of Cr(VI)	Addition of Cr(VI)	Addition of Cr(VI)
	7				
	8		Addition of Cr(VI)	Addition of Cr(VI)	
	9				
	10		Addition of Cr(VI)	Addition of Cr(VI)	
	11				
	12		Addition of Cr(VI)	Addition of Cr(VI)	
	13				
	14		Addition of Cr(VI)	Addition of Cr(VI)	
	15				
	16		Addition of Cr(VI)	Addition of Cr(VI)	
	17				
	18		Addition of Cr(VI)	Addition of Cr(VI)	
	19				
	20		Addition of Cr(VI)	Addition of Cr(VI)	
	21				
	22		Addition of Cr(VI)	Addition of Cr(VI)	
	23				
	24		Addition of Cr(VI)	Addition of Cr(VI)	
	25				
	26		Addition of Cr(VI)	Addition of Cr(VI)	
	27				
	28		Addition of Cr(VI)	Addition of Cr(VI)	
	29				
	30		Addition of Cr(VI)	Addition of Cr(VI)	
	31				
32	Evaluation of Senescence by β-galactosidase staining				



As can be observed on **Figure 3.11**, cells exposed constantly for four weeks to 0.5  $\mu\text{M}$  Cr(VI) had preponderant rounded-shape morphology, disorganized structure and noticeably less confluence. These characteristics could also be seen on 0.25  $\mu\text{M}$  Cr(VI)-exposed cells, although in a minor extent.

An interesting effect could be observed on wo.Cr(VI) cells. As images on Figure 3.10 revealed, two different cellular sub-populations are visibly co-existing: round-like, possibly senescent cells, on a lower layer and spindled-like, apparently normal, cells on a top layer. The morphologic phenotypes co-existence may suggest that senescent cells, on the top layer, are reversing their phenotype and so recovering the normal phenotype, because the Cr(VI)-pressure was removed. This hypothesis was further supported on evaluating the cells' viability ratio, obtained through MTT assay (**Figure 3.12**).

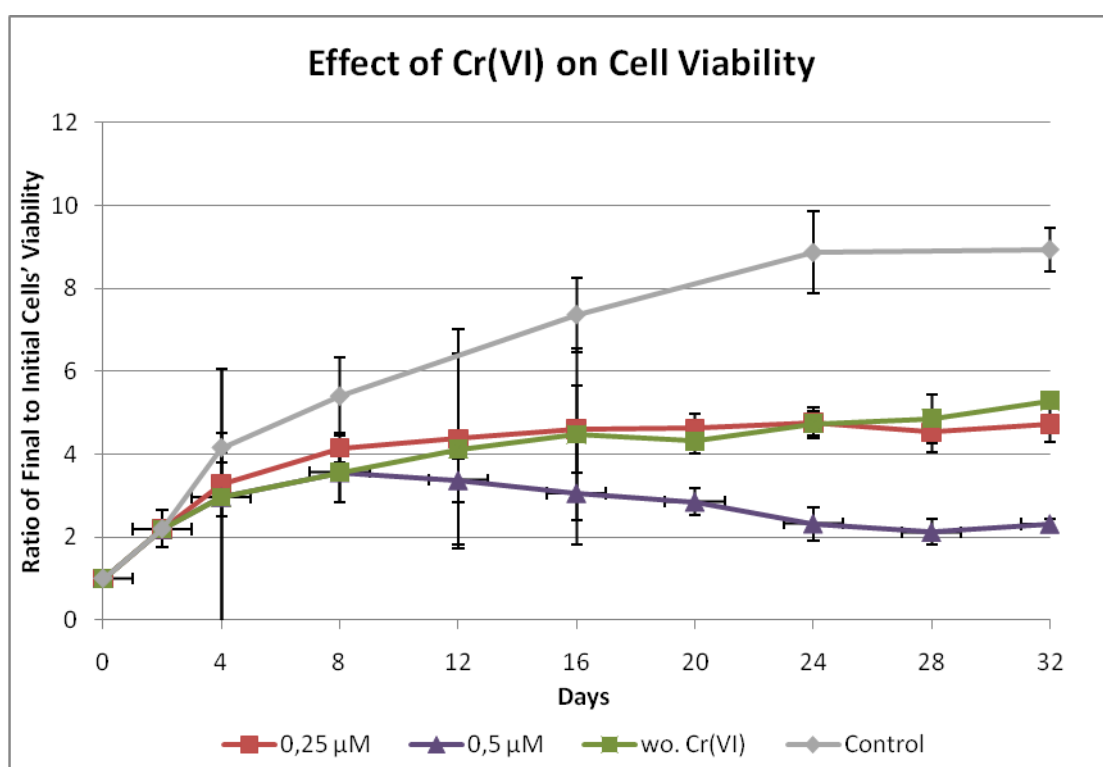


**Figure 3.12:** Cr(VI) effects on in CBR passage 8 cells viability. Cr(VI) addition was carried out 48 hours after cells' plating and the medium replaced every two days along 32 days culture, except for wo.Cr(VI) cell cultures, whose medium contained 0.5  $\mu\text{M}$  Cr(VI) during one week, followed by medium without Cr(VI) during the next three weeks. Control experiments were performed similarly but in the absence of Cr(VI). Cells' viability in culture, was evaluated by MTT assay every four days. The results, expressed as the ratio of final to initial cells' viability are the mean  $\pm$  SD of at least experiments carried out in triplicated.

**Table 3.13:** Cr(VI) effects on in CBR passage 8 cells viability. Cr(VI) addition was carried out 48 hours after cells' plating and the medium replaced every two days along 32 days culture, except for wo.Cr(VI) cell cultures, whose medium contained 0.5  $\mu\text{M}$  Cr(VI) during one week, followed by medium without Cr(VI) during the next three weeks. Control experiments were performed similarly but in the absence of Cr(VI). Cells' viability in culture, was evaluated by MTT assay every four days. The results, expressed as the ratio of final to initial cells' viability are the mean  $\pm$  SD of at least experiments carried out in triplicated.

[Cr(VI)] ( $\mu\text{M}$ )	Passage Number	Cell Density (cell/cm <sup>2</sup> )	Days											
			Ratio of Final to Initial cells' Viability	2	SD Value	4	SD Value	8	SD Value	12	SD Value	16	SD Value	
Control	8	20000	2,20	0,45	4,16	0,34	5,40	0,94	ND	ND	7,36	0,89		
0.25 $\mu\text{M}$	8	20000	2,20	0,45	3,28	0,77	4,15	0,35	4,38	2,65	4,60	1,05		
0.5 $\mu\text{M}$	8	20000	2,20	0,45	2,97	3,09	3,57	0,72	3,38	0,53	3,06	1,25		
wo. Cr(VI)	8	20000	2,20	0,45	2,97	3,09	3,57	0,72	4,13	2,30	4,48	2,06		
Continuation	[Cr(VI)] ( $\mu\text{M}$ )	Passage Number	Cell Density (cell/cm <sup>2</sup> )	Days										
	Ratio of Final to Initial cells' Viability	20	SD Value	24	SD Value	28	SD Value	32	SD Value					
	Control	8	20000	ND	ND	8,87	0,99	ND	ND	8,94	0,53			
	0.25 $\mu\text{M}$	8	20000	4,63	0,34	4,76	0,38	4,53	0,48	4,73	0,42			
	0.5 $\mu\text{M}$	8	20000	2,85	0,32	2,33	0,40	2,12	0,30	2,32	0,13			
wo. Cr(VI)	8	20000	4,31	0,30	4,74	0,30	4,86	0,59	5,29	0,15				

As illustrated (**Figure 3.12**), after 4 weeks, the viability of CBR cells exposed constantly one week to 0.5  $\mu\text{M}$  Cr(VI) (wo.Cr(VI) condition) overlapped the 32 days 0.25  $\mu\text{M}$  Cr(VI) continuously exposed cells. Simultaneously, 0.5  $\mu\text{M}$  Cr(VI)-exposed cells confirm to be growth arrested after approximately three weeks in culture. The hypothesis that this 0.5  $\mu\text{M}$  Cr(VI)-continuous exposed cells were mostly senescent was confirmed by the SA- $\beta$ -gal assay (**Figure 3.13**).

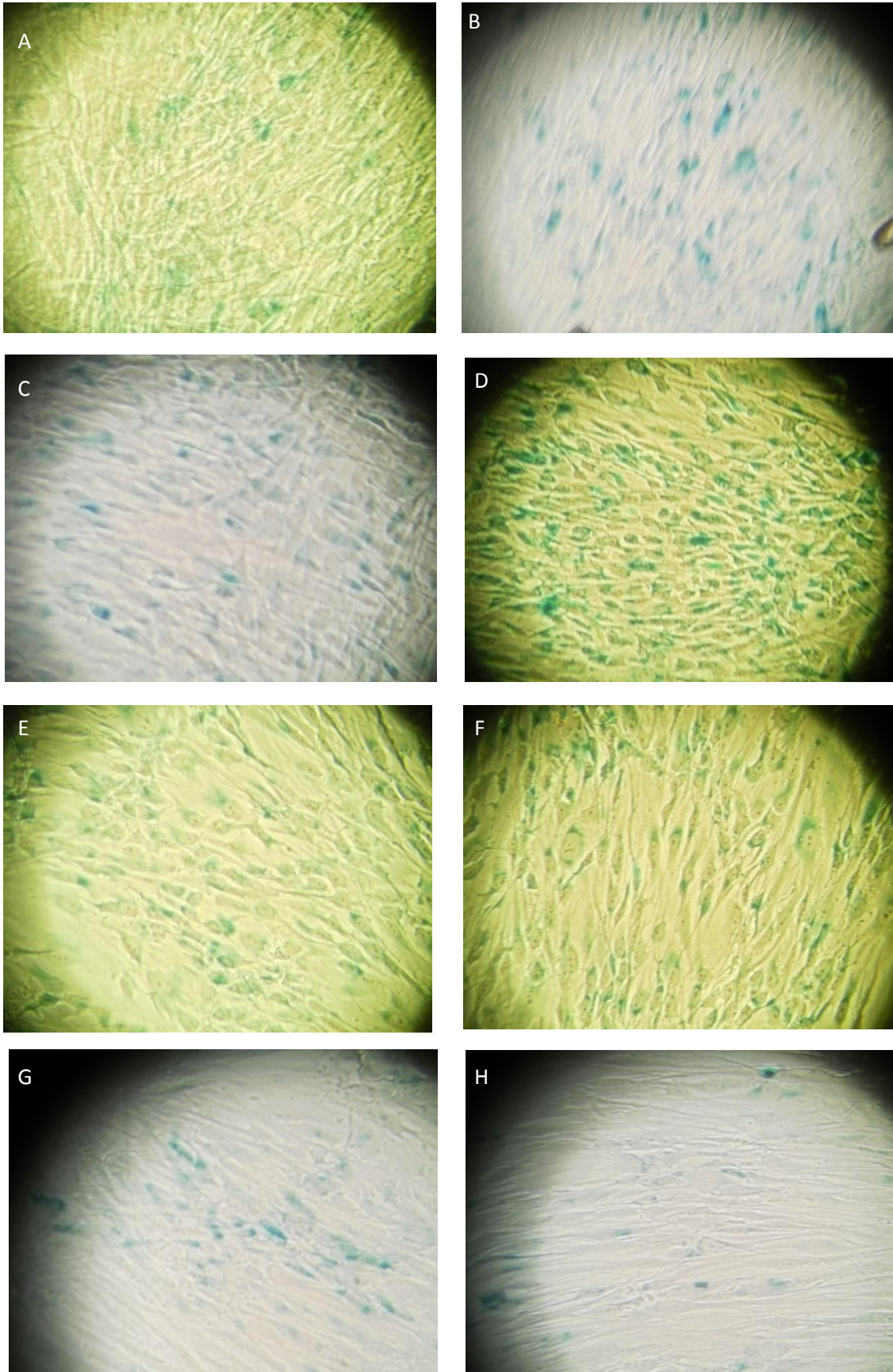


**Figure 3.13:** Representative images of the of CBR passage 8 cells with SA-β-gal senescent staining, day 32 in culture. Control (A), 0.25  $\mu$ M (B, C), 0.5  $\mu$ M (D, E, F) and wo.Cr(VI) (G, H), all magnified 100X.

As pointed up in **Figure 3.12 (D-F)**, the extensive blue staining associated with SA- $\beta$ -gal activity, portrayed by 0.5  $\mu$ M Cr(VI)-exposed cells, revealed that cells had a senescent phenotype. The slight staining observed for 0.25  $\mu$ M Cr(VI)-exposed cells, as well as for control cells, suggested that some of these cells were senescent possibly as result of confluence, more noticeable in the case of control cells (**Figures 3.11 and 3.12 A**). As to wo.Cr(VI) cells, the slight staining observed revealed that the senescent phenotype is reversible once the 0.5  $\mu$ M Cr(VI)-insult is removed (**Figure 3.12 G and H**).

Although hypoxia is known to delay the onset of senescence and in cancerous cells promote cell proliferation [**Welford et al., 2006**] recent work suggested that cycles of hypoxia and food deprivation may induce a state of stress-induced senescence [**Choi et al., 2011**]. Based on these studies, others experiments were carried out attempting to evaluate whether cycles of hypoxia followed by food deprivation would inhibit the senescence reverse observed in wo.Cr(VI) cultures once the Cr(VI)-insult was removed.

For deprivation studies CBR cells, once constantly exposed during a week to 0.5  $\mu$ M Cr(VI)-insult, had their medium changed only once a week instead of every two days. As to hypoxia, CBR cells once exposed a week to 0.5  $\mu$ M Cr(VI)-insult, the multiwell plates were sealed with parafilm although the medium was changed every two days. Combined experiments were also performed, *i.e.*, one week hypoxia followed by another week of food deprivation. Controls were carried out simultaneously with Cr(VI) untreated CBR cells (**Table 3.14**).

**Table 3.14:** Four week-long experiments using CBR passage 9 and 10 cells exposed a week to 0.5  $\mu$ M Cr(VI) and medium renewed with fresh 0.5  $\mu$ M Cr(VI) medium every 2 days for a week. From week two onward, cells were submitted to cycles of hypoxia, deprivation or hypoxia and deprivation. Control experiments were performed in the absence of Cr(VI).

	Condition	Passage Number	Cell Density (cell/cm <sup>2</sup> )		Week			
					1	2	3	4
Hypoxia and Deprivation Cycles	Control	9	20000	Plating	DMEM/F12	DMEM/F12	DMEM/F12	DMEM/F12
	Treated	9	20000		0.5 $\mu$ M Cr(VI)	Hypoxia	Deprivation	Hypoxia
Continuous Hypoxia and Continuous Deprivation	Control	10	20000		DMEM/F12	DMEM/F12	DMEM/F12	DMEM/F12
	Hypoxia	10	20000		0.5 $\mu$ M Cr(VI)	Hypoxia	Hypoxia	Hypoxia
	Deprivation	10	20000		0.5 $\mu$ M Cr(VI)	Deprivation	Deprivation	Deprivation

As revealed by SA- $\beta$ -gal activity staining images, the alternated cycles of hypoxia and deprivation could not inhibit the reversal senescence following removal of the Cr(VI)-insult (**Figure 3.14**).

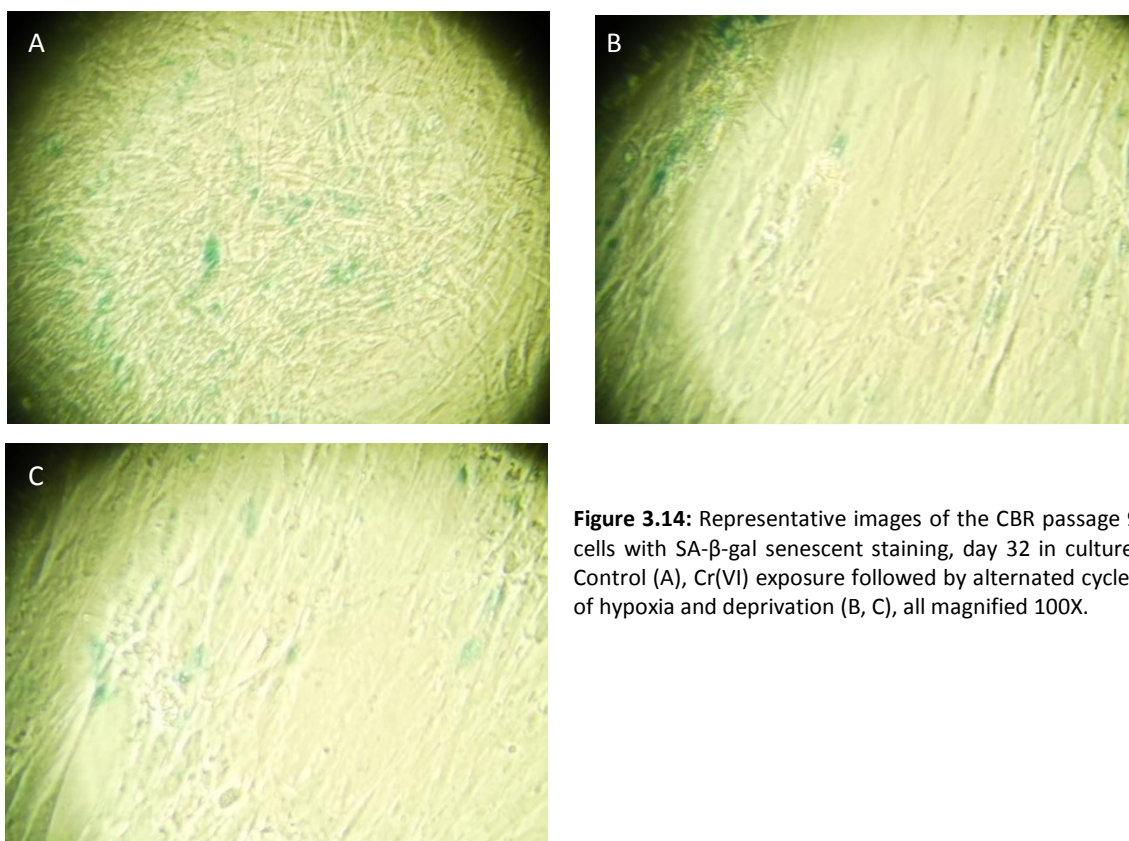


**Figure 3.14:** Representative images of the CBR passage 9 cells with SA- $\beta$ -gal senescent staining, day 32 in culture. Control (A), Cr(VI) exposure followed by alternated cycles of hypoxia and deprivation (B, C), all magnified 100X.

As illustrated in **Figure 3.15**, cells submitted three weeks to hypoxia showed morphological similarities to 0.25  $\mu$ M Cr(VI)-continuously exposed cells (**Figure 3.11, B and C**), while cells submitted for three weeks to deprivation appeared morphologically very similar to cells continuously exposed 0.5  $\mu$ M Cr(VI) along 4 weeks in culture (**Figure 3.11, D-F**). Moreover, a one week Cr(VI)-insult followed by either hypoxia or deprivation induced extensive senescence.

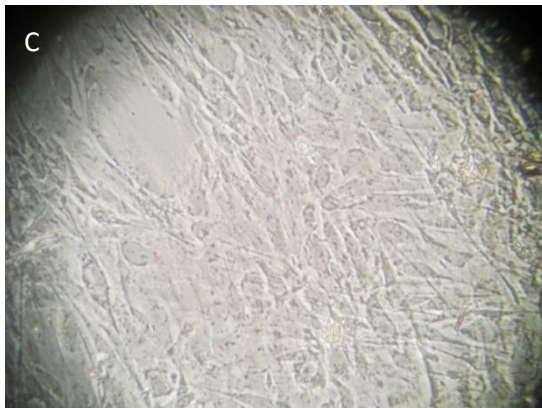
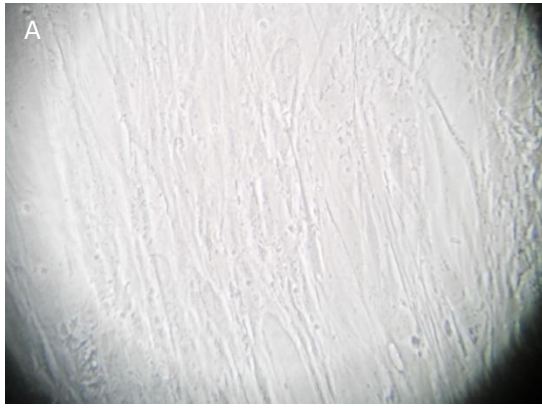


**Figure 3.15:** Representative images of the morphology of CBR passage 9 cells, day 32 in culture. Control (A), hypoxia exposed Cells (B) and deprivation exposed Cells (C), all magnified 100X.

As illustrated (**Figure 3.16**) morphological changes correlated with senescent staining coinciding in both hypoxia and deprivation conditions.

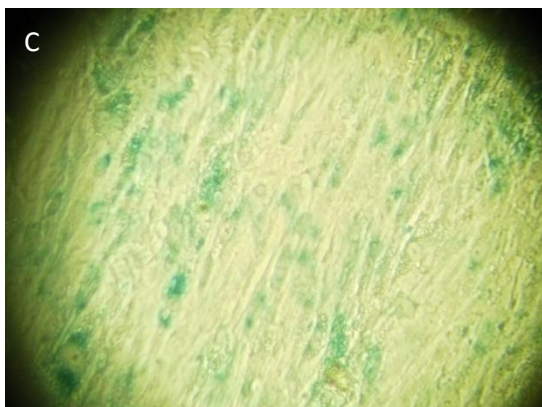
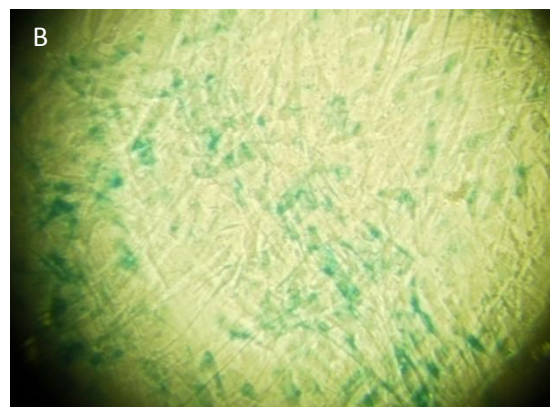
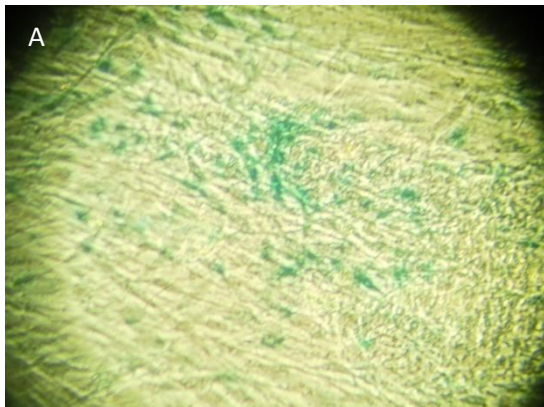


**Figure 3.16:** Representative images of the of CBR passage 8 cells with SA-β-gal senescent staining, day 32 in culture. Control (A), hypoxia exposed Cells (B) and deprivation exposed Cells (C), all magnified 100X.

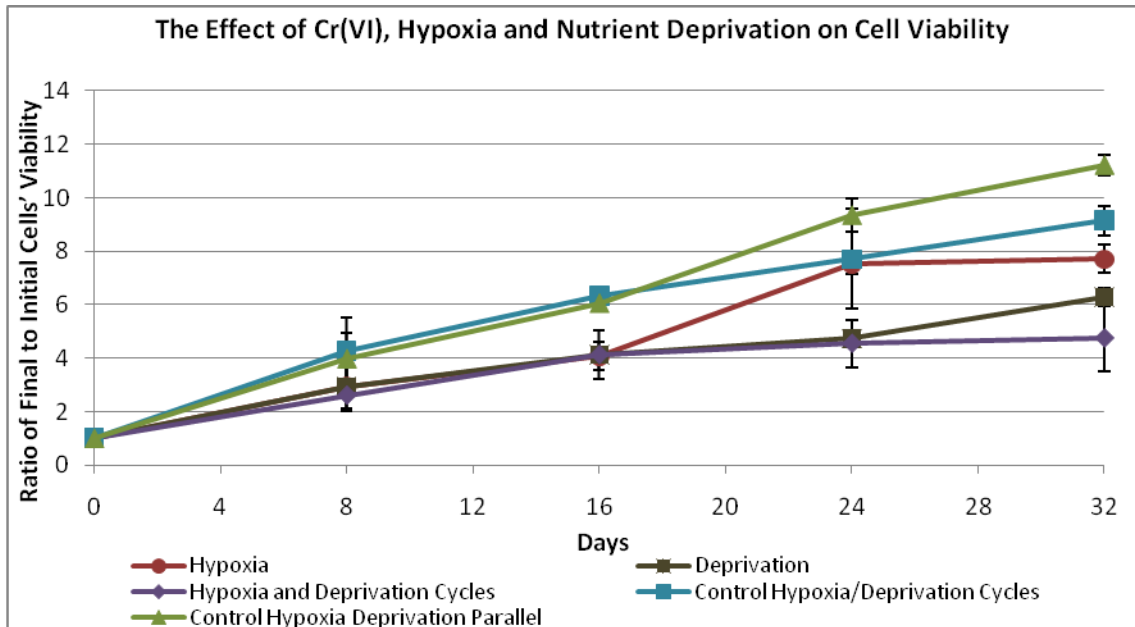


**Figure 3.17:** Representative effects of hypoxia, deprivation, and cycles of hypoxia and deprivation on CBR cells' viability. Cells were exposed for a week to 0.5  $\mu\text{M}$  Cr(VI) with medium changed every two days, followed by either hypoxia or deprivation, and alternative cycles of hypoxia and deprivation. The results are expressed as the ratio of final to initial cell viability evaluated by the MTT assay and represent the mean  $\pm$  SD of three independent experiments.

**Table 3.15:** Representative effects of hypoxia, deprivation, and cycles of hypoxia and deprivation on CBR cells' viability. Cells were exposed for a week to 0.5  $\mu\text{M}$  Cr(VI) with medium changed every two days, followed by either hypoxia or deprivation, and alternative cycles of hypoxia and deprivation. The results are expressed as the ratio of final to initial cell viability evaluated by the MTT assay and represent the mean  $\pm$  SD of three independent experiments.

	Condition	Passage Number	Cell Density (cell/cm <sup>2</sup> )	Ratio of Final to Initial cells' Viability	Week							
					1	SD Value	2	SD Value	3	SD Value	4	SD Value
Hypoxia and Deprivation Cycles	Control	9	20000		4,28	1,25	6,32	0,31	7,70	1,87	9,14	0,56
	Treated	9	20000		2,61	0,51	4,13	0,91	4,55	0,88	4,75	1,23
Continuous Hypoxia and Continuous Deprivation	Control	10	20000		3,98	0,95	6,05	0,15	9,34	0,60	11,22	0,40
	Hypoxia	10	20000		2,94	0,91	4,07	0,51	7,53	0,40	7,70	0,53
	Deprivation	10	20000		2,94	0,91	4,13	0,21	4,73	0,28	6,28	0,34

Considering cell viability, morphological changes and senescent-staining, all these results can seem to be contradictory. Firstly, although cells exposed to hypoxia and deprivation cycles showed a cell viability arrest, the senescent-staining was not strong enough to warrant the consideration of this condition as capable of inducing and retaining senescence.

It can be proposed that this arrest was not due to entering the state of senescence but related to a lag phase, being the cells in the process of adaptation to new conditions, having never reached an exponential growth phase, that would be reflected on a cell viability increase, due to constant change of conditions.

At the same time, constant hypoxia and deprivation conditions showed staining and morphology changes similar to 0.25 and 0.5  $\mu\text{M}$  Cr(VI) continuous exposure, considered the best conditions for senescence. This was not totally correlated in terms of cell viability as there is no significant long-term viability ratio stagnation. However, it can be observed that between the third and fourth weeks of the experiment, hypoxia-treated cells did not show a significant increase in viability ratio ( $\Delta$  ratio = 0.17) while between the second and third weeks, deprivation-treated cells showed little increase in viability ratio ( $\Delta$  ratio = 0.60).

This data, correlated with the senescent staining and morphology changes, suggest that further weeks of experiment would be needed to obtain a conclusive result. Meanwhile, these results suggest that, possibly, the senescence-inducing pathways activated by hypoxia and deprivation treatment would be different from the ones activated by Cr(VI) exposure only.

### **3.3.3. IMMUNOCYTOCHEMICAL CHARACTERIZATION OF SENESCENT FIBROBLASTS**

Immunocytochemistry analysis was used to characterize CBR passage 9 fibroblasts continuously exposed to 0.25 and 0.5  $\mu\text{M}$  Cr(VI) for 6 weeks. As expected, both control and 0.25 and 0.5  $\mu\text{M}$  continuously exposed cells, stained positive for vimentin. The ubiquitous distribution of this protein confirmed the fibroblast nature of these cells (**Figure 3.18**).

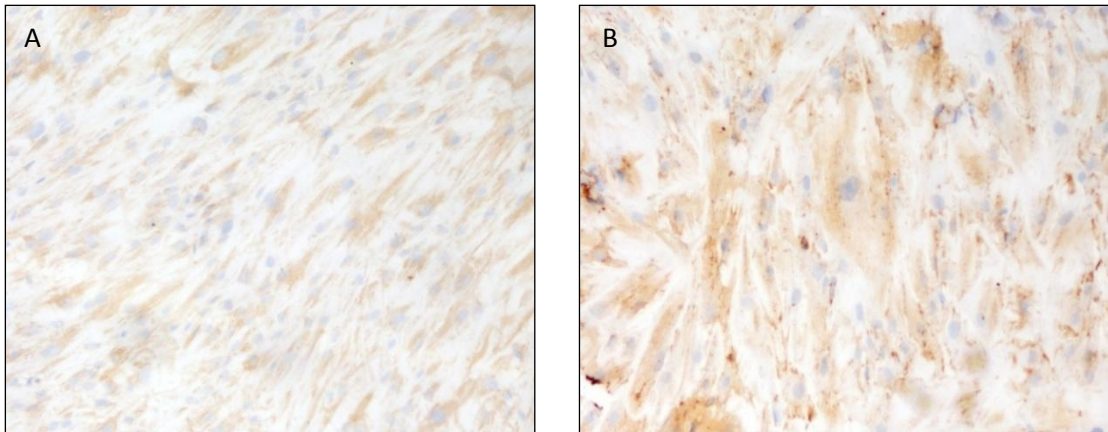


**Figure 3.18:** Representative images of fibroblasts, CBR passage 9 exposed to Cr(VI), immunocytochemical staining. Cells had been previously plated on top of microscopic slides for staining later on for vimentin as described in Materials and Methods. Control (A), and 0.25  $\mu$ M Cr(VI) (B), amplified 100x (A, B). Orange staining: Vimentin. Blue staining: Nuclei.

However, as revealed in **Figures 3.19 and 3.20**, the CBR cultures were not homogeneous since three sub-populations could be clearly identified: (i) a sub-population composed by cells with large nucleus; (ii) another sub-population composed of cells with small nuclei; (iii) a sub-population composed of cells with elongated nucleus. Positive staining for,  $\alpha$  smooth muscle actin ( $\alpha$ -SMA), a biomarker of mesenchymal and myofibroblasts cells, was particularly abundant in cultures exposed to Cr(VI) (**Figures 3.19 and 3.20**). In fact, the abundance of cells with elongated nucleus increased as Cr(VI) concentration increased, while the abundance of the other populations decreased, particularly the small nucleus cells. The morphology of the cells with elongated nucleus revealed they are mesenchymal-like fibroblasts and not myofibroblast-like cells (small nucleus). It appears that mesenchymal-like fibroblasts are more resistant to Cr(VI) exposure than myofibroblasts.

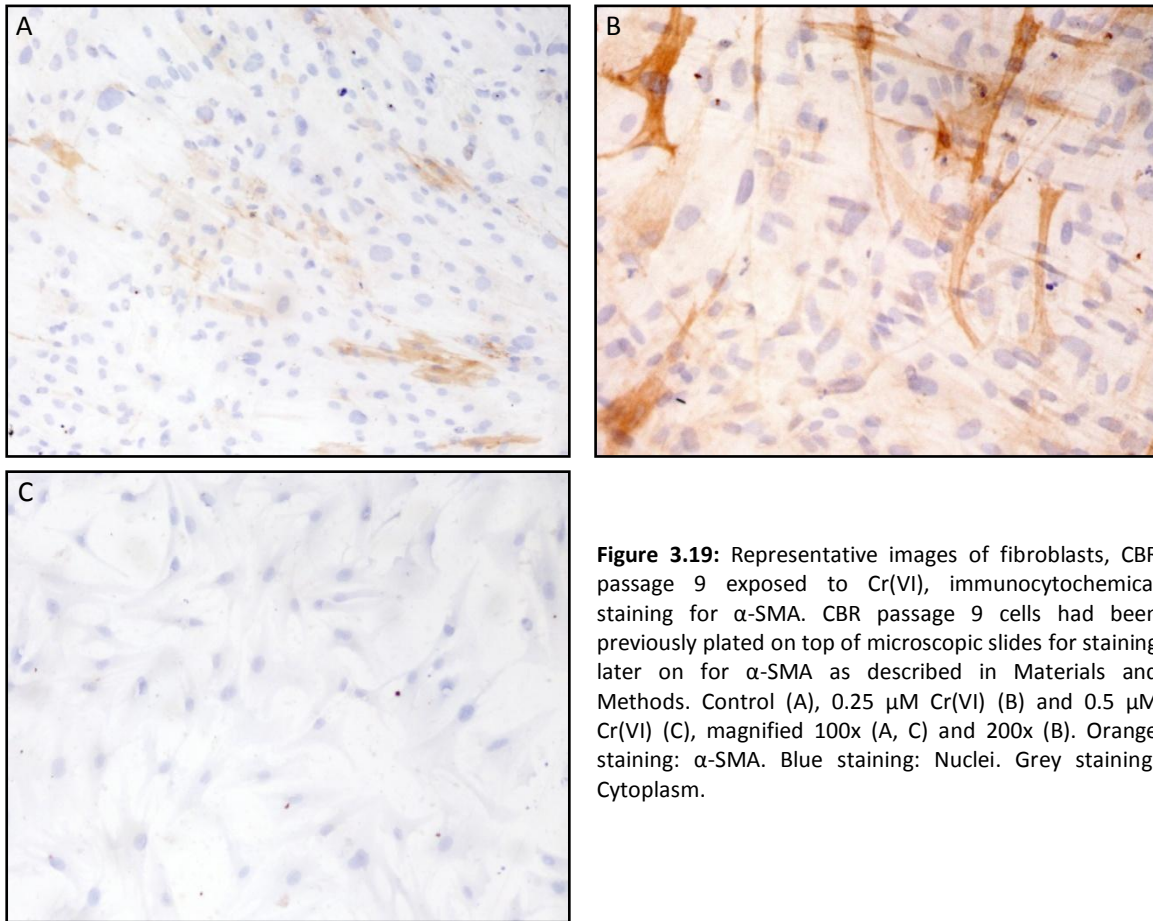


**Figure 3.19:** Representative images of fibroblasts, CBR passage 9 exposed to Cr(VI), immunocytochemical staining for  $\alpha$ -SMA. CBR passage 9 cells had been previously plated on top of microscopic slides for staining later on for  $\alpha$ -SMA as described in Materials and Methods. Control (A), 0.25  $\mu$ M Cr(VI) (B) and 0.5  $\mu$ M Cr(VI) (C), magnified 100x (A, C) and 200x (B). Orange staining:  $\alpha$ -SMA. Blue staining: Nuclei. Grey staining: Cytoplasm.

Regarding the staining with MNF-116, control cells showed a mild staining; however it was not strong enough to justify a positive staining (**Figure 3.20**). As to Cr(VI) exposed cells, the negative MNF-116 revealed an apparent absence of epithelial cells, ruling out a EMT under Cr(VI) stress. However, the positive staining of very few cells for E-Cadherin in cultures exposed to 0.5  $\mu$ M Cr(VI) may suggest the formation of myoepithelial cells through a mesenchymal to epithelial transition (MET) (**Figure 3.21**).

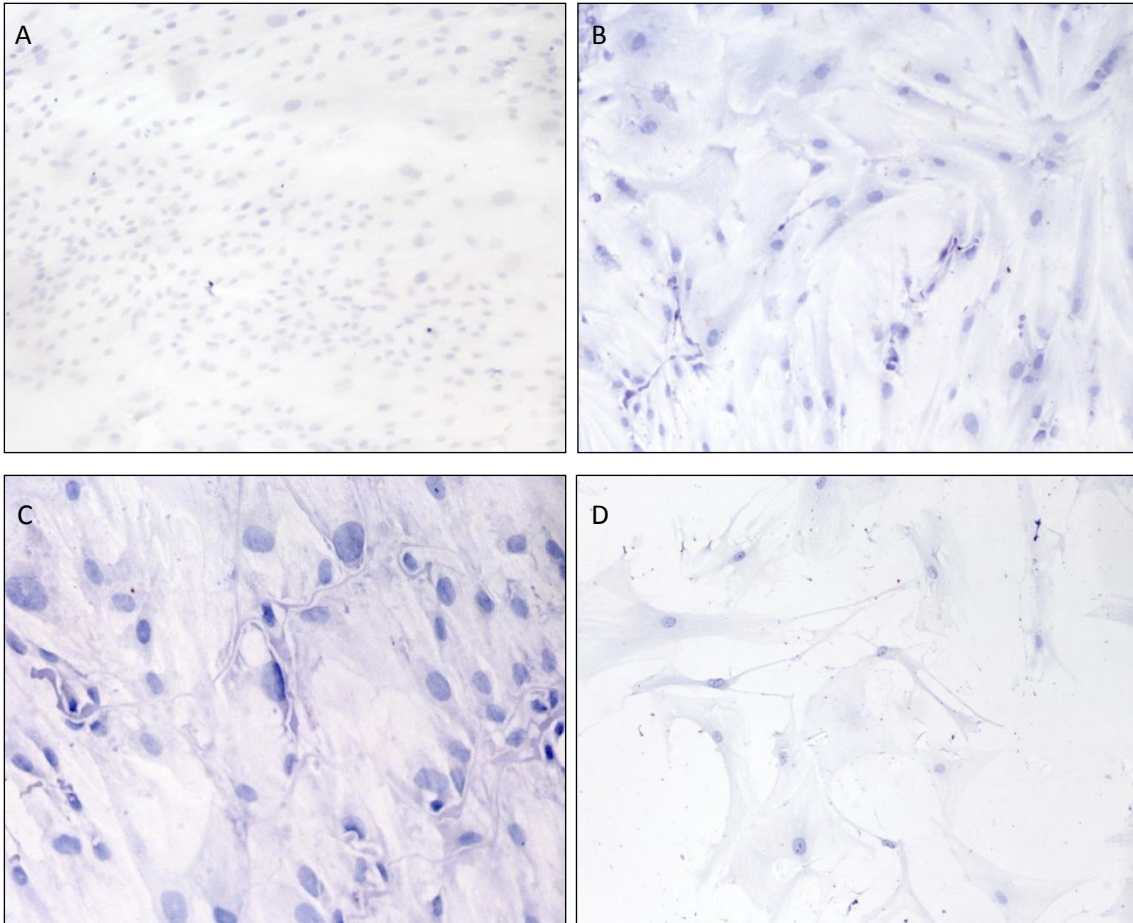


**Figure 3.20:** Representative images of fibroblasts, CBR passage 9 exposed to Cr(VI), immunocytochemical staining. CBR passage 9 cells had been previously plated on top of microscopic slides for staining later on for MNF-116 as described in Materials and Methods. Control (A), 0.25  $\mu$ M Cr(VI) (B, C) and 0.5  $\mu$ M Cr(VI) (D). Magnification: 100x (A, B, D) and 200x (C). Dark Blue staining: MNF-116. Blue staining: Nuclei. Grey staining: Cytoplasm.

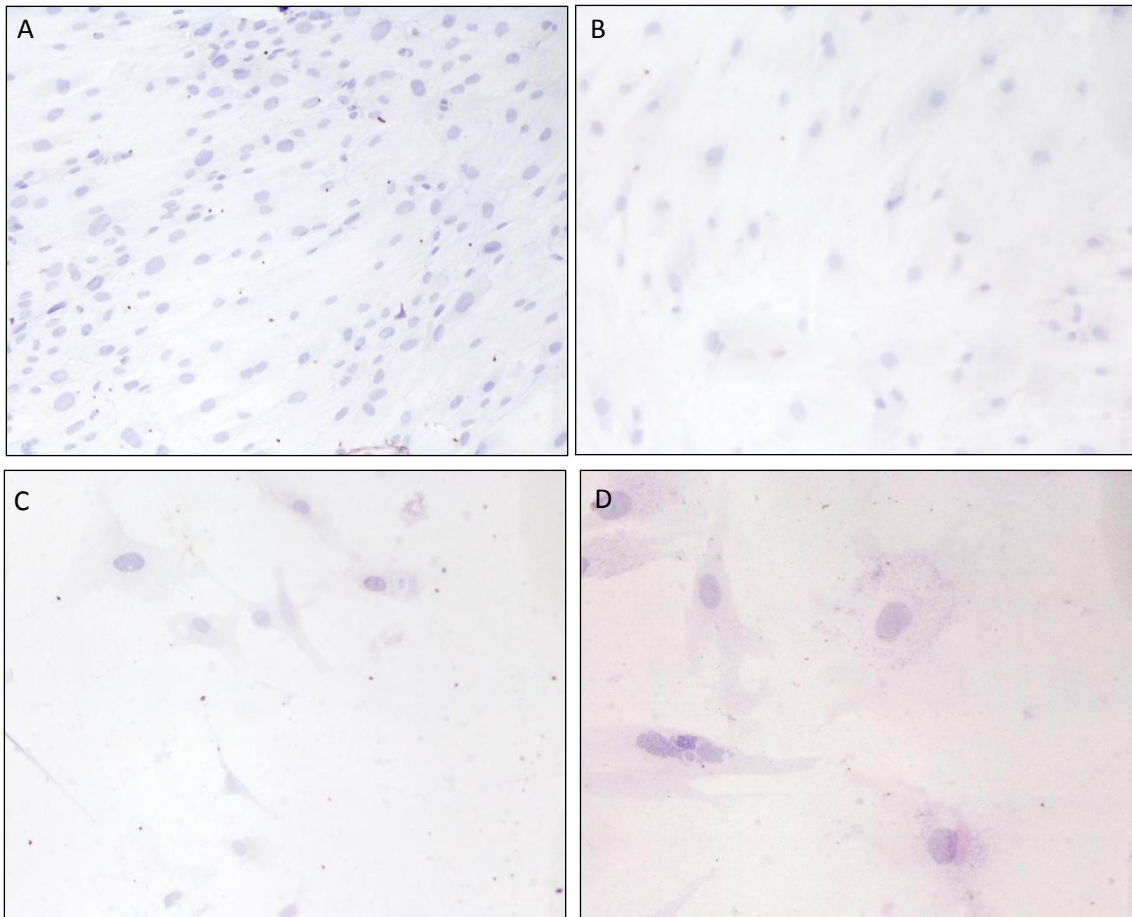


**Figure 3.21:** Representative images of fibroblasts, CBR passage 9 exposed to Cr(VI), immunocytochemical staining for E-Cadherin. CBR passage 9 cells had been previously plated on top of microscopic slides for staining later on for E-Cadherin as described in Materials and Methods. Control (A), 0.25  $\mu$ M Cr(VI) (B) and 0.5  $\mu$ M Cr(VI) (C, D), magnified 100x (A, B, C) and 200x (D). Pink staining: E-Cadherin. Blue staining: Nuclei. Grey staining: Cytoplasm.

Finally, the Cr(VI)-induced senescent-phenotype of CBR, passage 9, cells could be characterized as a predominant mesenchymal population, with small expression of  $\alpha$ -SMA and cytokeratins. These two protein' small expression could be related with the morphological changes in the cell in terms of nuclei and cell form, as they lost their previously organized state to a rounder-shape.

While there is the possibility of the senescent fibroblasts to be associated with a MET, through the results of E-Cadherin staining, it should be noted that further studies must be done in order to really assess the depth of the occurring changes, although the possibility of a MET could explain the effect of senescent fibroblasts on epithelial cells growth and disorganization in co-culture

### 3.4. CO-CULTURES: THE EFFECTS OF SENESCENT FIBROBLASTS ON BEAS-2B CELLS PROLIFERATION

The effects of Cr(VI)-senescent fibroblasts on bronchial epithelial cells proliferation and morphology were studied using the co-culture model of Chanson and collaborators [Wiszniewski *et al.*, 2006]. To this end, E7A passage 4 fibroblasts were first exposed to either 0.25 or 0.5  $\mu\text{M}$  Cr(VI), according to Table 3.12 (section 3.3), as these exposure regimens would guarantee that senescence would be achieved within 4 weeks of continuously exposure to Cr(VI). These 4 weeks treated fibroblasts were used as feeder layers in the co-culture experiments with BEAS-2B passage 5 cells on the top of gelatine coated transwells (**Table 3.16**).

**Table 3.16:** Co-Culture Experiments using either E7A passage 4 normal or Cr(VI)-senescent fibroblasts and BEAS-2B passage 5 In all experiments with Cr(VI) (added 3 days after BEAS-2B cells plating), the medium was renewed every three days along time in culture as described in Materials and Methods.

		Fibroblasts E7A		
		Control	Passage 4 0.25 $\mu\text{M}$ Cr(VI)	Cell Density 20000 cell/cm <sup>2</sup> Senescent 0.5 $\mu\text{M}$ Cr(VI)
BEAS-2B	Control	Yes	Yes	Yes
Passage 5	0.25 $\mu\text{M}$ Cr(VI)	Yes	Yes	
Cell Density 45000 cell/cm <sup>2</sup>	0.5 $\mu\text{M}$ Cr(VI)	Yes		Yes

As observed in **Figure 3.22**, within the first 24 hours co-cultures of BEAS-2B with 0.5  $\mu\text{M}$  Cr(VI)-induced-senescent fibroblasts were more confluent than co-cultures of BEAS-2B with normal fibroblasts. However, as revealed in **Figure 3.23** no additional changes were observed when the co-cultures were performed in presence of Cr(VI).

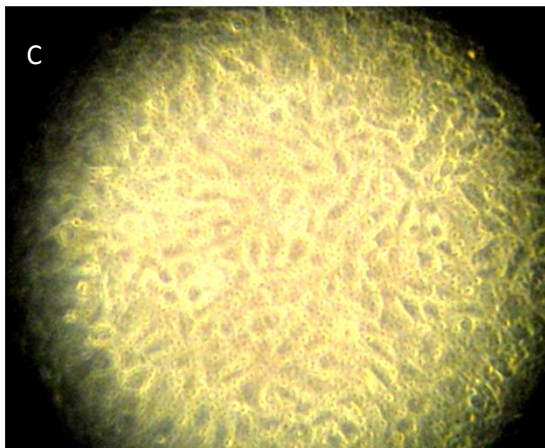
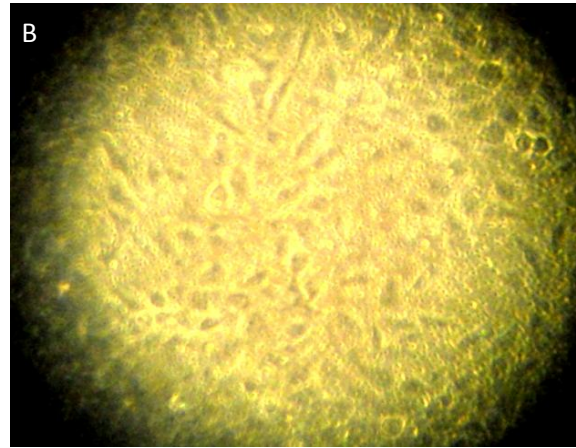
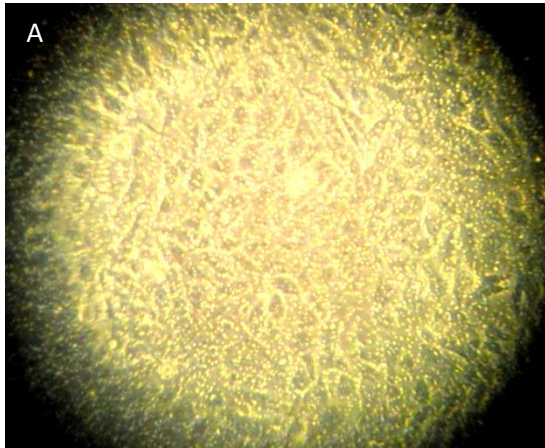


**Figure 3.22:** Representative images of the morphology of BEAS-2B passage 5 cells, day 1 in co-culture. With Control Fibroblasts (A), 0.25  $\mu\text{M}$  Cr(VI)-Induced Senescent Fibroblasts (B) and 0.5  $\mu\text{M}$  Cr(VI)-Induced Senescent Fibroblasts (C), all magnified 100X.

Prolonged co-cultivation showed no additional changes even in presence of Cr(VI) (**Figure 3.23**). This is due to the fact that BEAS-2B are immortalized cells and therefore their growth rate is greater than normal bronchial epithelial cells, leading to a quicker confluency and therefore a smaller Cr(VI) concentration per cell, resulting in a much smaller effect.

These results were then inconclusive regarding the effect of senescent fibroblasts in bronchial epithelial cells proliferation, whether in the presence or absence of Cr(VI), mainly due to the initial epithelial cell density

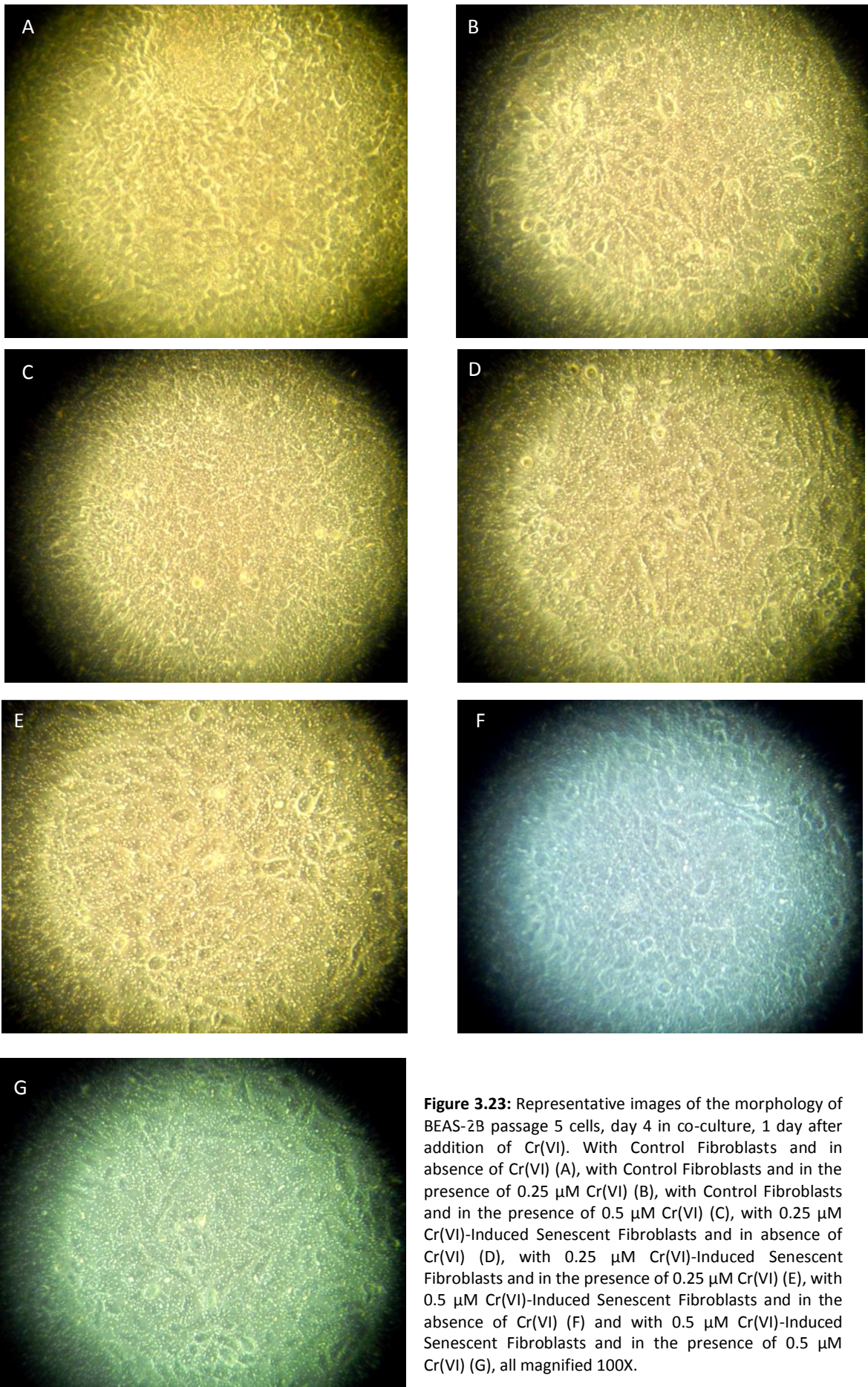


**Figure 3.23:** Representative images of the morphology of BEAS-2B passage 5 cells, day 4 in co-culture, 1 day after addition of Cr(VI). With Control Fibroblasts and in absence of Cr(VI) (A), with Control Fibroblasts and in the presence of 0.25  $\mu\text{M}$  Cr(VI) (B), with Control Fibroblasts and in the presence of 0.5  $\mu\text{M}$  Cr(VI) (C), with 0.25  $\mu\text{M}$  Cr(VI)-Induced Senescent Fibroblasts and in absence of Cr(VI) (D), with 0.25  $\mu\text{M}$  Cr(VI)-Induced Senescent Fibroblasts and in the presence of 0.25  $\mu\text{M}$  Cr(VI) (E), with 0.5  $\mu\text{M}$  Cr(VI)-Induced Senescent Fibroblasts and in the absence of Cr(VI) (F) and with 0.5  $\mu\text{M}$  Cr(VI)-Induced Senescent Fibroblasts and in the presence of 0.5  $\mu\text{M}$  Cr(VI) (G), all magnified 100X.

**Conclusions**

**&**

**Final Remarks**



In the concluding and final remarks of this work it is possible to focus that, effectively, cell culture techniques are a very useful tool of research, as most of the results were based on these techniques.

Firstly, primary cultures of both bronchial fibroblasts and bronchial epithelial cells were obtained, albeit the degree of success cannot be considered 100% due to problems already referred in sections 3.1 and 3.2. Therefore, in future projects, related with the use of primary cultures as an end result, the exact methodology for this aim should be perfected.

In this work it was possible to observe that Cr(VI) is able to induce changes in bronchial fibroblasts associated with senescence, being confirmed by the expression of SA- $\beta$ gal. Considering this, one great result was the establishment of a model of exposure to Cr(VI) that allows bronchial fibroblasts to express a stable senescent phenotype, being able to be maintained up to 4 weeks in culture afterwards. This model requires a cell density of 20000 cells/cm<sup>2</sup>, with 0.25 and 0.5  $\mu$ M Cr(VI) addition every two days, for 4 weeks, as detailed on section 3.3.2.

Also, regarding the effect of Cr(VI) and induction of senescent, it was observed that both deprivation and hypoxia conditions, after 0.5  $\mu$ M Cr(VI) exposure, were able to induce senescence on bronchial fibroblasts.

Still regarding senescent fibroblasts, it was shown that, in terms of immunocytochemistry, the primary cultures had several populations initially but only one thrived in Cr(VI) exposure conditions, leading to a predominantly mesenchymal-like phenotype, with elongated nuclei, that characterized the 0.5  $\mu$ M Cr(VI) senescent cells, as seen on section 3.3.3.

Although promising, these results did not answer any questions regarding the mechanisms by which senescence was attained in these fibroblasts, although it was not the focus of this work. Therefore, for this aim, further studies are required, focusing mainly on DNA damage response and ROS formation, as well as identifying which, between pRb and p53, if not both pathways, leads to the obtained senescent state in bronchial fibroblasts.

Also, further characterization of these senescent fibroblasts should be done, namely their metabolism, *e.g.* answering if glycolysis rate increases, as well as oxidative phosphorylation rate, as well as secreted factors, comparing this phenotype to the secretory senescent phenotype described in literature.

As for the final aim of the work, co-cultures have been shown to be a viable way to mimic *in vivo* situations, considering the existence of a supportive and dynamic layer beneath epithelial cells.

Yet, for the proposed objective of observing if there was any change in proliferation and differentiation of bronchial epithelial cells, in the presence of senescent fibroblasts and Cr(VI), the results were inconclusive. This was due mainly to the cell type used, as BEAS-2B are an immortalized cell line, being used in substitution of bronchial epithelial cells primary culture, have a greater proliferation rate. This, associated with the initial cell density used, based on literature considering the use of cell co-culture, resulted in the main flaws of the final work section (section 3.4).

Therefore, to realize the effects of senescent fibroblasts on bronchial epithelial cells in co-culture, closely to an *in vivo* situation, it is essential that, first of all, primary cultures of epithelial cells are successfully obtained and, most importantly, are able to be sub-cultured, using a correct protocol.

It should be also noted, that the decisions of BEAS-2B usage in the co-culture section and regarding the cell density used, were greatly influenced by the amount of time left until the official deadline for the master's thesis conclusion.

Considering that the work was mostly based on literature, without any previous results regarding primary cell culture and senescence studies on fibroblasts that could be related to this project, it can be said that the project was fairly ambitious for a one year master's thesis.

# References



Andriani F., Margulis A., Lin N., Griffey S., Garlick J.A. (2003); *Analysis of microenvironmental factors contributing to basement membrane assembly and normalized epidermal phenotype*. J Invest Dermatol., 120(6), 923-31.

Barceloux D.G. (1999); *Chromium*. J Toxicol Clin Toxicol., 37(2), 173-94

Bartling B., Rehbein G., Silber R.E., Simm A. (2006); *Senescent fibroblasts induce moderate stress in lung epithelial cells in vitro*. Exp Gerontol., 41(5), 532-9

Bello-DeOcampo D., Kleinman H.K., Deocampo N.D., Webber M.M. (2001); *Laminin-1 and  $\alpha 6\beta 1$  Integrin Regulate Acinar Morphogenesis of Normal and Malignant Human Prostate Epithelial Cells*. Prostate, 46(2), 142-53

Berman J.J. (2009); *Neoplasms: principles of development and diversity. First Edition*. Jones & Bartlett Publisher, LLC

BéruBé K., Prytherch Z., Job C., Hughes T. (2010); *Human primary bronchial lung cell constructs: The new respiratory models*. Toxicology., 278(3), 311-8

Biedermann K.A., Landolph J.R. (1987); *Induction of anchorage independence in human diploid foreskin fibroblasts by carcinogenic metal salts*. Cancer Res., 47(14), 3815-23

Bissell M.J., Kenny P.A., Radisky D.C. (2005); *Microenvironmental Regulators of Tissue Structure and Function Also Regulate Tumor Induction and Progression: The Role of Extracellular Matrix and Its Degrading Enzymes*. Cold Spring Harb Symp Quant Biol., 70, 343-56

Bissell M.J., Rizki A., Mian I.S. (2003); *Tissue architecture: the ultimate regulator of breast epithelial function*. Curr Opin Cell Biol., 15(6), 753-62

Campisi J. (2005); *Senescent Cells, Tumor Suppression, and Organismal Aging: Good Citizens, Bad Neighbors*. Cell., 120(4), 513-22

Campisi J., d'Adda di Fagagna F. (2007); *Cellular senescence: when bad things happen to good cells*. Nat Rev Mol Cell Biol., 8(9), 729-40

Cancer Research UK – Stats from February 2011:  
[http://info.cancerresearchuk.org/prod\\_consump/groups/cr\\_common/@nre/@sta/documents/generalcontent/crukmig\\_1000ast-2972.pdf](http://info.cancerresearchuk.org/prod_consump/groups/cr_common/@nre/@sta/documents/generalcontent/crukmig_1000ast-2972.pdf)

Choi H.R., Cho K.A., Kang H.T., Lee J.B., Kaeberlein M., Suh Y., Chung I.K., Park S.C. (2011); *Restoration of senescent human diploid fibroblasts by modulation of the extracellular matrix*. Aging Cell., 10(1), 148-57

Cooper G.M., Hausman R.E. (2009); *The Cell – A Molecular Approach. Fifth Edition*. ASM Press and Sinauer Associates, Inc., Washington D.C.

Coppé J.P., Boesen M., Sun C.H., Wong B.J.F., Kang M.K:K, Park N.H., Desprez P.Y., Campisi J., Krtolica A. (2008a); *A Role for Fibroblasts in Mediating the Effects of Tobacco-Induced Epithelial Cell Growth and Invasion*. Mol Cancer Res., 6(7), 1085-98

Coppé J.P., Patil C.K., Rodier F., Sun Y., Muñoz D.P., Goldstein J., Nelson P.S., Desprez P.Y., Campisi J. (2008b); *Senescence-associated secretory phenotypes reveal cell-nonautonomous functions of oncogenic RAS and the p53 tumor suppressor* PLoS Biol., 6(12), 2853-68

Costa A.N., Moreno V., Prieto M.J., Urbano A.M., Alpoim M.C. (2010); *Induction of Morphological Changes in BEAS-2B Human Bronchial Epithelial Cells Following Chronic Sub-Cytotoxic and Mildly Cytotoxic Hexavalent Chromium Exposures*. Mol Carcinog., 49(6), 582-91

Cotton, F.A., Wilkinson, G. (1998); *Advanced Inorganic Chemistry. Fifth edition*. Wiley-Interscience, New York

Crystal R.G., Randell S.H., Engelhardt J.F., Voynow J., Sunday M.E. (2008); *Airway Epithelial Cells: current concepts and challenges*. Proc Am Thorac Soc., 5(7), 772-7

Data Sheet: Cell Culture Manual, 2005-2006, Sigma, Sigma-Aldrich

del Moral P.M., De Langhe S.P., Sala F.G., Veltmaat J.M., Tefft D., Wang K., Warburton D., Bellusci S. (2006); *Differential role of FGF9 on epithelium and mesenchyme in mouse embryonic lung*. Dev Biol., 293(1), 77-89

Dimri G.P., Lee X., Basile G., Acosta M., Scott G., Roskelley C., Medrano E.E., Linskens M., Rubelj I., Pereira-Smith O., Peacocke M., Campisi J. (1995); *A biomarker that identifies senescent human cells in culture and in aging skin in vivo*. Proc Natl Acad Sci U S A., 92(20), 9363-7

Feng Z., Hu W., Teresky A.K., Hernando E., Cordon-Cardo C., Levine A.J. (2007); *Declining p53 function in the aging process: A possible mechanism for the increased tumor incidence in older populations*. Proc Natl Acad Sci U S A., 104(42), 16633-8

- Freshney R.I. (2002); *Culture of Epithelial Cells. Second Edition*. Wiley-Liss, Inc., New York
- Freshney R.I. (2004); *Culture of Human Tumour Cells. First Edition*. John Wiley & Sons, Inc. Hoboken, New Jersey
- Freshney R.I. (2005); *Culture of Animal Cells – Manual of Basic Technique*. Fifth Edition, Wiley–New Jersey
- Ghajar C.M., Bissell M.J. (2008); *Extracellular matrix control of mammary gland morphogenesis and tumorigenesis: insights from imaging*. *Histochem Cell Biol.*, 130(6), 1105-18
- Goodwin E., Yang E., Lee C.J., Lee H.W., DiMaio D., Hwang E.S. (2000); *Rapid induction of senescence in human cervical carcinoma cells*. *Proc Natl Acad Sci U S A.*, 97(20), 10978-83
- Hanahan D., Weinberg R.A. (2011); *Hallmarks of cancer: the next generation*. *Cell.*, 144(5), 646-74
- Herbst R.S., Heymach J.V., Lippman S.M. (2008); *Lung Cancer*. *N Engl J Med.*, 359(13), 1367-80
- Holgate S., Davies D.E., Lackie P.M., Wilson S.J., Puddicombe S.M., Lordan J.L. (2000); *Epithelial-mesenchymal interactions in the pathogenesis of asthma*. *J Allergy Clin Immunol.*, 105(2 Pt 1), 193-204
- Hsu P.P., Sabatini D.M. (2008); *Cancer cell metabolism: Warburg and beyond*. *Cell.*, 134(5), 703-7
- Hu M., Polyak K. (2008); *Microenvironmental regulation of cancer development*. *Curr Opin Genet Dev.*, 18(1), 27-34
- Hyatt B.A., Shangguan X., Shannon J.M. (2004); *FGF-10 induces SP-C and Bmp4 and regulates proximal-distal patterning in embryonic tracheal epithelium*. *Am J Physiol Lung Cell Mol Physiol.*, 287(6), 1116-26
- Johnson L.N., Koval M. (2009); *Cross-Talk Between Pulmonary Injury, Oxidant Stress, and Gap Junctional Communication*. *Antioxid Redox Signal.*, 11(2), 355-67
- Junqueira L.C., Carneiro J. (2008); *Histologia Básica. Eleventh edition*. Editora Guanabara Koogan S/A, Rio de Janeiro
- Kenny P.A., Bissell M.J. (2003); *Tumor Reversion: Correction of Malignant Behavior by Microenvironmental Cues*. *Int J Cancer.*, 107(5), 688-95

Knight D. (2001); *Epithelium–fibroblast interactions in response to airway inflammation*. Immunol Cell Biol., 79(2), 160-4

Knowles M., Selby P. (2005); *Introduction to the Cellular and Molecular Biology of Cancer; Fourth Edition*; Oxford University Press; New York

Komuro T (1990); *Re-evaluation of fibroblasts and fibroblast-like cells*. Anat Embryol (Berl.), 182(2), 103-12

Krtolica A., Campisi J. (2002); *Cancer and aging: a model for the cancer promoting effects of the aging stroma*. Int J Biochem Cell Biol., 34(11), 1401-14

Krtolica A., Ortiz de Solorzano C., Lockett S., Campisi J. (2002); *Quantification of epithelial cells in coculture with fibroblasts by fluorescence image analysis*. Cytometry., 49(2), 73-82

Krtolica A., Parrinello S., Lockett S., Desprez P.Y., Campisi J. (2001); *Senescent fibroblasts promote epithelial cell growth and tumorigenesis: A link between cancer and aging*. Proc Natl Acad Sci U S A., 98(21), 12072-7

Laberge R.M., Awad P., Campisi J., Desprez P.Y. (2011); *Epithelial-Mesenchymal Transition Induced by Senescent Fibroblasts*. Cancer Microenviron. 2011 Jun 25. [Epub ahead of print]

Lebeche D., Malpel S., Cardoso W.V. (1999); *Fibroblast growth factor interactions in the developing lung*. Mech Dev., 86(1-2), 125-36.

Lisanti M.P., Martinez-Outschoorn U.E., Chiavarina B., Pavlides S., Whitaker-Menezes D., Tsirigos A., Witkiewicz A., Lin Z., Balliet R., Howell A., Sotgia F. (2010); *Understanding the "lethal" drivers of tumor-stroma co-evolution: emerging role(s) for hypoxia, oxidative stress and autophagy/mitophagy in the tumor micro-environment*. Cancer Biol Ther., 10(6), 537-42

Littlepage L.E., Egeblad M., Werb Z. (2005); *Coevolution of cancer and stromal cellular responses*. Cancer Cell., 7(6), 499-500

Lodish H., Berk A., Kaiser C.A., Krieger M., Scott M.P., Bretscher A., Ploegh H., Matsudaira P. (2004); *Molecular Cell Biology. Fifth Edition*. New York: W.H. Freeman and Co.

Luca M.R., Ciubar R., Ciofrangeanu C.L., Mitran V., Cimpean A., Iordachescu D. (2007); *Response of Antioxidant Defense System to Chromium (VI) - Induced Oxidative Stress in Embryonary Fibroblasts*. Biometals., 23(1), 161-72

Maeda Y., Davé V., Whitsett J.A. (2007); *Transcriptional Control of Lung Morphogenesis*. *Physiol Rev.*, 87(1), 219-44

Manahan S. E. (2003); *Toxicological Chemistry and Biochemistry. Third Edition*. Lewis Publishers, CRC Press Company

Martinez-Outschoorn U.E., Balliet R.M., Rivadeneira D.B., Chiavarina B., Pavlides S., Wang C., Whitaker-Menezes D., Daumer K.M., Lin Z., Witkiewicz A.K., Flomenberg N., Howell A., Pestell R.G., Knudsen E.S., Sotgia F., Lisanti M.P (2010); *Oxidative stress in cancer associated fibroblasts drives tumor-stroma co-evolution: A new paradigm for understanding tumor metabolism the field effect and genomic instability in cancer cells*. *Cell Cycle.*, 9(16), 3256-76

Mills K. (2002); *Molecular Analysis of Cancer – An Overview. Methods in Molecular Medicine*, *Methods Mol Med.*, 68, 1-5

Mori N., Doi Y., Hara K., Yoshizuka M., Ohsato K., Fujimoto S. (1992); *Role of multipotent fibroblasts in the healing colonic mucosa of rabbits Ultrastructural and immunocytochemical study*. *Histol Histopathol.*, 7(4), 583-90

Narita M., Nuñez S., Heard E., Narita M., Lin A.W., Hearn S.A., Spector D.L., Hannon G.J., Lowe S.W. (2003); *Rb-mediated heterochromatin formation and silencing of E2F target genes during cellular senescence*. *Cell.*, 113(6), 703-16

O'Brien J., Ceryak S., Patierno S.R. (2003); *Complexities of chromium carcinogenesis: Role of cellular response, repair and recovery mechanisms*. *Mutat Res.*, 533(1-2), 3-36

Olumi A.F., Grossfeld G.D., Hayward S.W., Carroll P.R., Tlsty T.D., Cunha G.R. (1999); *Carcinoma-associated Fibroblasts Direct Tumor Progression of Initiated Human Prostatic Epithelium*. *Cancer Res.*, 59(19), 5002-11

Panno J. (2005); *Cancer – The Role of Genes, Lifestyle and Environment. First Edition*. The New Biology; New York

Parrinello S., Coppé J.P., Krtolica A., Campisi J. (2005); *Stromal-epithelial interactions in aging and cancer: senescent fibroblasts alter epithelial cell differentiation*. *J Cell Sci.*, 118(Pt 3), 485-96

Passos J.F., Nelson G., Wang C., Richter T., Simillion C., Proctor C.J., Miwa S., Olijslagers S., Hallinan J., Wipat A., Saretzki G., Rudolph K.L., Kirkwood T.B.L., von Zglinicki T. (2010),

*Feedback between p21 and reactive oxygen production is necessary for cell senescence.* Mol Syst Biol., 6, 347

Pohl C., Hermanns M.I., Uboldi C., Bock M., Fuchs S., Dei-Anang J., Mayer E., Kehe K., Kummer W., Kirkpatrick C.J. (2009); *Barrier functions and paracellular integrity in human cell culture models of the proximal respiratory unit.* Eur J Pharm Biopharm., 72(2), 339-49

Reddel R.R., et al. (1989); *Immortalized human bronchial epithelial mesothelial cell lines*; US Patent 4,885,238

Reynolds M., Stoddard L., Bepalov I., Zhitkovich A. (2007); *Ascorbate acts as a highly potent inducer of chromate mutagenesis and clastogenesis: linkage to DNA breaks in G2 phase by mismatch repair.* Nucleic Acids Res., 35(2), 465-76

Rodier F., Campisi J., Bhaumik D. (2007); *Two faces of p53: aging and tumor suppression.* Nucleic Acids Res., 35(22), 7475-84

Rodier F., Campisi J. (2011); *Four faces of cellular senescence.* J Cell Biol., 192(4), 547-56

Rodrigues C.F.D., Urbano A.M., Matoso E., Carreira I., Almeida A., Santos P., Botelho F., Carvalho L., Alves M., Monteiro C., Costa A.N., Moreno V., Alpoim M.C. (2009); *Human bronchial epithelial cells malignantly transformed by hexavalent chromium exhibit an aneuploid phenotype but no microsatellite instability.* Mutat Res., 670(1-2), 42-52

Ruddon R.W. (2007); *Cancer Biology. Fourth Edition.* Oxford Press University Press

Salnikow K., Zhitkovich A. (2008); *Genetic and Epigenetic Mechanisms in Metal Carcinogenesis and Cocarcinogenesis: Nickel, Arsenic and Chromium.* Chem Res Toxicol., 21(1), 28-44

Schulz W.A. (2005); *Molecular Biology of Human Cancers - An Advanced Student's Textbook.* Springer, New York

Skibinski G., Elborn J.S., Ennis M. (2007); *Bronchial epithelial cell growth regulation in fibroblast cocultures: the role of hepatocyte growth factor.* Am J Physiol Lung Cell Mol Physiol., 293(1), 69-76

Spiro S.G., Silvestri G.A. (2005); *One hundred years of lung cancer.* Am J Respir Crit Care Med., 172(5), 523-9

Stern R.M., Thomsen E. and Furst A. (1984); *Cr(VI) and other metallic mutagens in fly ash and welding fumes.* Toxicol Environ Chem., 8, 95-108

Sugiura H., Liu X., Duan F., Kawasaki S., Togo S., Kamio K., Wang X.Q., Mao L., Ahn Y., Ertl R.F., Bargar T.W., Berro A., Casale T.B., Rennard S.I. (2007); *Cultured lung fibroblasts from ovalbumin-challenged "asthmatic" mice differ functionally from normal*. Am J Respir Cell Mol Biol., 37(4), 424-30

Urbano A.M., Rodrigues C.F.D., Alpoim M.C. (2008); *Hexavalent Chromium Exposure, Genomic Instability and Lung Cancer*. Chem Res Toxicol., 19(11), 1492-8

Vergel M., Marin J.J., Estevez P., Carnero A. (2010); *Cellular senescence as a target in cancer control*. J Aging Res., 2011, 725365

Weber G.F. (2007); *Molecular Mechanisms of Cancer*. Springer; New York

Weinberg R. (1996); *How Cancer Arises*. Sci Am., 275(3), 62-70

Weir B.A., Woo M.S., Getz G., Perner S., Ding L., Beroukhi R., Lin W.M., Province M.A., Kraja A., Johnson L.A., Shah K., Sato M., Thomas R.K., Barletta J.A., Borecki I.B., Broderick S., Chang A.C., Chiang D.Y., Chirieac L.R., Cho J., Fujii Y., Gazdar A.F., Giordano T., Greulich H., Hanna M., Johnson B.E., Kris M.G., Lash A., Lin L., Lindeman N., Mardis E.R., McPherson J.D., Minna J.D., Morgan M.B., Nadel M., Orringer M.B., Osborne J.R., Ozenberger B., Ramos A.H., Robinson J., Roth J.A., Rusch V., Sasaki H., Shepherd F., Sougnez C., Spitz M.R., Tsao M.S., Twomey D., Verhaak R.G., Weinstock G.M., Wheeler D.A., Winckler W., Yoshizawa A., Yu S., Zakowski M.F., Zhang Q., Beer D.G., Wistuba I.I., Watson M.A., Garraway L.A., Ladanyi M., Travis W.D., Pao W., Rubin M.A., Gabriel S.B., Gibbs R.A., Varmus H.E., Wilson R.K., Lander E.S., Meyerson M. (2007); *Characterizing the cancer genome in lung adenocarcinoma*. Nature., 450(7171), 893-8

Welford S.M., Bedogni B., Gradin K., Poellinger L., Broome Powell M., Giaccia A.J. (2006); *HIF1alpha delays premature senescence through the activation of MIF*. Genes Dev., 20(24), 3366-71

Wikipedia: [http://en.wikipedia.org/wiki/File:Haemocytometer\\_Grid.png](http://en.wikipedia.org/wiki/File:Haemocytometer_Grid.png)

Wisniewski L., Jornot L., Dudez T., Pagano A., Rochat T., Lacroix J.S., Suter S., Chanson M. (2006); *Long-Term Cultures of Polarized Airway Epithelial Cells from Patients with Cystic Fibrosis*. Am J Respir Cell Mol Biol., 34(1), 39-48

Wright W.E., Shay J.W. (2002); *Historical claims and current interpretations of replicative aging*. Nat Biotechnol., 20(7), 682-8

Zhitkovich A. (2005); *Importance of Chromium-DNA Adducts in Mutagenicity and Toxicity of Chromium(VI)*. Chem Res Toxicol., 18(1), 3-11



